

**Euclidean classical solutions in
quantum field theory and gravity:
Higgs vacuum metastability and the hierarchy problem**

THÈSE N° 8911 (2018)

PRÉSENTÉE LE 22 NOVEMBRE 2018

À LA FACULTÉ DES SCIENCES DE BASE

LABORATOIRE DE PHYSIQUE DES PARTICULES ET DE COSMOLOGIE

PROGRAMME DOCTORAL EN PHYSIQUE

ÉCOLE POLYTECHNIQUE FÉDÉRALE DE LAUSANNE

POUR L'OBTENTION DU GRADE DE DOCTEUR ÈS SCIENCES

PAR

Andrey SHKERIN

acceptée sur proposition du jury:

Prof. V. Savona, président du jury
Prof. M. Chapochnikov, directeur de thèse
Prof. G. Dvali, rapporteur
Prof. R. Gregory, rapporteuse
Prof. J. Penedones, rapporteur



ÉCOLE POLYTECHNIQUE
FÉDÉRALE DE LAUSANNE

Suisse
2018

Abstract

The thesis is dedicated to two groups of questions arising in modern particle physics and cosmology. The first group concerns with the problem of stability of the electroweak (EW) vacuum in different environments. Due to its phenomenological significance, the problem attracts high attention in recent research. We contribute to this research in two directions.

First, we study decay rate of the EW vacuum at the inflationary stage of the universe. While in a low density, low temperature environment characteristic of the present-day universe the Standard Model EW vacuum is safely long-lived, the situation may be different during inflation. We estimate tunneling transition via Coleman-De Luccia instanton in this case and confirm that it is exponentially suppressed, contrary to the claims made in the literature.

Second, we compute the lifetime of the EW vacuum in a scale-invariant extension of the Standard Model and gravity, known as the Higgs-Dilaton theory. The theory passes phenomenological tests and provides us with a plausible cosmological scenario. To confirm its viability, it is necessary to check if the EW vacuum in this theory is sufficiently safe. We perform this check and find that features of the Higgs-Dilaton theory yield additional stabilization of the low-energy vacuum, compared to the Standard Model case.

Another group of questions addressed in the thesis is related to the hierarchy problem. Combining quantum scale invariance with the absence of new degrees of freedom above the EW scale leads to stability of the latter against perturbative quantum corrections. Nevertheless, the hierarchy between the weak and the Planck scales remains unexplained. We suggest that this hierarchy can be a manifestation of a non-perturbative effect relating low-energy and strong-gravity domains of the theory. To support this suggestion, we construct instanton configurations and investigate their contribution to the vacuum expectation value of the Higgs field.

The effect we find relies on properties of the theory in the ultraviolet regime. Non-minimal coupling of the Higgs field to the Ricci scalar and an approximate Weyl invariance of the theory in this regime are important ingredients of the mechanism. Dynamical gravity plays a crucial role in the effect as it leads to existence of instanton solutions suitable for generating the EW scale.

Keywords: electroweak vacuum, electroweak scale, vacuum stability, vacuum expectation value, inflation, gravity, instantons, scale invariance, hierarchy problem

Résumé

Cette thèse est consacrée aux deux groupes de questions qui se posent en physique des particules et cosmologie. Le premier groupe concerne le problème de la stabilité du vide électrofaible dans différents environnements. Grâce à son importance phénoménologique, ce problème attire l'attention de recherches actuelles. Nous contribuons à ces recherches dans deux directions.

D'une part, nous étudions le taux de décroissance du vide électrofaible pendant l'inflation cosmique. Tandis que le vide dans le modèle standard est assez sûr à basses densités et températures qui sont caractéristiques de l'univers actuel, la situation pourrait être différente lors de l'inflation. Nous estimons le taux de transition du vide via instanton de Coleman-De Luccia dans ce cas et confirmons qu'il est supprimé exponentiellement, contrairement aux déclarations faites dans la littérature.

D'autre part, nous calculons la durée de vie moyenne du vide électrofaible dans une extension du modèle standard et de la gravitation, connue sous le nom de théorie de Higgs-Dilaton. La théorie passe des tests phénoménologiques et nous fournit un scénario cosmologique plausible. Pour confirmer sa viabilité, il est nécessaire de vérifier que le vide à basse énergie est suffisamment sûr dans cette théorie. Nous effectuons cette vérification et constatons que les caractéristiques de la théorie de Higgs-Dilaton permettent une stabilisation supplémentaire du vide, par rapport au cas du modèle standard.

Un autre groupe des questions abordées dans la thèse est lié au problème de la hiérarchie. La combinaison de l'invariance par changements d'échelle et l'absence de degrés de liberté nouveaux au-dessus de l'échelle électrofaible améliore la stabilité de cette dernière contre les corrections quantiques perturbatives. Cependant, la hiérarchie entre l'échelle faible et l'échelle de Planck reste inexpliquée. Nous suggérons que cette hiérarchie peut être une manifestation d'un effet non-perturbatif qui relie les domaines d'énergies faibles et de gravitation forte de la

théorie. Pour soutenir cette suggestion, nous construisons des configurations euclidiennes classiques d'un certain type et étudions leurs contributions à la valeur moyenne dans le vide du champ de Higgs.

L'effet que nous trouvons dépend des propriétés de la théorie dans le régime ultraviolet. Le couplage non-minimal du champ de Higgs au scalaire de Ricci et une invariance de Weyl approximative de la théorie dans ce régime sont les ingrédients importants du mécanisme. La gravitation dynamique joue un rôle fondamentale dans l'effet car elle conduit à l'existence de solutions instantanées adaptées à la génération de l'échelle électrofaible.

Mots clés: vide électrofaible, échelle électrofaible, stabilité du vide, valeur moyenne dans le vide, inflation, gravitation, instanton, invariance par changements d'échelle, problème de la hiérarchie

Acknowledgements

I would like to express my gratitude to Mikhail Shaposhnikov for supervising my research and for his constant benevolence and attention.

I am grateful to Sergey Sibiryakov for being my co-author and to Georgi Dvali, Ruth Gregory, Joao Penedones and Vincenzo Savona for accepting to be members of the jury.

I also thank Fedor Bezrukov, Georgios Karananas, Alexander Monin, Emin Nugaev and Javier Rubio for many fruitful discussions.

Contents

Abstract	i
Résumé	iii
Acknowledgements	v
1 Introduction	1
1.1 General remarks	1
1.2 Introduction to part I	4
1.3 Introduction to part II	5
I On electroweak vacuum stability	8
2 Electroweak vacuum stability during inflation	9
2.1 Bounces in de Sitter space	11
2.1.1 Hawking-Moss instanton	12
2.1.2 Coleman-De Luccia bounce	13
2.2 Discussion of approximations	14
3 Bounce in the Higgs-Dilaton theory	16
3.1 Review of the Higgs-Dilaton theory	17
3.2 Bounce in the Higgs-Dilaton theory	22
3.2.1 Equations of motion and boundary conditions	22
3.2.2 Running couplings	23
3.2.3 Effective potential	25
3.2.4 Decay rate	28
3.2.5 EW vacuum stability in the Higgs-inflation scenario	30
3.3 Discussion	31
3.4 Summary	33
II Towards a non-perturbative approach to the hierarchy problem	34
4 Motivation and setup	35
5 Outline of the idea	40

6	Singular instanton in the Dilaton model	44
6.1	The Dilaton model	44
6.2	Classical configurations and Instanton action	46
7	“Higgs+gravity” models	51
7.1	The warm-up model	52
7.2	Implementation of the mechanism	54
7.2.1	Making the instantaneous scalar field source	54
7.2.2	Attempting to compute the vev in the simple model	56
7.2.3	Shaping the large-field limit with derivative operators	59
7.2.4	Making the hierarchy of scales with polynomial operators	61
7.3	Implications for the hierarchy problem	64
7.4	Summary	65
8	“Higgs+dilaton+gravity” models	68
8.1	Instantons in scale-invariant gravity with two scalar fields	69
8.1.1	Model setup	69
8.1.2	Polar field variables	71
8.1.3	Instanton in a model without higher-dimensional terms	74
8.1.4	Regularization of the instanton by a higher-dimensional term	77
8.1.5	Source enhancement	79
8.2	New scale via the instanton	81
8.3	Implications for the hierarchy problem	85
8.3.1	On quantum corrections in the Higgs-Dilaton theory	85
8.3.2	Higgs vev generation in the Higgs-Dilaton setting	86
9	Discussion and outlook	90
10	Conclusion	93
A	Singular instanton in curved space	95
B	Derivative operators of higher degrees	98
C	More on short-distance behavior of the instanton	100
	Bibliography	102

Chapter 1

Introduction

1.1 General remarks

It is intrinsic for human mind to search for principles organizing the world around us. Among different ways of building causal chains out of events we witness, the scientific method proved in centuries to be the most useful in providing us with the means of knowledge about our universe. Here, physics and, in particular, particle physics and cosmology are intended to uncover the rules governing Nature at very small as well as very large length scales. It is very interesting to note in this regard that the laws of microscopic physics have direct imprint on the structure of the world at cosmological distances, and by observing remote patches of the universe, one can judge about elementary particles, their properties and interactions.

There has to be an irresistible attraction in the idea of a *final* theory unifying all known forms of matter and interaction. The 20th century saw the impressive progress towards implementing this idea. The Standard Model (SM) of particle physics, which unifies three out of four fundamental forces, shows a great success of theoretical physics in explaining phenomena that occur at distances as small as 10^{-16} cm (or, equivalently, at energies as large as ~ 100 GeV). However, despite of its great predictive power, we cannot treat the SM as the final theory. The list of experimental and observational data that require a step out of the Model includes neutrino oscillations, dark matter, dark energy, baryon asymmetry of the universe. This is why a significant amount of efforts today are focused on searches for new physics. The latter is often placed at energy scales at the frontier of what we can access with the current experimental facilities, or much above that frontier.

A reasonable strategy to probe new physics at high energy scales, to which we have no direct access, is to ask what kind of high-energy behaviour can possibly explain a given fact about low-energy observables, which otherwise lacks a complete explanation. One way to address such questions is to do it with non-perturbative tools. The latter imply the use of classical aspects of a theory at hand and, in particular, of solutions of classical equations of motion — solitons and instantons. This thesis is dedicated to several problems in particle physics and cosmology, which seem to be well suited for being treated in this way.

Although the current understanding of fundamental laws of Nature is based on principles of quantum theory, it is true that a lot of information can be obtained by studying classical configurations arising in a theory and, in particular, solutions of classical equations of motion [1]. Often these solutions represent localized lumps of fields that exhibit a particle-like behavior, although the standard definition of a particle in quantum field theory refers to second quantization [2]. Existing thanks to nonlinear effects, such lumps are of non-perturbative nature. Hence, they do not show up within the perturbation theory built on top of a homogeneous classical vacuum. In turn, perturbation theory must be built above a classical solution, and the latter is a valid leading-order approximation in the semiclassical expansion provided that the corresponding semiclassical parameter is small (see, e.g., [3, 4]).

Localized particle-like or extended configurations of finite energy or energy density, which live in a spacetime with lorentzian signature, are referred to as solitons [5] (see also [6]). Often they are absolutely stable due to their topological properties or conservation laws and can propagate with maintaining their shape [7, 8].¹ The notion of soliton is crucial in many branches of modern physics. Their significance is due to numerous applications in nonlinear optics [9], condensed matter physics [10], particle physics and cosmology [11, 12]. Solitons are predicted in theories beyond the SM [13] and in gravity [14], hence they are of large phenomenological interest.

Another class of nonlinear classical objects are finite-action configurations arising in a theory continued to euclidean space. These objects are similar to solitons in their mathematical structure; however, unlike solitons, they are localized in time, albeit euclidean time [3]. Because of this, they are referred to as instantons or

¹One also speaks of these objects as solitary waves, while reserving the name soliton for configurations that maintain their form when interacting with each other.

pseudoparticles [15].² At the classical level, one often has a correspondence between static soliton solutions of a theory in d dimensions and instanton solutions of the same theory in $d+1$ dimensions [1]. However, the effects engendered by instantons in quantum field theory are very different from those caused by solitons. Instantons are responsible for many non-perturbative phenomena which are important for the current understanding of Nature. Among them are violation of quantum numbers, false vacuum decay and phase transitions [17]. Instantons are ample in modern theories including the SM and its extensions and gravity [13, 18]. The non-perturbative nature of instantons allows them to link physics at different energy domains of a theory.

In this thesis,³ we use semiclassical method to obtain and study euclidean classical configurations of certain types arising in theories of scalar fields and gravity. Despite the fact that the large part of the thesis is devoted to theoretical discourse, our goal is to address actual problems standing in particle physics and cosmology. It is these problems that help us navigate through the vastness of opportunities and select particulars for close analysis. They also limit the depth of the analysis, although many features of the objects we will study are of interest on their own. This particularly refers to instantons in theories of gravity, which are allowable for analytical treatment.

One type of classical configurations we are interested in is a regular bounce determining the semiclassical decay of false vacuum [16, 23]. In euclidean space, this solution describes a motion from a false vacuum to a region of true vacuum and back, hence the name. Our purpose here is to clarify some questions regarding metastability of the electroweak (EW) vacuum in different environments. This is the topic of the first part of the thesis, which comprises chapters 2 and 3.

The second part of the thesis includes chapters 4—9. There we study specific singular configurations in theories of one or two scalar fields and dynamical gravity. Our focus is on scale-invariant models and on the models where global scale symmetry is broken explicitly in the gravitational sector. Our goal is to use singular solutions to address the so-called hierarchy problem — a long-standing challenge of particle physics that concerns with the smallness of the ratio of the observed values of the EW and the Planck energy scales.⁴

²A regular solution of euclidean equations of motion with exactly one negative mode is also called a bounce [16].

³The content of the thesis is based on [19–22].

⁴Speaking more strictly, the problem is seen whenever an energy scale much above the EW scale appears, associated with particles that are coupled to the Higgs field; see chapter 4 and references therein.

Below we outline more specifically the questions addressed in the thesis. For convenience, the rest of this chapter is divided in two sections corresponding to the two parts of the thesis.

1.2 Introduction to part I

Part I of the thesis is dedicated to analyzing the lifetime of the EW vacuum in different settings. In the SM, the tree-level Higgs potential has an absolute minimum corresponding to this vacuum. It is known that quantum corrections modify the potential drastically through the Renormalization Group (RG) running of the Higgs quartic coupling λ [24–31], and a new minimum can develop at large energy scales, making the EW vacuum unstable.

The shape of the Higgs potential at large energy scales is very sensitive to the SM parameters and, in particular, to the Higgs mass m_H and the top quark mass m_t . At the moment, the largest uncertainty in the parameters of the potential is due to the uncertainties in top mass measurements [32]. The value of m_t is extracted from the Monte-Carlo analysis of decay products of the top quark, and it depends on the decay channels taken into account [33, 34]. Further uncertainties to the value of m_t come from theoretical analysis where they are related to the difference between the Monte-Carlo and the pole masses of the quark. These uncertainties leave the possibility for λ to stay positive all the way up to the Planck scale, in which case no second minimum appears [32]. However, for the current best-fit values of the SM parameters, λ crosses zero at the scale $\sim 10^{11}$ GeV, and reaches its negative minimum at the scale $\sim 10^{17}$ GeV [35, 36]. Hence, the possible metastability of the EW vacuum must be properly taken care of, and the question of whether its lifetime exceeds significantly the current age of the universe deserves a special attention.

The issue of stability of the EW vacuum attracts significant attention in recent studies. These include the investigation of the lifetime assuming no gravity and no physics beyond the SM [30, 31, 37], of gravitational and thermal corrections to the decay rate [38–41], investigation of vacuum stability in the different cosmological epochs [42–45] and in the presence of local inhomogeneities such as black holes [46–49]. In chapters 2 and 3 we contribute to this research by addressing two questions. Namely, in chapter 2, which follows [19], we study the EW vacuum stability during the inflationary period of the universe, and in chapter 3, based on [20], our concern is with the lifetime of the EW vacuum in a particular

theory extending the SM and General Relativity, known as the Higgs-Dilaton theory [50, 51].

1.3 Introduction to part II

In the second part of the thesis we suggest a fresh look at the hierarchy problem between the Fermi and the Planck scales. We ask if the observed smallness of the Higgs vacuum expectation value (vev), as compared to M_P , can be a manifestation of some non-perturbative effect relating the low-energy and the Planck-scale physics. This is a step out of the currently accepted paradigm which asserts that at low energies the theory must be organized so that the value of the EW scale is stable against modifications of the theory in the ultraviolet regime. This paradigm implies the necessity for new physics right above the EW scale [52], which goes in tension with the absence of its signatures at the LHC [53]. Confronted with this fact and with the success of the SM in describing the low-energy phenomena, we adopt the conjecture that no new physics interferes between the weak and the Planck scales and that the former is generated from the latter due to instanton effects.

In addressing the hierarchy problem, it is tempting to make use of the conformal symmetry [54]. Indeed, since at the classical level the SM Lagrangian acquires the conformal invariance (CI) once m_H is put to zero, one can imagine to start from the conformally-invariant classical SM which has no EW symmetry breaking and generate the Higgs mass due to the CI violation.

One of the possible ways to generate the Higgs mass within the CI setting is associated with quantum conformal anomaly (see, e.g., [55]). Indeed, the UV regularisation of renormalizable field theories necessarily introduces a parameter with the dimension of mass, which violates CI at the quantum level and thus makes it to be anomalous. As a result, the effective potential for the Higgs field, accounting for higher-order radiative corrections, may develop a minimum displaced from the origin, potentially leading to the vev of the Higgs field v small compared with M_P or the GUT scale [24, 56].

The Coleman-Weinberg (CW) scenario [24] in the SM can indeed be realised [26, 57, 58], but it leads to the Higgs and the top quark masses $m_H \simeq 7$ GeV and $m_t \lesssim 80$ GeV being far from those observed experimentally. If we take the physical values of dimensionless Higgs quartic coupling λ and top quark Yukawa

coupling y_t , the effective potential of the conformally-symmetric SM has a minimum around the QCD scale $\Lambda_{\text{QCD}} \sim 100$ MeV, associated with confinement and quark condensates [59], which is too far from the one realised in Nature. If the value of the top quark Yukawa coupling is smaller than some critical value, $y_t < y_{\text{crit}}$, this minimum is unique. For $y_t > y_{\text{crit}}$ yet another minimum is generated by the CW mechanism [60], with the vev $v \gtrsim M_P$, now many orders of magnitude larger than the EW scale. Due to the uncertainties discussed above, it is not known yet whether y_t is larger or smaller than y_{crit} , but in any event the predictions of the conformally-invariant SM are in sharp contrast with experiment.

In spite of this failure, the no-scale theories look very attractive and motivated many authors to search for different extensions of the SM, in which the mechanism may work and be phenomenologically acceptable. We mention just a few. The extended scalar sector was discussed on general grounds in [61], more recent works deal with the SM extended by right-handed neutrinos and a real scalar field [62], by an Abelian $B - L$ gauge field [63–65], or by non-abelian gauge groups [66, 67].

All considerations of the theories with CI up to date were carried out without gravity. There is a clear rationale for this, based on (nearly scale-invariant) perturbation theory [68]: any perturbative corrections to the effective potential of the Higgs field coming from gravity are suppressed by the Planck mass [69], and in the absence of heavy particles they are numerically small. In the SM, the largest contribution is of order $y_t^6 h^6 / M_P^2$, which is negligible at the weak scale.

We argue that, in fact, gravity is capable of generating a new mass scale of the order of v , but in a non-perturbative way. Non-perturbative effects can manifest themselves in various ways. As one example, they can be associated with a strong-coupling scale around which the content of a theory is reorganized and, in particular, the physical degrees of freedom are rearranged.⁵ Another possibility is provided by instantons that contribute to correlation functions of the theory and may eventually result in drastic changes in the low-energy observables.⁶

After all, it is not difficult to come to an idea that instantons or, more precisely, their large actions may somehow be involved in generating the hierarchy. To motivate this kind of reasoning, note that one can write

$$v \sim M_P e^{-\bar{W}} , \quad (1.1)$$

⁵For discussion of this possibility in context with the hierarchy problem see, e.g., [70].

⁶Perhaps, the most instructive example here is a discrete symmetry restoration in quantum mechanics of one dimension [71].

where, in order to match with experiment, one should take $\bar{W} \approx 37$. Eq. (1.1) gives a hint that the non-zero value of v could result from an exponentially strong suppression of the Planck scale via instanton effects. In turn, the Planck mass may stand explicitly in the gravitational Lagrangian or else appear, say, due to spontaneous breaking of global scale symmetry. The latter option points towards an interesting scenario in which one starts with the classically scale-invariant theory, generates classically the Planck scale, and then semiclassically — the EW scale in a natural way. In this thesis, we discuss the both scenarios.

The quantity \bar{W} can be viewed as resulting from a saddle-point approximation of some functional integral. At this point euclidean classical configurations come into play. As was mentioned before, part II of the thesis, which is based on [21, 22], is mostly devoted to analyzing these configurations in particular models and to the extent that allows to use them in deriving Eq. (1.1).

The plan of part II is the following. In chapter 4 more motivation to address the hierarchy problem with non-perturbative tools is given. There we also specify the framework in which the semiclassical analysis will be performed. Chapter 5 outlines a method that allows to endow Eq. (1.1) with the physical meaning. In chapter 6 we study instantons of a special type in a simple model that allows for analytical treatment of classical configurations. The results of these studies are used in chapters 7 and 8, where more realistic theories are considered and an implication for the hierarchy problem is provided. Chapter 9 contains a general discussion of the results and outlines future prospects. Finally, chapter 10 concludes the thesis.

Part I

On electroweak vacuum stability

Chapter 2

Electroweak vacuum stability during inflation

As was pointed out in introduction, in the SM framework and for the current best-fit values of the parameters, the Higgs field self-coupling λ changes sign at large RG scale $\mu_0 \sim 10^{11}$ GeV and reaches a negative minimum at $\mu_* \sim 10^{16} \div 10^{18}$ GeV, see Fig. 2.1 for illustration. It is worth stressing that this RG evolution is obtained under the assumption of no new physics interfering with the running of λ . As a result, the effective Higgs potential¹

$$V_h = \frac{\lambda(h)h^4}{4} \quad (2.1)$$

goes much below the EW vacuum at large values of the field, as shown schematically in Fig. 2.2. This makes the EW vacuum metastable.

While in a low density, low temperature environment characteristic of the present-day universe the SM vacuum is safely long-lived (see, e.g., [37]), the situation may be different during primordial inflation. Indeed, most inflationary models predict the Hubble expansion rate during inflation H_{inf} to be much higher than the measured Higgs mass. Thus, if the Higgs does not have any other couplings besides those present in SM, it behaves at inflation as an essentially massless field and develops fluctuations of order H_{inf} . Denote by h_{max} the value of h corresponding to the top of the barrier separating the EW vacuum from the runaway region. Then, even if h is originally placed close to the origin, it will roll beyond the barrier with order-one probability for $H_{inf} > h_{max}$ [42, 43, 73–76].

¹We neglect the SM mass term which is tiny compared to all contributions appearing below.

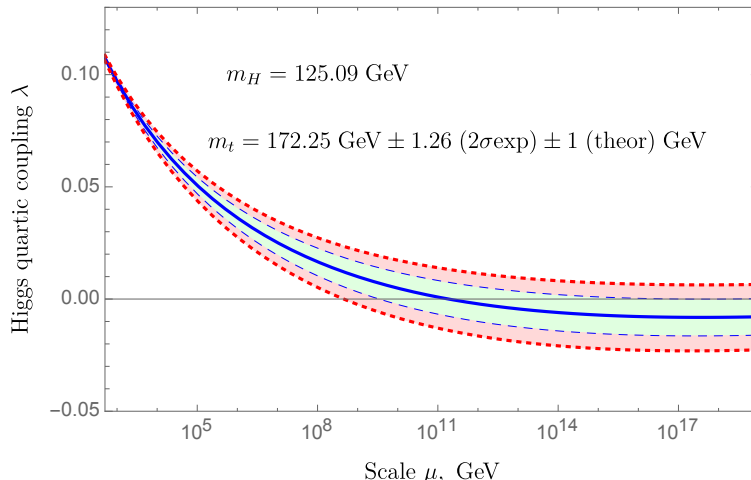


FIGURE 2.1: Running of the Higgs quartic coupling in the Standard Model at NNLO in the $\overline{\text{MS}}$ scheme. The RG equations are solved using the code based on [29, 72]. Blue solid line corresponds to the best-fit values of the Standard Model parameters [35, 36]. Blue dashed lines correspond to 2σ experimental uncertainty in the measurement of the top-quark mass [36] and red dotted lines — to the theoretical uncertainty discussed in [32].

A simple cure to the problem is to endow the Higgs with an effective mass $m_{eff} \gtrsim H_{inf}$ during the inflationary stage. This can be due, for example, to a non-minimal coupling to gravity², $V_{hR} = \xi R h^2/2$ [42, 77], or a coupling between h and the inflaton field³ ϕ of the form $V_{h\phi} = f(\phi)h^2/2$ [43, 74]. This raises the potential barrier and suppresses the over-barrier transitions. In this situation the EW vacuum is still able to decay via quantum tunneling.

Tunneling from a false vacuum in (quasi-) de Sitter spacetime can proceed in two distinct regimes: via the Hawking-Moss (HM) instanton [79] which describes quantum jumps on top of the potential barrier, or via Coleman-De Luccia (CDL) bounce [23] corresponding to genuinely under-barrier penetration. While HM transitions have been extensively discussed in connection with the Higgs behavior during inflation (see e.g. [42, 73, 75, 76]), the CDL tunneling is usually discarded with the common lore that it is sufficiently suppressed. However, the verification of this assertion was missing in the literature.⁴ Moreover, Ref. [73] which explicitly addressed this question had reported an opposite result that the CDL decay of the EW vacuum is enhanced, instead of being exponentially suppressed.

²We work in the signature $(-, +, +, +)$, so that the curvature of de Sitter space is positive, $R = 12H_{inf}^2$.

³We assume that the inflaton is distinct from the Higgs, unlike the case of Higgs inflation [78].

⁴Note that the thin-wall approximation, which is often invoked in the analysis of the CDL tunneling and which makes the exponential suppression manifest, is not applicable in the case of the Higgs field.

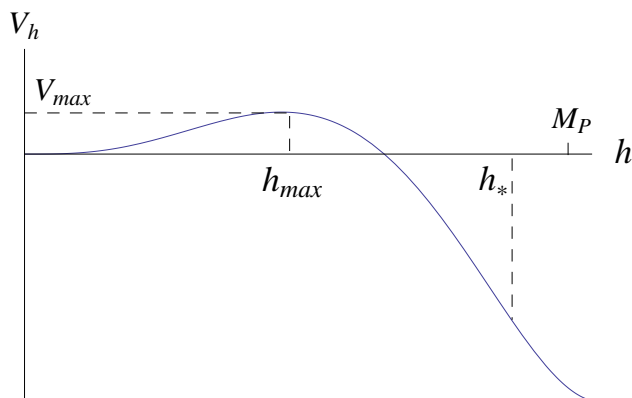


FIGURE 2.2: Schematic form of the effective Higgs potential (not to scale).

In this chapter we clarify the above issue. We will estimate the CDL tunneling rate and confirm that it is exponentially suppressed. The suppression exponent will be found to be essentially the same as in flat spacetime, up to small corrections which are estimated analytically.

2.1 Bounces in de Sitter space

In this section we assume that the energy density of the universe is dominated by the inflaton with negligible back-reaction of the Higgs field on the metric. The validity of this assumption will be discussed later. Then, neglecting the slow-roll corrections, we arrive to the problem of a false vacuum decay in external de Sitter spacetime. This process is described by the Euclidean version of the Higgs action

$$S_E = \int d^4x \sqrt{g_E} \left(\frac{1}{2} g_E^{\mu\nu} \partial_\mu h \partial_\nu h + V_h(h) \right), \quad (2.2)$$

where $g_{E\mu\nu}$ is the metric of a 4-dimensional sphere, which is the analytic continuation of the de Sitter metric [23] (see also [80]),

$$ds_E^2 = d\chi^2 + \rho^2(\chi) d\Omega_3^2, \quad \rho = \frac{1}{H_{inf}} \sin(H_{inf}\chi), \quad 0 \leq \chi \leq \frac{\pi}{H_{inf}}. \quad (2.3)$$

Here $d\Omega_3$ is the line element on a unit 3-sphere. We search for a smooth solution of the Higgs equations of motion following from Eq. (2.2). Assuming $O(4)$ symmetry, one reduces the action to

$$S_E = 2\pi^2 \int_0^{\pi/H_{inf}} d\chi \rho^3 \left(\frac{h'^2}{2} + V_h \right), \quad (2.4)$$

which yields the equation for the bounce $h_b(\chi)$,

$$h_b'' + 3H_{inf} \operatorname{ctg}(H_{inf}\chi) h_b' = \frac{dV_h}{dh}. \quad (2.5a)$$

To be regular, the solution must obey the boundary conditions,

$$h_b'(0) = h_b'(\pi/H_{inf}) = 0. \quad (2.5b)$$

The probability of false vacuum decay per unit time per unit volume scales as

$$\frac{dP}{dt d\mathcal{V}} \propto \exp(-S_E), \quad (2.6)$$

where the action is evaluated on the solution $h_b(\chi)$.

2.1.1 Hawking-Moss instanton

Equations (2.5) always have a constant solution with the Higgs field sitting on top of the potential barrier, $h_b = h_{max}$ (see Fig. 2.2). This instanton can be interpreted as describing the over-barrier jumps of the Higgs field due to non-zero de Sitter temperature, $T_{dS} = H_{inf}/(2\pi)$ [81]. The rate of such transitions is given by Eq. (2.6) with the action

$$S_E^{(HM)} = \frac{8\pi^2 V_{max}}{3 H_{inf}^4}. \quad (2.7)$$

The transition rate is exponentially suppressed if $H_{inf} \lesssim V_{max}^{1/4}$. In the pure SM $V_{max}^{1/4}$ is of order 10^9 GeV [30] implying that the EW vacuum is stable with respect to HM transitions whenever $H_{inf} < 10^9$ GeV and unstable otherwise. In the latter case new contributions into the Higgs potential that raise V_{max} are required to stabilize the SM vacuum. A simple option is to endow h with an effective mass m_{eff} during inflation. The potential becomes

$$V_h = \frac{\lambda(h) h^4}{4} + \frac{m_{eff}^2 h^2}{2}. \quad (2.8)$$

For $H_{inf} \gtrsim 10^{10}$ GeV the qualitative picture is captured by neglecting the slow logarithmic dependence of the coupling on the field and normalizing it at a fixed scale above μ_0 , so that λ is negative and is of order 0.01 in the absolute value. This gives for the position and height of the potential barrier,

$$h_{max} = \frac{m_{eff}}{\sqrt{|\lambda|}}, \quad V_{max} = \frac{m_{eff}^4}{4|\lambda|} \quad (2.9)$$

leading to the instanton action,

$$S_E^{(HM)} = \frac{8\pi^2}{3|\lambda|} \left(\frac{m_{eff}}{H_{inf}} \right)^4. \quad (2.10)$$

As expected, the transitions are strongly suppressed provided the mass is bigger than $|\lambda|^{1/4} H_{inf}$. Note that for these values of the mass h_{max} lies above μ_0 , which justifies our approximation of constant negative λ . For the case when the Higgs mass is due to non-minimal coupling to gravity one has $m_{eff}^2 = 12\xi H_{inf}^2$, so that the suppression (2.10) does not depend on the Hubble parameter and is large already for $\xi \gtrsim 0.1$ [42, 77, 82].

2.1.2 Coleman-De Luccia bounce

Another decay channel is described by inhomogeneous solutions of Eq. (2.5) which interpolate between the false vacuum and a value h_* in the run-away region. These correspond to genuinely under-barrier tunneling. To understand their properties, let us first neglect the running of λ normalizing it at a high enough scale, so that $\lambda < 0$. If we further neglect the mass and spacetime curvature, we obtain the setup of tunneling from the top of an inverted quartic potential in flat space. This is described by a family of bounces,

$$h_{\bar{\chi}}(\chi) = \sqrt{\frac{8}{|\lambda|}} \frac{\bar{\chi}}{\chi^2 + \bar{\chi}^2}, \quad (2.11)$$

parameterized by their size $\bar{\chi}$. The action of these solutions is independent of $\bar{\chi}$ due to the classical scale invariance of the setup,

$$S_E = \frac{8\pi^2}{3|\lambda|}. \quad (2.12)$$

The mass and finite Hubble rate break the degeneracy. Assuming that the size of the instanton is small compared to the length

$$l = \min(m_{eff}^{-1}, H_{inf}^{-1}) \quad (2.13)$$

characterizing the breaking of scale symmetry, one can estimate the corrections to the bounce action perturbatively. Substituting Eq. (2.11) into Eq. (2.4) and expanding to the order $O((l/\bar{\chi})^2)$ we obtain,

$$S_E^{(CDL)}(\bar{\chi}) = \frac{8\pi^2}{3|\lambda|} \left[1 + 3(m_{eff}^2 - 2H_{inf}^2)\bar{\chi}^2 \log(l/\bar{\chi}) \right], \quad (2.14)$$

where we have kept only the log-enhanced contributions. The tunneling rate is given by the configuration minimizing the action. If the minimal suppression is reached at the configuration of zero size⁵, $\bar{\chi} = 0$, and coincides with the flat-space result (2.12). One observes that in this case the assumption $\bar{\chi} \ll l$ is justified. In the opposite case, $m_{eff}^2 < 2H_{inf}^2$, the correction due to the expansion of the universe dominates and makes the solution spread over the whole 4-sphere. We have checked numerically that the only solution in this case is the HM instanton.

We now restore the running of couplings which provides additional source of the scale invariance breaking. This enters into the calculations through the loop corrections in the instanton background. For instantons of the size smaller than l these corrections can be evaluated neglecting both the mass m_{eff} and the Hubble H_{inf} . Thus, they are the same as in the flat space [84] and roughly amount to substituting in Eq. (2.14) the coupling constant evaluated at the scale of inverse instanton size, $\mu = \bar{\chi}^{-1}$. Numerically, for the best-fit values of the SM parameters, this dependence on $\bar{\chi}$ turns out to be much stronger than the one introduced by the effective mass and the Hubble expansion. This freezes the size of the instanton at the value corresponding to the minimum of the running coupling constant, $\bar{\chi}_*^{-1} \approx \mu_* \sim 10^{16} \div 10^{18}$ GeV. The total answer for the suppression is then given by Eq. (2.14) evaluated at $\bar{\chi}_*$. The corrections due to m_{eff} and H_{inf} are small as long as⁶ $m_{eff}, H_{inf} \lesssim 10^{15} \div 10^{17}$ GeV.

2.2 Discussion of approximations

We have obtained Eq. (2.14) under the assumption that the transition happens in an external de Sitter spacetime. Let us check its validity. First, the Hubble rate during inflation is not exactly constant, but slowly varies. We have seen that the size of the bounce is much smaller than the horizon size. This implies that the formation of the bubble of the new phase inside the false vacuum occurs very fast⁷. Thus neglecting the change in the Hubble rate during the formation of the bubble is justified.

Second, in the case when the effective Higgs mass is given by the coupling to the inflaton, the Higgs exerts a force on the inflaton during tunneling. This force

⁵A proper interpretation of this singular bounce is given within the formalism of constrained instantons [83].

⁶The bound on the primordial tensor perturbations [85] constrains $H_{inf} \lesssim 10^{14}$ GeV during last ~ 60 e-folds of inflation.

⁷The time of the bubble formation should not be confused with the vacuum decay time, which is exponentially long.

should not lead to large displacements of ϕ that could change its energy density. One estimates the shift of ϕ due to the Higgs force as

$$\square\delta\phi = \frac{h^2}{2} \frac{dm_{eff}^2}{d\phi} \implies \delta\phi \sim \frac{h_*^2}{H^2} \frac{dm_{eff}^2}{d\phi}, \quad (2.15)$$

where \square stands for the Laplacian on the 4-sphere and $h_* = \sqrt{8/|\lambda(\bar{\chi}_*^{-1})|} \bar{\chi}_*^{-1}$ is the value of the Higgs in the center of the instanton. Requiring $V'_{inf}\delta\phi \ll V_{inf}$ we obtain the condition

$$\frac{dm_{eff}^2}{d\phi} \ll \frac{V'_{inf}}{6\epsilon h_*^2}, \quad (2.16)$$

where $\epsilon = (M_p V'_{inf})^2 / (16\pi V_{inf}^2)$ is the slow-roll parameter. This condition is satisfied if the dependence of m_{eff} on the inflaton is weak enough.

Last, but not least, one should check if the energy density of the Higgs field is smaller than that of the inflaton. This requirement turns out to be violated in the center of the CDL bounce for realistic values of H_{inf} . What saves the day is the fact that the size of the region where this violation occurs is of order $\bar{\chi}_*$. On the other hand, the log-enhanced corrections in Eq. (2.14) come from the region of order $\sim l$, which is much larger. Thus they are not modified by the back-reaction of the Higgs field on the geometry.

The effects of the back-reaction can be taken into account neglecting completely the inflaton energy density, i.e. in the same way as in the case of the false vacuum decay in the flat space [38, 40, 41]. They give an additional contribution to the bounce action⁸,

$$\Delta S_E^{(CDL)} = \frac{256\pi^3(1-6\xi)^2}{45(M_p\bar{\chi}\lambda)^2}. \quad (2.17)$$

For moderate values of ξ these corrections are small as long as $\bar{\chi}_*^{-1} < 5 \cdot 10^{16}$ GeV. Finally, further corrections to the bounce action can come from Planck-suppressed higher-order operators in the Higgs action. The analysis of these corrections is the same as in flat spacetime. Note that they can be quite significant due to the fact that the size of the instanton is close to Planckian [86].

⁸Here we assume that gravity is described by Einstein's general relativity at least up to the scale $\bar{\chi}^{-1}$.

Chapter 3

Bounce in the Higgs-Dilaton theory

The Higgs-Dilaton theory was introduced in [87] and studied in detail in [50, 51]. It is an effective field theory whose properties allow to account for many issues in particle physics and cosmology, which still lack of the complete explanation. For example, it makes a step towards the solution of the hierarchy problem by reformulating the latter in terms of dimensionless quantities. This is achieved by demanding the theory to be scale-invariant both at classical and perturbative quantum levels.¹ All scales are hence generated dynamically. Next, it is able to provide us with a plausible cosmological scenario, including inflation, dark matter and dark energy domination epochs of the universe. Hence, the theory is phenomenologically acceptable in a wide range of scales.

Further tests of viability of the Higgs-Dilaton theory include the question of whether the EW vacuum in this setting is sufficiently safe compared to the case of SM. In this chapter, we answer the question by considering the decay rate of the EW vacuum in the present-day universe,²

$$\Gamma = Ae^{-B}, \quad B = S_E(\text{bounce}) - S_E(FV). \quad (3.1)$$

In this formula $S_E(\text{bounce})$ is an euclidean action of the theory computed on a bounce solution interpolating between the EW vacuum and the true vacuum region, $S_E(FV)$ is an euclidean action of the EW vacuum, and A is a prefactor. Below we will mainly focus on computing the exponential coefficient B . The SM

¹Such scale-invariant scalar-tensor theories are discussed in detail in chapter 8.

²Unlike the situation considered in chapter 2, in the Higgs-Dilaton theory the Higgs field is responsible for inflation and there appears no question with vacuum stability during that period; see also [88].

vacuum decay rate prefactor was computed in flat space [37, 89], and we take this result as an approximation of the prefactor in the Higgs-Dilaton theory; see also section 3.3. We will find that in a wide range of parameters of the theory, the tunneling probability is safely small. Moreover, the decay rate is suppressed significantly compared to the SM case. The conclusion is that the features of the Higgs-Dilaton theory lead to additional stabilization of the false vacuum.

We start in section 3.1 with a brief overview of the Higgs-Dilaton theory, aiming to fix the notation and to introduce a particular set of field coordinates in which it is convenient to perform the analysis of classical solutions of euclidean equations of motion. In section 3.2 we first study the bounce analytically, and then find it numerically and compute B at different values of the parameters. We discuss our findings and some properties of the bounce in section 3.3. Finally, in section 3.4 the results are summarized.

3.1 Review of the Higgs-Dilaton theory

The Higgs-Dilaton theory is a moderate extension of the SM and General Relativity that possesses no dimensional parameters at the classical level. The attractiveness of the theory is due to its ability to explain certain cosmological observations as well as to provide some input into theoretical puzzles of particle physics. In particular, as we will see shortly, scale symmetry allows to reformulate the hierarchy problem in terms of dimensionless quantities. The theory naturally incorporates the Higgs inflation scenario [90–92], hence it predicts a successful inflationary period followed by a graceful exit to the hot Big Bang theory.

The theory contains Higgs ϕ and dilaton χ fields coupled to gravity in a non-minimal way and the rest of the SM content unchanged. The presence of the massless dilaton is necessary for the model to match observational data [50]. The fields ϕ and χ are allowed to interact in the way that preserves the scale symmetry. The Higgs-Dilaton sector of the theory is written as ³

$$\frac{\mathcal{L}_{\chi,\phi}}{\sqrt{-g}} = \frac{1}{2}(\xi_\chi \chi^2 + 2\xi_h \phi^\dagger \phi)R - \frac{1}{2}(\partial\chi)^2 - \frac{1}{2}(\partial\phi)^2 + V(\chi, \phi^\dagger \phi), \quad (3.2)$$

³We do not take into account possible boundary terms, since they do not affect the action of the bounce solution [93] (see also [94]).

where $(\partial\phi)^2 \equiv \nabla_\mu\phi\nabla^\mu\phi^*$ and the potential is given by

$$V(\chi, \phi^\dagger\phi) = \lambda \left(\phi^\dagger\phi - \frac{\alpha}{2\lambda}\chi^2 \right)^2 + \beta\chi^4. \quad (3.3)$$

The full Lagrangian of the theory is obtained from Eq. (3.2) by supplementing the latter with the rest of the SM fields. As we will see, the bounce solution is built from the metric and the two scalars; hence, one can ignore the presence of other degrees of freedom when computing the decay rate in the leading-order semiclassical approximation.

Matching predictions of the theory with observations constrains possible values of its parameters. In particular, the non-minimal couplings ξ_χ and ξ_h are restricted by inflationary data. Specifically, they are bounded from measurements of the amplitude and the tilt of the primordial scalar spectrum. In Fig. 3.1 the allowable region for ξ_χ and ξ_h is shown, according to [50]. The precise form of this region depends on details of post-inflationary processes; however, in any case

$$\xi_\chi \ll 1 \ll \xi_h. \quad (3.4)$$

The parameters α , β and λ in the potential (3.3) determine the low-energy physics around the ground state of the theory. The latter is specified by constant values of the dilaton and Higgs fields, $(\chi_0, h_0)^T$, where χ_0 can be chosen arbitrarily and

$$h_0^2 = \frac{\alpha}{\lambda}\chi_0^2 + \frac{\xi_h}{\lambda}R, \quad R = \frac{4\beta\lambda\chi_0^2}{\lambda\xi_\chi + \alpha\xi_h}. \quad (3.5)$$

The values of α and β are converted into the ratios between different scales present in the SM and gravity. For example, exploiting the ratio between the Higgs and Planck masses, one obtains⁴

$$m_H^2 \sim \frac{\alpha M_P^2}{\xi_\chi} \quad \Rightarrow \quad \alpha \sim 10^{-34}\xi_\chi, \quad (3.6)$$

where the Planck mass is defined as

$$M_P^2 \equiv \xi_\chi\chi_0^2 + \xi_h h_0^2. \quad (3.7)$$

⁴In this and the following estimates we take λ equal its low-energy value, $\lambda \sim 10^{-1}$, and assume the cosmological constant to be sufficiently small.

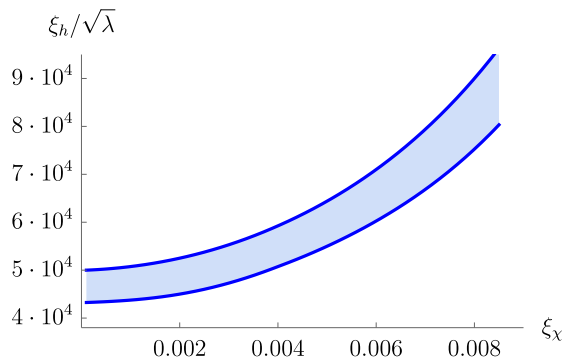


FIGURE 3.1: The parameter region for which the amplitude and the tilt of the scalar spectrum lie in the observationally allowed region, see [50] for details.

For the hierarchy between the Planck scale and the observed value of the cosmological constant Λ , we have

$$\Lambda \sim \frac{\beta M_P^4}{\xi_\chi^2} \Rightarrow \beta \sim 10^{-56} \alpha^2. \quad (3.8)$$

We see that the constraints (3.6) and (3.8) both involve big numbers. They are nothing but reformulations in the Higgs-Dilaton setting of the hierarchy problem and the cosmological constant problem accordingly.

For our purposes, one can safely neglect contributions from the terms $\propto \chi^2 \phi^2$ and $\propto \chi^4$ and set $\alpha = \beta = 0$. Indeed, such approximation is clearly applicable as long as $\lambda |\varphi|^2 \gg \alpha M_P^2$. However, as will be shown later, the contribution to the decay exponent from the region of $|\varphi|$ where this condition violates is itself negligible if Eqs. (3.4), (3.6) and (3.8) are satisfied. Hence, the approximation is justified for all values of $|\varphi|$. Choosing the unitary gauge for the Higgs field, $\varphi^T = (0, h/\sqrt{2})$, we rewrite the potential (3.3) as follows,

$$V(h) = \frac{\lambda}{4} h^4. \quad (3.9)$$

Finally, the euclidean form of the Lagrangian (3.2) is written as

$$\frac{\mathcal{L}_{\chi,h,E}}{\sqrt{g}} = -\frac{1}{2}(\xi_\chi \chi^2 + \xi_h h^2)R + \frac{1}{2}(\partial h)^2 + \frac{1}{2}(\partial \chi)^2 + V(h). \quad (3.10)$$

Whenever non-minimal couplings of scalar fields to gravity are non-zero, one can perform the metric redefinition

$$\tilde{g}_{\mu\nu} = \Omega^2 g_{\mu\nu} \quad (3.11)$$

to rewrite a theory in the form in which such couplings are absent. This form is referred to as the Einstein (E)-frame, while the original Lagrangian (3.2) is said to be written in the Jordan (J)-frame.⁵ To arrive at the E-frame, the conformal factor Ω^2 has to be chosen as

$$\Omega^2 = M_P^{-2}(\xi_h h^2 + \xi_\chi \chi^2). \quad (3.12)$$

Making use of the standard relations between the J- and E-frames [96],

$$\sqrt{g} = \Omega^{-4} \sqrt{\tilde{g}}, \quad R = \Omega^2(\tilde{R} + 6\tilde{\square} \log \Omega - 6\tilde{g}^{\mu\nu} \partial_\mu \log \Omega \partial_\nu \log \Omega), \quad (3.13)$$

one obtains the following Lagrangian,

$$\frac{\mathcal{L}_E}{\sqrt{\tilde{g}}} = -\frac{M_P^2}{2} \tilde{R} + \frac{1}{2} \tilde{K}(h, \chi) + \tilde{V}(h, \chi). \quad (3.14)$$

The kinetic term \tilde{K} has a non-canonical form,

$$\tilde{K}(h, \chi) = \gamma_{ij} \tilde{g}^{\mu\nu} \partial_\mu \phi^i \partial_\nu \phi^j, \quad (3.15)$$

where we have introduced the notation $(\phi^1, \phi^2) \equiv (h, \chi)$. The quantity γ_{ij} can be interpreted as a metric in the two-dimensional field space spanned by h and χ , in the E-frame. It is given by

$$\gamma_{ij} = \frac{1}{\Omega^2} \left(\delta_{ij} + \frac{3}{2} M_P^2 \frac{\partial_i \Omega^2 \partial_j \Omega^2}{\Omega^2} \right). \quad (3.16)$$

Finally, the transformed potential is written as

$$\tilde{V}(h, \chi) = \frac{V(h)}{\Omega^4}. \quad (3.17)$$

We now look for further redefinition of the fields of the theory, aiming to recast the field space metric (3.16) into a diagonal form. To this end, we exploit the scale symmetry of the model. Consider the infinitesimal scale transformation of the fields in the E-frame,

$$\tilde{g}_{\mu\nu} \rightarrow \tilde{g}_{\mu\nu}, \quad \phi^i \rightarrow \phi^i + \sigma \Delta \phi^i, \quad (3.18)$$

⁵The scalar-tensor theories, related to each other by a transformation of the form (3.11), are classically equivalent. For discussion of their equivalence at the quantum level see, e.g, [95].

where σ is a small constant. The current corresponding to this transformation reads as follows,

$$\tilde{J}^\mu = \frac{1}{\sqrt{\tilde{g}}} \frac{\partial \mathcal{L}_E}{\partial \partial_\mu \phi^i} \Delta \phi^i = \tilde{g}^{\mu\nu} \frac{M_P^2}{2(\xi_\chi \chi^2 + \xi_h h^2)} \partial_\nu ((1 + 6\xi_\chi) \chi^2 + (1 + 6\xi_h) h^2). \quad (3.19)$$

Following [50], we introduce a new set of variables $(\phi'^1, \phi'^2) \equiv (\rho, \theta)$ that transform under the scale transformations as

$$\rho \rightarrow \rho + \sigma M_P, \quad \theta \rightarrow \theta. \quad (3.20)$$

Due to the scale symmetry, the field ρ can only enter the Lagrangian through its derivatives. Requiring the metric γ'_{ij} corresponding to the fields (ρ, θ) to be diagonal, we have

$$\tilde{J}^\mu = M_P \tilde{g}^{\mu\nu} \gamma'_{\rho\rho} \partial_\nu \rho. \quad (3.21)$$

Comparing the currents (3.19) and (3.21), we deduce the following expression for ρ ,

$$\rho = \frac{M_P}{2} \log \left(\frac{(1 + 6\xi_\chi) \chi^2 + (1 + 6\xi_h) h^2}{M_P^2} \right). \quad (3.22)$$

One observes that ρ can be viewed as a radial coordinate in the field space spanned by the vectors $\sqrt{1 + 6\xi_\chi} \chi$ and $\sqrt{1 + 6\xi_h} h$. We can choose θ to be an angular coordinate in this space, that is

$$\theta = \arctan \left(\sqrt{\frac{1 + 6\xi_h}{1 + 6\xi_\chi}} \frac{h}{\chi} \right). \quad (3.23)$$

By construction, θ does not transform under the scale transformations, in agreement with Eq. (3.20). In terms of θ and ρ , the Lagrangian (3.14) is written as

$$\frac{\mathcal{L}_E}{\sqrt{g}} = -\frac{M_P^2}{2} \tilde{R} + \frac{a(\theta)}{2} (\partial\rho)^2 + \frac{b(\theta)}{2} (\partial\theta)^2 + \tilde{V}(\theta), \quad (3.24)$$

with the potential

$$\tilde{V}(\theta) = \frac{\lambda}{4\xi_h^2} M_P^4 \left(\frac{1}{1 + \varsigma \cot^2 \theta} \right)^2, \quad (3.25)$$

where

$$a(\theta) = \frac{1 + 6\xi_h}{\xi_h} \frac{1}{\sin^2 \theta + \varsigma \cos^2 \theta}, \quad b(\theta) = \frac{M_P^2 \varsigma}{\xi_\chi} \frac{\tan^2 \theta + \xi_\chi / \xi_h}{\cos^2 \theta (\tan^2 \theta + \varsigma)^2}, \quad (3.26)$$

and

$$\varsigma = \frac{(1 + 6\xi_h) \xi_\chi}{(1 + 6\xi_\chi) \xi_h}. \quad (3.27)$$

We see that the fields ρ and θ are almost decoupled, and, what is more important, the potential \tilde{V} depends on θ only. This simplifies significantly the study of euclidean classical solutions in the theory.

3.2 Bounce in the Higgs-Dilaton theory

3.2.1 Equations of motion and boundary conditions

Since we study vacuum decay in the homogeneous and isotropic environment, one can assume the bounce to be $O(4)$ -symmetric.⁶ Hence, the following ansatz for the metric can be chosen,

$$d\tilde{s}^2 = f^2(r)dr^2 + r^2d\Omega_3^2, \quad (3.28)$$

where r is a radial coordinate, and $d\Omega_3^2$ denotes the line element of a unit 3-sphere. As we will see shortly, this somewhat nonstandard form of the ansatz results in a particular simple form of the Einstein equations.

In what follows, we neglect spacetime curvature arising due to non-zero cosmological constant Λ_0 and assume that the false vacuum geometry is flat. As will be shown later, this is a reasonable approximation as long as $m_H \gg \Lambda_0^{1/4}$. In this case, the function f is required to approach the flat space limit at infinity and the euclidean anti-de Sitter limit at the origin. The scalar fields ρ and θ are required to have a good behavior at infinity, in order to ensure the finiteness of the action, and to be regular at the origin.

Applying the ansatz (3.28) to the equations of motion following from the Lagrangian (3.24), one finds,

$$\rho' = C \cdot \frac{f}{a(\theta)r^3}, \quad (3.29)$$

with C some constant. It is easy to make sure that the requirement for θ to approach a finite true vacuum value θ_0 at the origin is not satisfied whenever $C \neq 0$. Hence, the tunneling solution must obey $\rho = \rho_0 = \text{const}$, and the value of ρ_0 is fixed by the false vacuum state, $h_{FV} = 0$, $\chi_{FV} = M_P/\sqrt{\xi_\chi}$ [50].⁷ From Eq. (3.22) we have

$$\rho_0 = \frac{M_P}{2} \log \left(\frac{1 + 6\xi_\chi}{\xi_\chi} \right). \quad (3.30)$$

⁶Although it was proven that the solution of maximal symmetry dominates the transition amplitude in flat space background [97, 98], no such proof is known in the case when gravity dynamics is included.

⁷We neglect corrections due to non-zero α and β .

Under the conditions (3.28) and (3.30), the equations of motion become

$$2rf^3\tilde{V}'(\theta) + 2rb(\theta)f'\theta' - f(rb'(\theta)\theta'^2 + 2b(\theta)(3\theta' + r\theta'')) = 0, \quad (3.31)$$

$$2f^2(3M_P^2 - r^2\tilde{V}(\theta)) = 6M_P^2 - r^2b(\theta)\theta'^2. \quad (3.32)$$

As a consequence of the choice of ansatz (3.28), the 00-component of the Einstein equations is reduced to Eq. (3.32) which is algebraic with respect to f .

The system (3.31), (3.32) is to be solved numerically. However, before plunging into numerics, it is useful to understand analytically qualitative behavior and asymptotic properties of the bounce. We proceed to this below.

3.2.2 Running couplings

Let us pause here and discuss quantum corrections to the Higgs-Dilaton Lagrangian (3.2). We choose to regularize the theory in the way that makes all loop diagrams finite and all symmetries of the classical action intact. Note that the Higgs-Dilaton theory is not renormalizable [51] (see also [99]), hence an infinite number of counter-terms with the structure different from that appearing in Eq. (3.2) is required to be added at the quantum level. Non-renormalizability of the theory does not pose a principal obstacle to its quantization, but its UV behavior cannot be uniquely fixed by the initial classical Lagrangian. The ambiguity in the choice of a set of subtraction rules is not fully removable, since it reflects our ignorance about the proper set of rules established by the unknown UV completion of the theory. Nevertheless, the underlying assumptions about the full theory, including the symmetry arguments, can constrain significantly the set of possible renormalization prescriptions.

With the aim to preserve *explicitly* the scale symmetry of the theory (3.2) at the perturbative quantum level, a scale-invariant renormalization procedure was developed in [100] (see also [101] for the original suggestion and [102–104] for further developments). It is based on dimensional regularization. The use of the latter is motivated by the well-known fact that loop corrections computed within this scheme are polynomial in masses and coupling constants [105]. This means, in particular, that in the absence of heavy particle's mass thresholds no large corrections to the Higgs mass are generated.

As an example, consider the renormalization of the Higgs quartic coupling λ . In d dimensions, one has

$$\lambda = \mu^{2\epsilon} \left(\tilde{\lambda} + \sum_{n=1}^{\infty} \frac{a_n}{\epsilon^n} \right), \quad d = 4 - 2\epsilon, \quad (3.33)$$

where by $\tilde{\lambda}$ we denote the dimensionless finite coupling, μ is a 't Hooft-Veltman normalization point [68] with the dimension of energy, and the series in ϵ corresponds to counter-terms. We now replace the scale μ by a field-dependent normalization point,

$$\mu^2 = F(\chi, h) \hat{\mu}^2. \quad (3.34)$$

The function F reflects the particular choice of the renormalization prescription and leads to different physical results, while the dimensionless parameter $\hat{\mu}$ plays the role of the usual choice of momentum scale in the RG equations and should disappear in the final result. The scheme (3.34) is manifestly scale-invariant, as soon as μ depends only on the fields h, χ . A change of the choice of the function F can be compensated by the change of the classical Lagrangian by adding a specific set of higher-dimensional operators.

One of the most natural possibilities in choosing F is to identify μ with the gravitational cutoff in the J-frame,

$$\mu_I \sim \xi_\chi \chi^2 + \xi_h h^2. \quad (3.35)$$

Another option is to choose the scale-invariant direction along the dilaton field, i.e.,

$$\mu_{II} \sim \xi_\chi \chi^2. \quad (3.36)$$

To test the ability of the Higgs-Dilaton model to describe correctly the inflationary physics, the careful analysis of the quantum corrections to the potential (3.9) during inflation is needed. Such analysis was performed in [51]. It was shown that at one-loop level the leading contribution to the potential is given by

$$\Delta V = -\frac{3m_t^4}{16\pi^2} \left(\log \frac{m_t^2}{\mu^2} - \frac{3}{2} \right), \quad (3.37)$$

where $m_t^2 = y_t^2 h^2/2$ stands for the effective top quark mass in the J-frame. It is convenient to fix the value of $\hat{\mu}$ such that the logarithmic contribution (3.37) is minimized for each value of h , $\hat{\mu}^2 \simeq \frac{y_t^2}{2} \frac{h^2}{F(h, \chi)/M_P^2}$. Depending on the choice of

the normalization point $\mu_{I,II}$, this gives,

$$\hat{\mu}_I^2(h, \chi) = \frac{y_t^2}{2} \frac{M_P^2 h^2}{\xi_h h^2 + \xi_\chi \chi^2}, \quad \hat{\mu}_{II}^2(h, \chi) = \frac{y_t^2}{2} \frac{M_P^2 h^2}{\xi_\chi \chi^2}. \quad (3.38)$$

Finally, we rewrite the expressions above in terms of the ‘‘polar’’ variables ρ and θ to obtain

$$\hat{\mu}_I^2(\theta) = \frac{y_t^2 M_P^2}{2\xi_h} \frac{1}{1 + \zeta \cot^2 \theta}, \quad \hat{\mu}_{II}^2(\theta) = \frac{y_t^2 M_P^2}{2\xi_h \varsigma} \cot^2 \theta \quad (3.39)$$

with ς given in Eq. (3.27). In accordance with the chosen regularization scheme, the momentum scale depends only on the scale-invariant quantity θ . The RG enhanced potential for the field θ is given by Eq. (3.25) with λ replaced by the running coupling $\lambda(\hat{\mu}_{I,II}(\theta))$.⁸

3.2.3 Effective potential

To get an insight into qualitative properties of the bounce, it is useful to rewrite the solution $\rho = \rho_0$, $\theta = \theta_b(r)$ in terms of the original variables h and χ . From Eq. (3.22) we obtain the relation between h_b and χ_b ,

$$(1 + 6\xi_\chi)\chi_b^2 + (1 + 6\xi_h)h_b^2 = M_P^{*2}, \quad M_P^* = M_P \sqrt{\frac{1 + 6\xi_\chi}{\xi_\chi}}. \quad (3.40)$$

One observes that the bounce trajectory draws a circle in the field space spanned by the vectors $\sqrt{1 + 6\xi_\chi}\chi$ and $\sqrt{1 + 6\xi_h}h$, as shown in Fig. 3.2. The relation (3.40) allows us to study the bounce using a single variable which is chosen to be h_b . Using Eqs. (3.40) and (3.23), one finds the relation between h_b and θ_b ,

$$h_b = \frac{M_P^*}{\sqrt{1 + 6\xi_h}} \sin \theta_b. \quad (3.41)$$

By definition (3.23), θ_b is confined in the interval $0 \leq \theta_b \leq \frac{\pi}{2}$. This condition, seeming obscuring in the polar field variables, becomes clear if we write it in terms of h_b ,

$$0 \leq h_b \leq \frac{M_P^*}{\sqrt{1 + 6\xi_h}}, \quad (3.42)$$

where it is seen to be the consequence of Eq. (3.40). The inequality (3.42) imposes a nontrivial constraint on the magnitude h_0 of the bounce. We will say more about this below.

⁸It what follows, we neglect the running of the non-minimal couplings ξ_h , ξ_χ . Such approximation is fair provided that the values of the couplings are far from the conformal limit.

Using Eqs. (3.25) and (3.40), one obtains the effective potential for the bounce,

$$V_{eff} = \frac{\lambda(\hat{\mu}(h_b))}{4} \left(\frac{1}{M_P^2} \frac{\xi_h - \xi_\chi}{1 + 6\xi_\chi} + \frac{1}{h_b^2} \right)^{-2}. \quad (3.43)$$

One minimum of this potential is achieved at $h_b = 0$, in accordance with the false vacuum solution $\theta_{FV} = 0$ of the equation of motion (3.31).⁹ Another, deeper minimum develops whenever $\lambda(\hat{\mu}_{I,II}(h_b))$ crosses zero at some energy scale h_* . Note also that, as long as the conditions (3.4) are fulfilled, the potential (3.43) possesses no singular points.

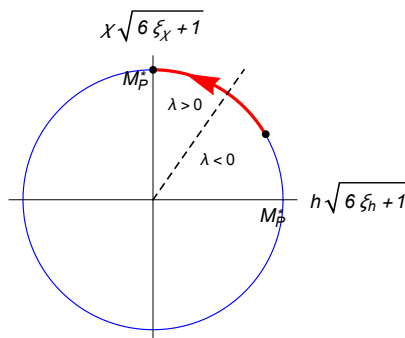


FIGURE 3.2: The bounce configuration in terms of the Higgs (h) and dilaton (χ) fields. The arrow points the direction in which r grows.

Now we would like to investigate how variations of different couplings, that are present in the potential (3.43), affect the decay rate (3.1). Presumably, the strongest effect on the bounce is caused by the variation of the Higgs quartic coupling $\lambda(\hat{\mu})$. For this reason, below we choose different values of the top quark mass m_t — the ones lying in the 1σ experimental uncertainty region according to [36]. However, the effect caused by the variation of m_t is well-known in the SM case, and we do not expect it to change much in the Higgs-Dilaton theory.

Next, we turn to the non-minimal couplings ξ_h and ξ_χ . We ask what the signs of variations $\frac{\delta B}{\delta \xi_h}$ and $\frac{\delta B}{\delta \xi_\chi}$ are in the cases when the normalization prescriptions (3.39) are implemented.

Prescription I. As will be seen later from numerics, under the conditions (3.4) the magnitude of the bounce satisfies

$$\frac{h_0^2 \xi_h}{M_P^2} \ll 1. \quad (3.44)$$

⁹We neglect corrections due to the non-zero vacuum expectation value of the Higgs field.

Then, using Eq. (3.41), one expresses the normalization point $\hat{\mu}_I$ through h_b as follows,

$$\hat{\mu}_I^2(h_b) = \frac{y_t^2 h_b^2}{2} \left(1 - \frac{\xi_h - \xi_\chi}{1 + 6\xi_\chi} \frac{h_b^2}{M_P^2} + O\left(\frac{h_b^4 \xi_h^2}{M_P^4}\right) \right). \quad (3.45)$$

If $h_* \ll h_0$, one expects the dominant contribution to the bounce action coming from the region of r at which the bounce solution is determined mainly by the behavior of the effective potential V_{eff} at large h_b . Hence, the variation of B is determined by the variation of the asymptotics of V_{eff} . From Eqs. (3.43) and (3.45) we have,

$$\frac{\delta|V_{eff}|}{\delta\xi_h} < 0, \quad \frac{\delta|V_{eff}|}{\delta\xi_\chi} > 0, \quad (3.46)$$

from which it follows that

$$\frac{\delta B}{\delta\xi_h} > 0, \quad \frac{\delta B}{\delta\xi_\chi} < 0. \quad (3.47)$$

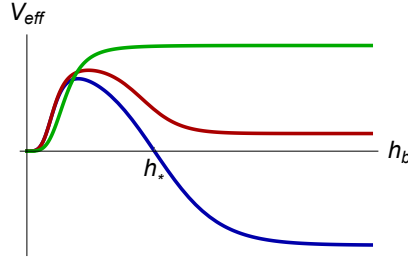


FIGURE 3.3: Possible forms of the effective potential for the field h_b .

Prescription II. Under the condition (3.44), the dependence of the normalization scale $\hat{\mu}_{II}$ on the variable h_b can be written as

$$\hat{\mu}_{II}^2(h_b) = \frac{y_t^2 h_b^2}{2} \left(1 + \frac{\xi_\chi(1 + 6\xi_h)}{1 + 6\xi_\chi} \frac{h_b^2}{M_P^2} + O\left(\frac{h_b^4 \xi_h^2 \xi_\chi^2}{M_P^4}\right) \right). \quad (3.48)$$

Using Eqs. (3.43) and (3.48), we arrive again at the result (3.46), from which the inequalities (3.47) follow. Thus, we expect that for both normalization prescriptions the exponential coefficient B grows when ξ_h increases or when ξ_χ decreases, making the tunneling less probable. These expectations are confirmed by numerical results.

3.2.4 Decay rate

Making use of the Einstein equations, one brings the euclidean action of the bounce to the form

$$S_E(\text{bounce}) \simeq -2\pi^2 \int_0^{m_H^{-1}} dr r^3 g_b(r) \tilde{V}(\theta_b(r)), \quad (3.49)$$

where g_b and θ_b are the bounce solution of Eqs. (3.31), (3.32). The integral is truncated from above by the non-zero Higgs mass. Indeed, as long as $r \ll m_H^{-1}$, the Higgs field is effectively massless, and the bounce exhibits a power-like asymptotics, $\theta_b \sim r^{-2}$, that contributes to the integral (3.49). At $r \gtrsim m_H^{-1}$, the bounce becomes decaying exponentially fast, and the contribution to the action from that region of r is negligible. This allows us to justify the approximation that we made for the potential $V(h, \chi)$. Namely, as long as $m_H^2 \gg \alpha M_P^2/\lambda$, the corrections to the bounce coming from the non-zero α and β can be neglected. It was shown in [50] that under the conditions (3.4) and (3.6), (3.8), the Higgs mass is given by

$$m_H^2 \sim \frac{\alpha M_P^2}{\lambda \xi_\chi}, \quad (3.50)$$

hence the required inequality is fulfilled. We can also justify the flat space approximation for the false vacuum state that we made when discussing the boundary conditions for the bounce solution. Indeed, as long as $m_H \gg \Lambda_0^{1/4}$, the integral (3.49) is insensitive to the nontrivial space geometry, and the flat space asymptotics can be used.

Now we turn to the calculation of the decay rate (3.1) and focus on the exponential coefficient B . In our case $S_E(FV) = 0$ and B is given by the r.h.s. of Eq. (3.49). We are interested in the ratio B/B_0 , where B_0 is the SM bounce action in flat space and for the same values of the SM parameters. We take the Higgs mass $m_H = 125.09$ GeV [35], and the top quark mass $m_t = 172.25$ GeV [36]. To see the effect from variation of m_t , we also compute B/B_0 for $m_t = 172.25 \pm 0.63$ GeV corresponding to the 1σ experimental uncertainty region.¹⁰ The results for the normalization points $\hat{\mu} = \hat{\mu}_{I,II}$, with $\hat{\mu}_{I,II}$ given in Eq. (3.39), are presented in Fig. 3.4.

We observe that the difference between the results obtained within different normalization prescriptions is small. The behavior of B as a function of the non-minimal couplings ξ_h and ξ_χ confirms the predictions (3.47) based on the qualitative analysis of the effective potential for the bounce solution. We also see

¹⁰Within this region, λ changes sign at some scale $h_* \ll M_P$, and the tunneling is possible.

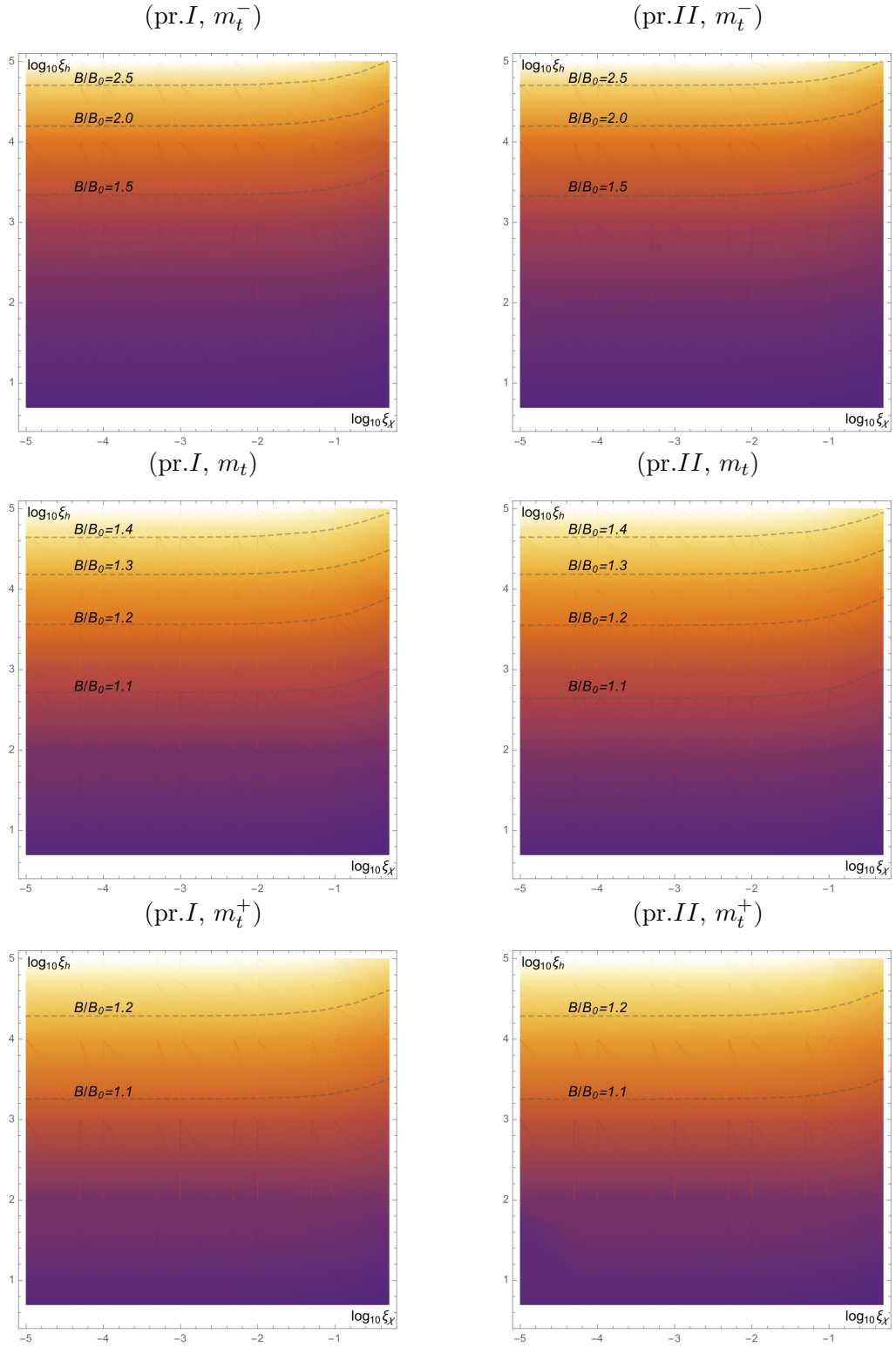


FIGURE 3.4: (see the text above) The ratio B/B_0 for the two choices of the normalization point (pr.I,II). We take the Higgs mass $m_H = 125.09$ GeV and the top quark masses $m_t = 172.25$ GeV and $m_t^\pm = 172.25 \pm 0.63$ GeV.

that necessarily $B > B_0$. This is to be expected, since the bounce interpolates between (approximately) flat space and anti-de Sitter space, and the gravitational effects are known to make the transition from Minkowski geometry to anti-de Sitter geometry less probable compared to the flat space limit [23].

3.2.5 EW vacuum stability in the Higgs-inflation scenario

Before we have discussed how the quantum corrections affect the shape of the effective potential for the bounce solution at the relevant energy scales. Let us now discuss the possibility that these corrections change the potential in the way that makes the possible metastability of the EW vacuum compatible with the Higgs-inflation scenario [92]. Renormalization effects due to the non-minimal coupling of the Higgs field can bring the Higgs self-coupling to positive values at inflationary scales, as shown schematically in Fig. 3.5. A typical energy at which these effects take over is of order $h_{inf} \sim M_P/\xi_h$. As long as this scale exceeds the magnitude of the bounce h_0 , the corrections do not affect the decay rate. On the other hand, if $h_0 \gtrsim h_{inf}$, we expect that the bounce changes significantly, yielding the further suppression of the tunneling probability. Somewhat surprisingly, numerical calculations show that for the values of ξ_h and ξ_χ that we consider here, h_0 never approaches h_{inf} . We illustrate this point in Fig. 3.6, where we choose, as an example, $m_t = 173.34$ GeV and $\hat{\mu} = \hat{\mu}_I$. The conclusion is that inflationary physics produces no effect on stability of the EW vacuum in the current low temperature background.

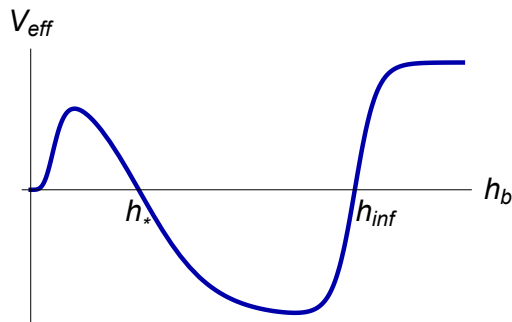


FIGURE 3.5: Schematic form of the effective potential in the Higgs-inflation scenario.

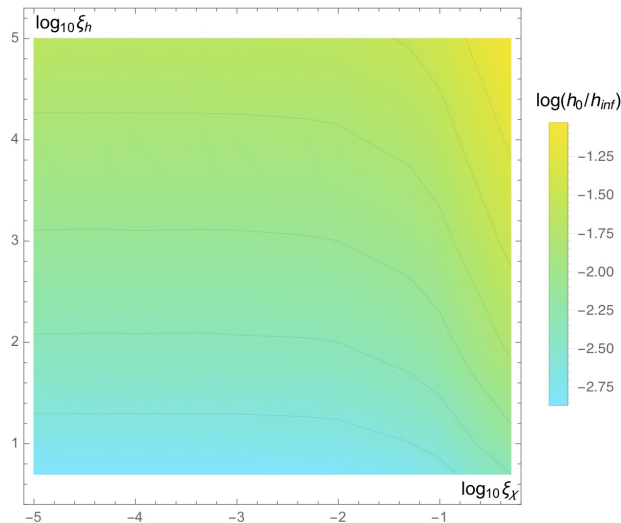


FIGURE 3.6: Magnitude of the bounce relative to the scale of the Higgs inflation. Here we take $m_t = 173.34$ GeV and $\hat{\mu} = \hat{\mu}_I$.

3.3 Discussion

Let us first make a general comment about the bounce solution in the Higgs-Dilaton theory. We would like to emphasize the fact that, according to the inequality (3.42), the theory restricts the largest energy scale the tunneling solution can hit by the value

$$h_{max} = M_P \sqrt{\frac{1 + 6\xi_\chi}{\xi_\chi(1 + 6\xi_h)}}. \quad (3.51)$$

This threshold is well below the Planck scale, provided that

$$\xi_\chi \xi_h \gg 1. \quad (3.52)$$

Moreover, as is seen from the numerical findings, for the values of parameters of the theory that we discuss here, including the range of them acceptable for phenomenology, the magnitude of the bounce satisfies the much stronger condition, $h_0 \ll M_P/\xi_h$. Note that the bound h_{max} is determined solely by ξ_h and ξ_χ and is independent of any other couplings of the theory. Being an effective theory, the Higgs-Dilaton model possesses a UV cutoff scale given by the effective Planck mass [51]. When approaching that scale, the theory is required to be supplemented by a sequence of higher-dimensional operators suppressed by the cutoff. If the inequality (3.52) holds, introduction of these operators produces no effect on the decay rate of the EW vacuum as long as they do not spoil the condition $\rho'_b = 0$. This observation reveals the difference between the tunneling

processes in the Higgs-Dilaton theory and in the SM. Indeed, it is known that the SM bounce can probe sub-Planckian energies, and that the Planck-suppressed operators, added to the theory, can change drastically the predictions for the EW vacuum decay rate [106]. We conclude that the tunneling probability in the Higgs-Dilaton theory at the range of parameters specified by Eq. (3.52) is less sensitive to new physics coming about at the Planck scale.

Let us now discuss the lifetime of the universe in the Higgs-Dilaton theory. Whenever the EW vacuum is not absolutely stable, there remains possibility for a transition towards another minimum of the Higgs potential. We would like to make sure that the calculations we have performed for the exponential factor B guarantee the expected lifetime to exceed the present age of the universe by many orders of magnitude. To this end, one needs to estimate the prefactor A introduced in Eq. (3.1). In flat spacetime, the good estimation for A is [84]

$$A \sim R^{-4}, \quad (3.53)$$

where R is the full-width-half-maximum of the bounce. We assume that Eq. (3.53) remains valid after gravitational corrections are taken into account. To the best of our knowledge, the computation of the prefactor has not been performed yet in the SM with gravity included. Our assumption about the validity of Eq. (3.53) is based on the observation that the Higgs-Dilaton bounce does not approach the Planck scale where quantum gravity effects come into play. Hence, one can expect the gravitational corrections to the prefactor to be suppressed by the ratio h_0/M_P . Then, the lifetime is given by [106]

$$\tau = \frac{R^4}{T_U^3} e^B, \quad (3.54)$$

where T_U is the age of the universe. For example, taking $m_H = 125.09$ GeV and $m_t = 173.34$ GeV, we have for the SM [107]

$$\tau_0 \sim 10^{600} T_U. \quad (3.55)$$

One can estimate the additional suppression of the decay rate in the Higgs-Dilaton model by computing the ratio τ/τ_0 for different values of ξ_h and ξ_χ . As an example, Fig. 3.7 shows the ratio with the choice $m_t = 173.34$ GeV and $\hat{\mu} = \hat{\mu}_I$. In particular, we observe that for the values of ξ_h acceptable for inflation, the lifetime of the EW vacuum is enhanced by at least 130 orders of magnitude compared to the SM. Thus, the Higgs-Dilaton low-energy vacuum is much safer than the SM vacuum.

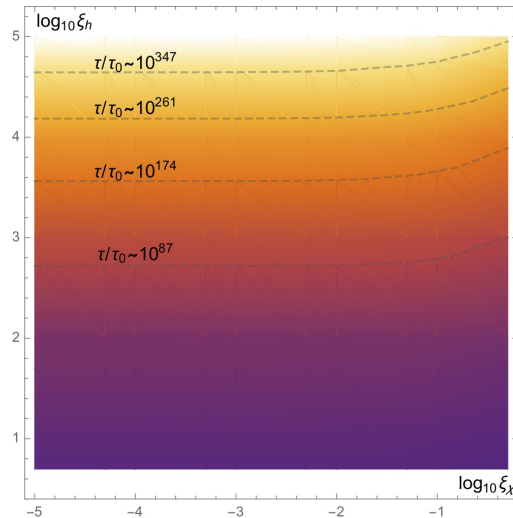


FIGURE 3.7: The ratio of the lifetime of the universe in the Higgs-Dilaton theory (τ) to that in the SM (τ_0). Here we choose $m_t = 173.34$ GeV and $\hat{\mu} = \hat{\mu}_I$.

3.4 Summary

Let us summarize our findings. In this chapter we computed the EW vacuum decay rate in the Higgs-Dilaton theory. We addressed the question of vacuum stability for the wide range of parameters of the theory. The stability of the EW vacuum against transitions towards another minimum of the Higgs potential is one of the necessary ingredients that make the theory phenomenologically acceptable. Our analysis showed that the transition probability is suppressed significantly compared to the SM case, yielding further stabilization of the vacuum. We also pointed out that possible corrections to the Higgs potential, coming from inflationary physics, do not change the lifetime of the vacuum. Furthermore, the decay rate in the Higgs-Dilaton theory is less sensitive to higher-dimensional Planck-suppressed operators than in the SM, provided that $\xi_h \xi_\chi \gg 1$.

Part II

Towards a non-perturbative approach to the hierarchy problem

Chapter 4

Motivation and setup

As suggested by the long quest for unification of fundamental interactions, it is natural to search for principles relating phenomena that occur at very different energy scales. To an underlying theory unifying diverse physical processes we assign a task to explain possible large differences in the measured fundamental quantities. One of the most striking differences, which has been a source of new ideas in particle physics for decades, is manifested in the ratio of the Fermi constant G_F , that sets the weak interaction scale, to the Newton constant G_N determining the gravitational force strength,¹

$$\frac{G_F \hbar^2}{G_N c^2} \sim 10^{33}. \quad (4.1)$$

It is tempting to speculate that some deep reason for the big number to appear in this relation may be hidden in a yet unknown theory encompassing the Standard Model (SM) and General Relativity.

At the classical level, the ratio (4.1) represents one face of the problem. Another aspect of it appears when we adopt the quantum field theory framework. It originates from the properties of the Higgs field through the vacuum expectation value (vev) of which the Fermi constant is defined. As it was realized long ago in studies of Grand Unified Theories, whenever new physics comes about with heavy degrees of freedom (dof) activating at some mass scale M_X , the heavy particle's loops are expected to produce an additive correction to the Higgs mass m_H [56, 108–111],²

$$\delta m_{H,X}^2 \sim M_X^2. \quad (4.2)$$

¹For illustrative purposes, here we write explicitly the Planck constant \hbar and the speed of light c . Everywhere further we work in natural units $\hbar = c = 1$.

²We assume that the new particles are coupled sufficiently strongly to the Higgs field.

As soon as M_X , if exists, is much larger than the observed value of m_H , Eq. (4.2) implies either a fine-tuning between various contributions to the Higgs mass or a mechanism of systematic suppression of those contributions. This puzzling fact about the SM Higgs field is known as the (electroweak) hierarchy problem. If one now treats the EW and gravitational forces within the quantum field theory framework, then one must include quantum gravity loop corrections to the Higgs mass. The naive power counting argument suggests these corrections to be of the order of the Planck mass,

$$\delta m_{H, grav.}^2 \sim M_P^2. \quad (4.3)$$

The validity of this estimation can be doubted by the observation that, unlike M_X , the Planck mass defines an interaction scale rather than a new particle's mass scale (see, e.g., [112]).³ Moreover, at the energies close to M_P gravity enters the strong-coupling regime where estimations based on perturbation theory lose the predictive power. Nevertheless, if we admit Eq. (4.3), then the observed difference in the interaction strengths (4.1) either requires a remarkable balance between the EW and the Planck scale physics, or it is an indication of specific properties of quantum gravity at strong coupling that result in the absence of the quadratic corrections to m_H , see [52, 53] for reviews of the problem.

The hierarchy problem was addressed in the literature many times and from various perspectives. The list of proposals dealing with the problem by introducing a new physics close to the EW scale includes supersymmetry, composite Higgs theories (for reviews see [115, 116] correspondingly), extra dimensions [117, 118]. The parameter spaces of the models extending the SM at the TeV scale are subject to constraints provided, in particular, by the LHC data. These constraints force such theories to be fine-tuned in order to remain compatible with experiment [53, 115, 119, 120]. More recent proposals attempt to overcome this issue [121–124]. Some of them suggest mechanisms of generation of exponentially small couplings to the Higgs field [114], or rely on a specific dynamics of the latter during the cosmological evolution [125] (see also [126, 127]).

Regardless the particular content of a model extending the SM at high energies, a common approach to the hierarchy problem lies within the effective field theory framework. The latter implies that the low-energy description of Nature, provided by the SM, can be affected by unknown UV physics only through a finite set of parameters. Two of them – the mass of the Higgs boson and the

³In fact, this observation can well be applied to the case of new physics much below the Planck scale. For example, in [113] an interpretation of the gauge coupling unification scale was proposed, which is not related to any new particle threshold; see also [114].

cosmological constant – are most sensitive to the scale and to the dynamics of physics beyond the SM, being quadratically and quartically divergent. In “natural” theories the quadratically divergent UV contributions to the Higgs mass are eliminated by introducing new physics right above the Fermi scale. It is this naturalness principle that is seriously questioned now in light of the absence of signatures of new physics at the TeV scale [53]. While some parameter regions of the theories with $M_X \sim 1$ TeV still survive at the price of a moderate fine-tuning, a relatively radical step would be to suggest that the UV physics can affect the low-energy behavior in a way that is not captured by the perturbation theory. Going back to the ratio (4.1), this would imply the existence of a non-perturbative effect linking the scales separated by 17 orders of magnitude.

Non-perturbative physics provides natural tools to establish links between the low-energy and the high-energy regimes of a theory. Perhaps, the most striking example of such a link, which strongly interferes phenomenology, is revealed in studying the EW vacuum decay. Indeed, as was discussed in section 3.3, depending on the structure of UV operators added to the SM at large energy scales, the decay rate of the EW vacuum can be changed drastically compared to the pure SM case [106]. Hence, having observed the sufficiently long-lived universe, one can make certain predictions about the physics complementing the SM at high energies (for a review see [32] and references therein).

The idea of some principle that can shape the behavior of a theory at very different energy scales is not novel to particle physics. For example, it is tempting to use such kind of reasoning when investigating a probable (near-)degeneracy of the minima of the SM Higgs potential, which is supported by the recent measurements of the Higgs and the top quark masses [29, 31]. A possible mechanism that makes the form of the potential special and, hence, predicts the values of the low-energy parameters, can manifest itself in a number of ways. For example, in [60] bounds on the Higgs and the top quark masses were put based on the principle of multiple point criticality [128], while in [129] the prediction of m_H was made, guiding by an asymptotic safety of gravity [130]. Inspired by these ideas, below we make an attempt to resolve the problem (4.1) by looking for an inherently non-perturbative effect relating the weak and the Planck scales.

The formulation of the hierarchy problem necessarily implies at least two scales in game. Considered isolated, the SM does not possess the problem due to the absence of thresholds with the energies above the EW scale, with which the Higgs mass is to be compared [54].⁴ But as soon as gravity is embedded into

⁴Here we leave aside an issue with the Landau pole in the scalar self-coupling.

the quantum field theory framework, one high-energy scale appears inevitably, raising the question about the origin of the big number in the r.h.s. of Eq. (4.1). Nonetheless, the no-scale scenario looks attractive [131–135], and motivates to search for the models which, alongside with incorporating the SM and gravity, do not contain dimensional parameters at the classical level [50, 51, 87, 136–143]. The advantage of this approach is that scale invariance and the absence of new heavy particles can protect the Higgs mass from large radiative corrections, thus making its value natural according to the 't Hooft definition [144]. This is a step forward in a solution of the hierarchy problem, although the big difference between the Fermi and the Planck scales remains unexplained.⁵ To study non-perturbative phenomena that can possibly affect the Higgs mass, it would be useful to have a theory in which the corrections coming at the perturbative level are suppressed, and one can achieve this by the means of scale symmetry and by requiring that no heavy dof appear beyond the SM.

In the scale-invariant framework, the Planck mass appears as a result of spontaneous breaking of the scale symmetry. In the subsequent chapters we argue that gravitational effects can generate non-perturbatively a new scale, associated with the classically zero vev of a scalar field. Dynamical gravity and global scale symmetry are important ingredients of a theory admitting this non-perturbative mechanism. The former ensures the existence of euclidean classical configurations of a special type — singular instantons — that contribute to the vev of the scalar field. The latter can protect the vev from large radiative corrections, provided that the scalar sector of a theory is additionally invariant under constant shifts of the field responsible for generating the Planck scale [100]. Our goal is to find if it is possible, in particular classes of theories, to make the new scale much smaller than M_P , in which case the hierarchy of scales emerges.

The existence of the desired instanton configuration relies on a specific structure of the theory in high-energy and large-field limits. In what follows, we will investigate this structure by the means of simple models containing the gravitational and scalar dof that mimic the Higgs-gravity sector of the theory we are eventually interested in. To apply the results of the non-perturbative analysis to the actual hierarchy problem (4.1), it is necessary to have a theory which is compatible with the models on which the mechanism is tested and is consistent with observations and experiment. Good candidates are the models of Higgs inflation studied in [90–92], or the Higgs-Dilaton model [50, 51, 131, 135, 145]. In

⁵As was discussed in section 1.3, the possibility to generate m_H via radiative correction to the Higgs field potential in the SM is not compatible with experiment.

chapters 7 and 8 we will show how Eq. (4.1) is reproduced in certain high-energy modifications of these theories.

Of course, the absence of an explicit UV completion of gravity engenders irremovable ambiguities in our analysis. The scale-invariant framework and the requirement of having a phenomenologically viable low-energy limit reduce partially this ambiguity. The resulting amount of possibilities for choosing a particular model for the analysis is, however, still quite large. For example, the Higgs-gravity sector of a theory under investigation can be governed by the Horndeski Lagrangian or its extensions [146–148]. We will focus on some possible examples in which the suggested mechanism of the exponential suppression of the Planck scale due to instantons exists. We do not intend to perform an extensive survey of all possible examples. Nor do we intend to argue that a toy model chosen to illustrate the mechanism can indeed be consistently embedded into the UV complete theory of gravity. Note, however, that Eq. (4.1) can be viewed as an argument in favor of those properties of the UV theory, that support the existence of the suppression mechanism.

Chapter 5

Outline of the idea

In this chapter, we provide a general idea of the method that allows to capture non-perturbative gravitational contributions to a one-point correlation function of a scalar field. We will use this method in chapters 7 and 8 where corrections coming from instantons to the vev of a scalar field are computed.

Consider the theory containing a real scalar field φ of a unit mass dimension, the metric field $g_{\mu\nu}$ and, possibly, other dof which we denote collectively by \mathcal{A} . In the euclidean signature, the (time-independent, spatially homogeneous) vev of φ is evaluated as¹

$$\langle \varphi \rangle = Z^{-1} \int \mathcal{D}\varphi \mathcal{D}g_{\mu\nu} \mathcal{D}\mathcal{A} \varphi(0) e^{-S}, \quad (5.1)$$

where Z denotes the partition function,

$$Z = \int \mathcal{D}\varphi \mathcal{D}g_{\mu\nu} \mathcal{D}\mathcal{A} e^{-S}, \quad (5.2)$$

and S is the euclidean action of the theory. If the theory admits the classical ground state of the form $\varphi = 0$, $g_{\mu\nu} = \delta_{\mu\nu}$, the numerator in Eq. (5.1) can be computed by the means of the standard perturbation theory. Let us instead attempt to reorganize it by exponentiating the scalar field variable in the region of large magnitudes of the latter,

$$\varphi \rightarrow \varphi_0 e^{\bar{\varphi}}, \quad \varphi \gtrsim \varphi_0, \quad (5.3)$$

¹Here and below we work with euclidean formulation of theories, without indicating this explicitly. We will comment on this later in this chapter.

where by φ_0 we understand an appropriate scale of the theory. The corresponding part of the path integral in Eq. (5.1) becomes

$$\int_{\varphi \gtrsim \varphi_0} \mathcal{D}\varphi \varphi(0) e^{-S} \rightarrow \varphi_0 \int_{\bar{\varphi} \gtrsim 0} \mathcal{D}\bar{\varphi} J e^{-W}, \quad (5.4)$$

where

$$W = -\bar{\varphi}(0) + S \quad (5.5)$$

and J is a Jacobian of the transformation (5.3).

Next, we want to evaluate the vev (5.1) in the saddle-point approximation (SPA). The partition function is evaluated via a ground state configuration. Suppose that the functional W admits appropriate saddle points through which the modified path integral can be evaluated as well. Then,

$$\langle \varphi \rangle \sim \varphi_0 e^{-\bar{W} + S_0}. \quad (5.6)$$

In this expression, \bar{W} is the value of W at a saddle and S_0 is the value of S at the ground state.

Clearly, the possible saddles of the functional W solve equations of motion for the field $\bar{\varphi}$ everywhere except the origin. At the origin, they satisfy the equation provided that the latter is supplemented with an instantaneous source of $\bar{\varphi}$,

$$\bar{\varphi}(0) = \int d^4x j(x) \bar{\varphi}(x), \quad j(x) = \delta^{(4)}(x). \quad (5.7)$$

The solutions of the equation with the source are expected to be singular at the point where the source acts. Despite this, they are valid saddle points of W (but not S).

Let us discuss the conditions under which the transition from Eq. (5.1) to Eq. (5.6) is possible. First, the theory must admit the singular configurations of the type described above, which approach the classical ground state away from the singular point. Second, the SPA must be justified by the presence in the theory of a suitable semiclassical parameter. The appearance of such parameter would ensure that $\bar{W} \gg 1$. If a particular calculation reveals \bar{W} to be of the order of one or negative, one concludes that Eq. (5.6) is not valid. Last, but not least, a physical argumentation is necessary in order to justify the change of the field variable made in Eq. (5.3).

In chapters 7 and 8 we will see in detail how the first two requirements mentioned above are satisfied in particular classes of models comprising gravity and scalar

fields. Here we just note that these conditions are, in fact, quite restrictive. It is easy to make sure that neither theories of a scalar field with no back-reaction on gravity nor theories with dynamical gravity and a minimal coupling of it to the scalar field possess classical configurations which would allow to arrive at Eq. (5.6).

The third requirement represents a more serious issue. Indeed, one would normally expect the value of $\langle\varphi\rangle$ to be independent of any transformations of the variables used in the intermediate computations. In the examples below we will see that what appears to be the canonical scalar field dof in the low-energy (or low-field) limit may not be so in the limit of large fields and energies. One may notice here an analogy with gauge theories, the valid description of the confinement phase of which is performed in terms of Wilson loops, not the gauge field itself [149]. One may also suggest that although the full calculation will indeed produce the same answer regardless the choice of variables, the *partial* answer that includes a finite amount of loops is sensitive to the background configuration upon which we build the perturbation theory. Hence, Eq. (5.6) may result from a certain resummation procedure. We leave any further discussion of this appealing possibility for future work.

Note that, because of the presence of gravity, the euclidean path integral in Eq. (5.1) must be taken with caution. Indeed, it is known that the action of the euclidean quantum gravity is unbounded below; in particular, it suffers from the so-called conformal factor problem [150] (see also the discussion in [151]). We assume that the properties of the theory in the UV regime result in a resolution of this problem in one or another way.

Eqs. (5.1)—(5.6) admit a straightforward generalization to the case when the vacuum geometry is not flat. In this case, the action of the theory must be supplemented by an appropriate boundary term, and the exponent in Eq. (5.6) will include the difference of the boundary terms taken at the ground state and at the configuration extremizing W . It is clear that the presence of the cosmological constant is not relevant for the analysis of classical configurations whose characteristic scale φ_0 is associated with the Planck scale. Note also that the non-zero vacuum energy can be realized in a scale-invariant theory without an explicit breaking of the scale symmetry [87, 152, 153].

The prefactor in Eq. (5.6) includes a parameter φ_0 with the dimension of mass. In scale-invariant theories a dimensionful parameter can arise due to a spontaneous symmetry breaking. If a theory possesses only one such parameter at the classical level, the vev of the field will inevitably be proportional to it. In this

case, the quantity \bar{W} can be viewed as a rate of suppression of the classical scale. Hence, Eq. (5.6) indicates the emergence of the hierarchy of scales, one of which is generated classically, and the other — non-perturbatively.

In evaluating the vev $\langle\varphi\rangle$ in the leading-order SPA, the fields of the theory, which do not participate in building the instanton configuration, are kept classically at their vacuum values. Fluctuations of the fields on top of the instanton are the source of perturbative corrections to the prefactor in Eq. (5.6). Evaluation of the prefactor with the accuracy beyond the naive dimensional analysis is difficult and is left for future work. However, the applicability of the SPA enables us to believe that the corrections coming with the fluctuation factor do not spoil the hierarchy of scales observed in the leading-order analysis. Moreover, as we will see later, the instanton value of W varies depending on the parameters of the theory, and this can compensate possible deviations of the value of the vev, caused by subleading contributions.

Chapter 6

Singular instanton in the Dilaton model

In this chapter, we consider a simple scale-invariant model admitting exactly solvable classical euclidean equations of motion. We will refer to it as the Dilaton model. We focus on the configurations solving these equations provided that the latter are accompanied with a scalar field source. These configurations share many important properties with their counterparts arising in more complicated theories which we study in chapters 7 and 8. The results obtained here will provide us with an intuition about certain properties a theory must possess in order to permit the mechanism of generating the hierarchy of scales, which was outlined in the previous chapter.

6.1 The Dilaton model

Consider the simplest scale-invariant model of one real scalar field coupled to gravity in a non-minimal way. The euclidean Lagrangian of the model is

$$\frac{\mathcal{L}}{\sqrt{g}} = -\frac{1}{2}\xi\varphi^2 R + \frac{1}{2}(\partial\varphi)^2 + \frac{\lambda}{4}\varphi^4, \quad (6.1)$$

where $(\partial\varphi)^2 \equiv g^{\mu\nu}\nabla_\mu\varphi\nabla_\nu\varphi$, and the non-minimal coupling constant ξ is taken to be positive. The euclidean action of the model,

$$S = \int d^4x \mathcal{L}, \quad (6.2)$$

must be supplemented with an appropriate boundary term (see, e.g., [154]). As we will see shortly, the latter should be taken in the form

$$I = - \int d^3x \sqrt{\gamma} K \xi \varphi^2, \quad (6.3)$$

where K denotes the external curvature of the space boundary and γ the determinant of the metric induced on the boundary.

The model is invariant under the global scale transformations¹

$$g_{\mu\nu}(x) \mapsto g_{\mu\nu}(qx), \quad \varphi(x) \mapsto q\varphi(qx) \quad (6.4)$$

with q a constant. Further, it admits the classical ground state of the form

$$\varphi = \varphi_0, \quad R = \frac{\lambda\varphi_0^2}{\xi}. \quad (6.5)$$

The latter breaks scale invariance spontaneously by introducing a classical scale φ_0 .

To simplify the analysis of classical configurations, it is convenient to rewrite the model in the form in which the non-minimal coupling is absent. To this end, we perform a Weyl transformation of the metric field. We have already encountered this type of transformation during the study of the bounce in the Higgs-Dilaton theory. To keep the kinetic term of the scalar field canonical (up to a constant multiplier) in the new coordinates, we also redefine the scalar field variable:²

$$\varphi = \varphi_0 \Omega, \quad \tilde{g}_{\mu\nu} = \Omega^2 g_{\mu\nu}, \quad \Omega = e^{\frac{\tilde{\varphi}}{\sqrt{\xi}\varphi_0}}. \quad (6.6)$$

The action becomes (see Eq. (3.13))

$$S = \int d^4x \tilde{\mathcal{L}} - 3 \int d^4x \sqrt{\tilde{g}} \xi \varphi_0^2 \tilde{\square} \log \Omega, \quad (6.7)$$

where $\tilde{\square} \equiv \tilde{g}^{-1/2} \partial_\mu \tilde{g}^{\mu\nu} \partial_\nu$. The exterior curvature transforms as

$$K = \Omega \tilde{K} + 3\tilde{n}^\mu \partial_\mu \Omega, \quad (6.8)$$

where \tilde{n}^μ is a unit normal to the boundary in the coordinate frame provided by $\tilde{g}_{\mu\nu}$. After using Gauss's theorem, the second contribution in Eq. (6.8)

¹The symmetry associated with the absence of dimensionful parameters can equivalently be written as an internal transformation, $g_{\mu\nu}(x) \mapsto q^{-2} g_{\mu\nu}(x)$, $\varphi(x) \mapsto q\varphi(x)$.

²The condition $\varphi > 0$ implied by Eq. (6.6) is not restrictive. In what follows, we will discuss the classical configurations which are monotonically-decreasing functions of a radial coordinate with the large-distance asymptotics $\varphi \rightarrow \varphi_0$.

cancels the total derivative term in Eq. (6.7). The transformed Lagrangian and boundary term are written as³

$$\frac{\tilde{\mathcal{L}}}{\sqrt{\tilde{g}}} = -\frac{1}{2}\xi\varphi_0^2\tilde{R} + \frac{1}{2a}(\tilde{\partial}\bar{\varphi})^2 + \frac{\lambda}{4}\varphi_0^4, \quad a = \frac{1}{6 + 1/\xi}, \quad (6.9)$$

$$I_{GH} = -\xi\varphi_0^2 \int d^3x \sqrt{\tilde{\gamma}} \tilde{K}, \quad (6.10)$$

where we denoted $(\tilde{\partial}\bar{\varphi})^2 \equiv \tilde{g}^{\mu\nu}\nabla_\mu\bar{\varphi}\nabla_\nu\bar{\varphi}$. In the first term of the Lagrangian we recognize the Planck mass,

$$M_P \equiv \sqrt{\xi}\varphi_0, \quad (6.11)$$

and Eq. (6.10) represents the usual Gibbons-Hawking term [93], which justifies Eq. (6.3).⁴ In the new coordinates, the scale transformations act as

$$\bar{\varphi}(x) \mapsto \bar{\varphi}(x) + q, \quad \tilde{g}_{\mu\nu}(x) \mapsto \tilde{g}_{\mu\nu}(x). \quad (6.12)$$

Note that the scalar field variable φ is related to the canonical variable $\bar{\varphi}$ via the exponential mapping, according to Eq. (6.6). Hence, the non-minimal coupling to gravity leads naturally to the appearance of the source term for $\bar{\varphi}$ in the process of evaluation of the vev $\langle\varphi\rangle$. Later, this observation will enable us to write Eq. (5.6) for a classically zero vev of the scalar field.

6.2 Classical configurations and Instanton action

In studying classical configurations arising in the Dilaton model, we restrict ourselves to the spherically-symmetric case. This is motivated by the fact that introducing the instantaneous source of the scalar field does not break the $O(4)$ -symmetry present in the theory. Should the less symmetric configurations suitable for our purposes exist, we assume that their contribution to the path integral is suppressed (see also footnote 6 in chapter 3). Furthermore, below we neglect the curvature of the background solution (6.5) by assuming that it has no impact on relevant properties of classical configurations whose characteristic energy scale exceeds significantly the scale of the background. This expectation is justified in appendix A where the case of non-zero R is considered.

³Note that without the boundary term taken into account, the Lagrangian (6.9) would contain the total derivative term, according to eq. (6.7), and this term would contribute to the action of a singular configuration, thus leading to an incorrect result.

⁴Of course, one can check directly that the boundary term (6.3) cancels the surface terms arising from the variation of the metric in the action (6.2).

We adopt the ansatz (3.28) for the metric field, which we quote here again for convenience:

$$d\tilde{s}^2 = f^2 dr^2 + r^2 d\Omega_3^2. \quad (6.13)$$

Here f is a function of the radial coordinate r and $d\Omega_3$ is the line element on a unit 3-sphere. The scalar field equation of motion and 00-component of the Einstein equations read as follows,

$$\partial_r \left(\frac{r^3 \bar{\varphi}'}{af} \right) = 0, \quad \frac{1}{f^2} = 1 + \frac{r^2 \bar{\varphi}'^2}{6aM_P^2}. \quad (6.14)$$

Equations of motion admit a solution of the form

$$\bar{\varphi} = 0, \quad f = 1, \quad (6.15)$$

which represents the classical ground state (6.5) of the model with $R = 0$. To find other configurations, we replace the first of Eqs. (6.14) by

$$\frac{r^3 \bar{\varphi}'}{af} = C \quad (6.16)$$

with C some non-zero constant. We require the classical configuration obeying Eq. (6.16) to approach the vacuum solution (6.15) at large distances. With this boundary condition, we obtain a one-parameter family of configurations distinguished by the value of C . Near the origin, the scalar field and the curvature behave as

$$\bar{\varphi} \sim -\gamma M_P \log(M_P r), \quad \tilde{R} \sim a M_P^{-4} r^{-6}, \quad \gamma = \sqrt{6a}, \quad r \rightarrow 0. \quad (6.17)$$

One observes that the physical singularity forms at the center of the configurations. Therefore, they are not valid solutions of Eqs. (6.14) at $r = 0$. In what follows we will refer to such configurations as “singular shots”.⁵

The divergence of a classical field configuration can be associated with a source of the field acting at the points of divergence. Therefore, such configuration can be regarded as a solution of equations of motion following from varying the action supplemented by a source term,

$$W = S - \int d^4x j(x) \bar{\varphi}(x). \quad (6.18)$$

⁵Configurations of this type were studied before in context with the cosmological initial value problem [155–158]. In those works, they are referred to as (singular) instantons. Here we would like to reserve the name “instanton” for a unique configuration of the family, for which Eq. (6.20) holds. The name “shot” was inspired by [159].

To reproduce the asymptotics (6.17), the source $j(x)$ must be instantaneous,

$$j(x) = M_P^{-1} \delta^{(4)}(x), \quad (6.19)$$

where we normalize the delta-function on the Planck scale as the latter is the only classical scale of the model. One of the singular configurations found above is obtained as a saddle point of the functional W . It is specified by

$$C = -M_P^{-1}. \quad (6.20)$$

This can be viewed as an additional boundary condition fixing the position of the center of the singular configuration and the strength of the source producing it. In what follows, we will call the solution of Eqs. (6.16), (6.20) the singular instanton. It is explicitly given by

$$\bar{\varphi}(r) = \sqrt{\frac{3a}{8}} M_P \log \left[\frac{\sqrt{1 + 6a^{-1} M_P^4 r^4} + 1}{\sqrt{1 + 6a^{-1} M_P^4 r^4} - 1} \right], \quad \frac{1}{f^2(r)} = 1 + \frac{a}{6M_P^4 r^4}. \quad (6.21)$$

As is seen from this equation, the singular instanton has a characteristic length scale $a^{1/4} M_P^{-1}$ determining the size of its core. In the core region, the gravitational field is affected strongly by the dynamics of the scalar field. In turn, the short-distance behavior of the scalar field is affected by gravity, see Fig. 6.1 for illustration.

We would like to note that the short-distance logarithmic divergence of the scalar field, expressed in Eqs. (6.17), reveals a nontrivial interplay between the scalar and gravitational sectors of the model. Indeed, in the flat space limit, the field $\bar{\varphi}$ in four dimensions exhibits the usual power-like massless asymptotics $\bar{\varphi} \sim r^{-2}$. We observe that gravity cures partially this divergence. This seems to be a promising sign of a general non-perturbative effect caused by gravity on the correlation functions in the scalar sector.⁶

Finally, we compute the euclidean action \bar{S} and the boundary term \bar{I}_{GH} of the singular instanton in the limit $\lambda = 0$, relative to the action S_0 and the boundary term $I_{GH,0}$ of the background solution. This gives

$$\bar{I}_{GH} - I_{GH,0} \sim a^{-1} M_P^{-2} r_s^{-2} \rightarrow 0, \quad r_s \rightarrow \infty, \quad \lambda = 0, \quad (6.22)$$

⁶Note that the solution of Eq. (6.20) can be viewed as an euclidean Green function of the massless scalar field propagating in the external gravitational background specified by the second of Eqs. (6.21).

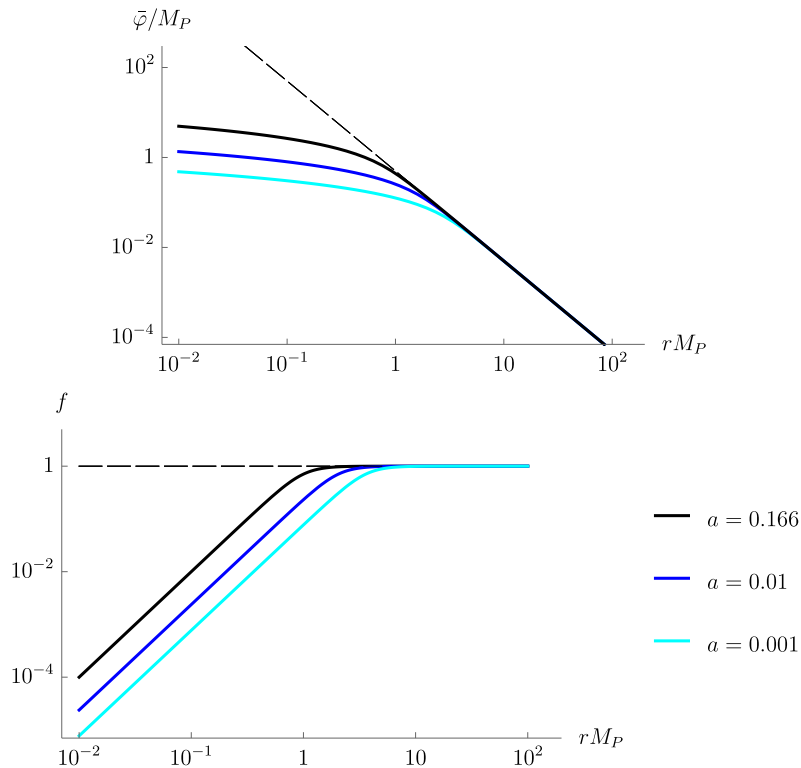


FIGURE 6.1: The profile of the singular instanton for the different values of a . The top panel demonstrates the logarithmic divergence of the scalar field $\bar{\varphi}$ in the core region of the instanton. The bottom panel shows the behavior of the metric function f in the same region. The dashed lines represent the static gravity limit.

where r_s is the radius of a 3-sphere, and

$$\bar{S} = S_0 = 0. \quad (6.23)$$

Hence, there is no contribution of order 1 from the instanton to the net euclidean action, neither to the net boundary term. Switching on the coupling λ does not change this result, once the instanton and the cosmological scales are well separated, see appendix A for details.

To summarize, the singular instanton found above is a legitimate solution of the variational problem $\delta W/\delta\bar{\varphi} = 0$ with W given in Eq. (6.18). This goes in accordance with the logic presented in chapter 5. However, in the Dilaton model, the classical scale is defined by the vev of the scalar field, and there is no room for the second scale to be generated via the singular instanton. Moreover, as we just saw, the model is not capable of providing the large instanton action. To fix these drawbacks, one should change the structure of the model in the region

of large $\bar{\varphi}$ and supplement it with the second scalar field whose vev is classically zero. We will proceed to this case in [chapter 8](#).

Chapter 7

“Higgs+gravity” models

In this chapter we demonstrate how singular instantons of the type studied before can contribute to the vev of the scalar field via the mechanism outlined in chapter 5, in the models of one scalar dof coupled to gravity in a non-minimal way.

Let us remind the framework which we will follow. According to the discussion in chapter 4, we would like to exclude from consideration possible quantum (perturbative) corrections to the Higgs field vev, coming with the heavy mass thresholds associated with new physics. To this end, we require no dof with the mass scales above the EW scale appear in the theory. That is, we demand the only classical dimensional parameter in the theory be the Planck mass. The vastness of possible models to consider is further restricted by the requirement to reproduce the SM Higgs sector and General Relativity at low energies and by the assumption that among higher-dimensional operators activating at high energies those are present that we find useful for the purpose of generating the hierarchy of scales.¹ Let us stress again that our goal here is to find a mere example of a model in which the mechanism of the exponential suppression of the Planck mass due to instantons exists.

We will find that the crucial ingredient of the theory admitting the instantons with the desired properties is the non-minimal coupling of the Higgs field to the Ricci scalar. This confirms the expectation coming from the analysis of the Dilaton theory. We will also find that the instantons generating the large hierarchy of scales favor the (approximate) Weyl invariance of the theory for large values of the scalar field.

¹The structure of theories at high energies can also be subject to constraints, e.g., by the requirement of asymptotic safety [130].

The plan of this chapter is as follows. In section 7.1 we introduce a simple model describing the dynamics of the gravitational and the classically massless scalar fields. The large-field limit of the model matches the Dilaton theory. We analyze euclidean classical configurations arising in this model, and discuss their possible influence on the vev of the scalar field. The results of the analysis motivate us to introduce certain modifications into the model. In section 7.2 we incorporate these modifications step by step. We find that contribution of the singular instanton to the scalar field vev can actually make the latter non-zero and, at the same time, many orders of magnitude smaller than the Planck scale. In section 7.3 we apply our findings to the actual hierarchy problem by identifying the scalar field with the Higgs field dof, and discuss the inclusion of other SM dof. Finally, section 7.4 summarizes our results.

7.1 The warm-up model

As a warm-up, in this section we study a simple model containing the real scalar field φ coupled to dynamical gravity. The purpose is to elucidate important properties of the singular instanton and to make connection with the results obtained within the Dilaton theory. We take the following Lagrangian,

$$\frac{\mathcal{L}_{\varphi,g}}{\sqrt{g}} = -\frac{1}{2}(M_P^2 + \xi\varphi^2)R + \frac{1}{2}(\partial\varphi)^2 + V(\varphi) \quad (7.1)$$

with

$$V(\varphi) = \frac{\lambda}{4}\varphi^4 \quad (7.2)$$

and $\xi > 0$. The Lagrangian (7.1) must be supplemented with the suitable boundary term. However, as we saw in section 6.2, the latter is not relevant for the analysis of classical configurations, and from now we will omit it.

The scalar sector of the model, represented by the last two terms in Eq. (7.1), exhibits global conformal invariance. Addition of gravity and the scalar-gravity interaction (the first two terms) breaks this symmetry explicitly. In the limit $|\varphi| \gg M_P/\sqrt{\xi}$, the global scale symmetry is acquired. Overall, the model (7.1) serves as a good prototype of the Higgs-gravity sector of a theory we are eventually interested in. Of course, in a more realistic setting operators of higher dimensions suppressed by a proper cutoff must be added to the Lagrangian. We will proceed with the study of particular types of such operators in section 7.2. Finally, the non-minimal coupling constant ξ and the quartic self-coupling constant λ can

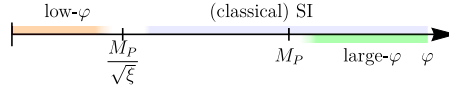


FIGURE 7.1: The regions of magnitudes of the scalar field of the model (7.1) with the condition (8.9) implemented.

be taken as functions of φ . The φ -dependence would mimic their RG-evolution once extra dof are included into the theory, that are coupled to the scalar field.

For the sake of simplicity, we require

$$\sqrt{\xi} \gg 1, \quad (7.3)$$

which provides us with a good separation of the Planck and the scale symmetry restoration scales. In what follows, we will refer to the range of magnitudes $|\varphi| \gg M_P/\sqrt{\xi}$ as the (classically) scale-invariant (SI) regime of the model, while the sub-range $|\varphi| \gg M_P$ will be referred to as the large- φ regime (see Fig. 7.1). Note that in the SI regime, the model (7.1) reduces to the Dilaton model studied above. Hence, one can expect that the properties of the singular instanton in the core region are the same in both theories.

Following the standard procedure, we rewrite the Lagrangian in the form in which the non-minimal coupling of the scalar fields to the Ricci scalar is absent. The corresponding Weyl transformation reads as follows,

$$\tilde{g}_{\mu\nu} = \Omega^2 g_{\mu\nu}, \quad \Omega^2 = \frac{M_P^2 + \xi\varphi^2}{M_P^2}, \quad (7.4)$$

and the E-frame Lagrangian is

$$\frac{\mathcal{L}_{\varphi,g}}{\sqrt{\tilde{g}}} = -\frac{1}{2}M_P^2\tilde{R} + \frac{1}{2a(\varphi)}(\tilde{\partial}\varphi)^2 + \tilde{V}(\varphi), \quad (7.5)$$

where

$$a(\varphi) = \frac{\Omega^4}{\Omega^2 + 6\xi^2\varphi^2/M_P^2}, \quad \tilde{V}(\varphi) = V(\varphi)\Omega^{-4}, \quad (7.6)$$

and by $(\tilde{\partial}\varphi)^2$ we understand the kinetic term in which the partial derivatives are contracted with the transformed metric $\tilde{g}^{\mu\nu}$.

As before, we restrict the analysis to the $O(4)$ -symmetric configurations and apply the metric ansatz (6.13). We further require the configuration to obey the vacuum boundary conditions at infinity. To stay close to the actual Higgs physics, we allow the quartic coupling λ as a function of φ to develop a domain

of negative values at some magnitudes of φ . In this case, the asymptotics

$$f^2(r) \rightarrow 1, \quad \varphi(r) \rightarrow 0, \quad r \rightarrow \infty \quad (7.7)$$

do not represent the true vacuum state of the theory. The model (7.5) then admits the bounce interpolating between the regions of the true and false vacua. Due to its regularity at the origin, the bounce is not an euclidean configuration suitable for our purposes. However, as we will see, some of the singular shots exhibit properties resemble to those of the bounce; hence it is instructive to compare these types of configurations.

Apart from the possible bounce, the model (7.5) admits a family of singular shots that also satisfy the boundary conditions (7.7). To find their large- φ asymptotics, we write the equations of motion following from the Lagrangian (7.5) in the SI regime and with the ansatz (6.13) applied,

$$\partial_r \left(\frac{r^3 \varphi'}{\varphi f} \right) = 0, \quad f^2 = 1 - \frac{r^2 \varphi'^2}{6a_{SI} \varphi^2}, \quad (7.8)$$

where

$$a_{SI} = \frac{1}{1/\xi + 6}. \quad (7.9)$$

From this we deduce the behavior of the singular shots near the origin

$$\varphi \sim r^{-\gamma}, \quad \tilde{R} \sim r^{-6}, \quad \gamma = \sqrt{6a_{SI}}, \quad r \rightarrow 0. \quad (7.10)$$

This coincides with Eq. (6.17) upon the exponential change $\varphi \rightarrow e^{\tilde{\varphi}}$ of the scalar field variable.

7.2 Implementation of the mechanism

7.2.1 Making the instantaneous scalar field source

Let us see how one of the singular shots obtained above becomes a valid singular instanton contributing to the vev of the scalar field. According to the discussion in chapter 5, we make the change of variable

$$\varphi \rightarrow M_P e^{\tilde{\varphi}/M_P}. \quad (7.11)$$

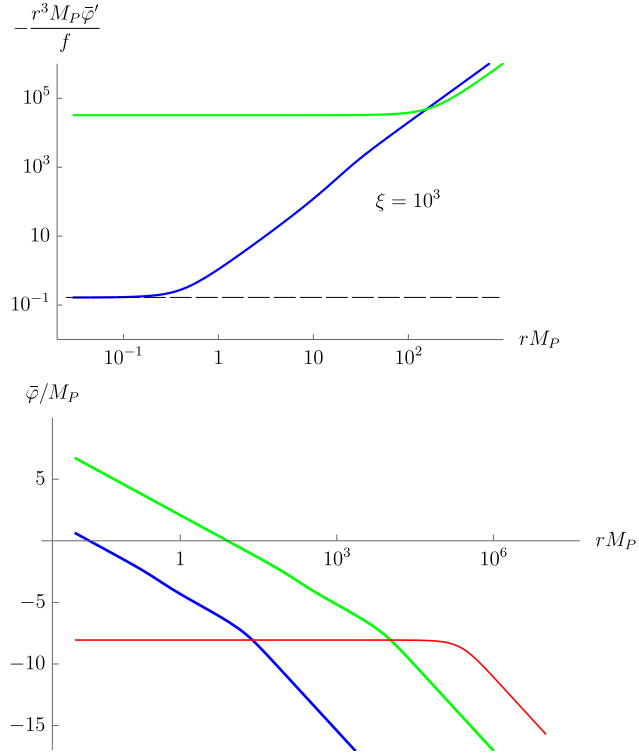


FIGURE 7.2: Two featured singular configurations of the model (7.5). The shot painted blue matches the scalar field source in the r.h.s. of Eq. (7.18), hence it is a valid singular instanton. The shot painted green is the one with the large euclidean action; for illustration, we choose for it $\bar{S}_E = 40$. We take the potential for the scalar field coinciding with the (RG-improved) Higgs potential in the SM with the central values of the top quark mass $m_t = 172.25$ GeV [36], the Higgs mass $m_H = 125.09$ GeV [35], and the field-dependent normalization point $\mu = \bar{\varphi}$. The top panel shows the short-distance asymptotics of the relevant combination of the fields, the dashed line marks the value $(6 + 1/\xi)^{-1}$. The bottom panel shows the behavior of $\bar{\varphi}$ as the singularity is approached. For illustrative purposes, the bounce is also plotted in red.

From Eq. (7.5) we see that $\bar{\varphi}$ is, in fact, a canonical variable for the scalar field in the limit $\varphi \gg M_P/\sqrt{\xi}$.² Therefore, we can endow Eq. (7.11) with the physical meaning by saying that it is $\bar{\varphi}$ that carries the valid dof of the scalar field at the large magnitudes of the latter. The field redefinition (7.11) results in the appearance of the desired source term in the process of evaluation of the vev $\langle \varphi \rangle$.

Introducing the source term as in Eqs. (6.18), (6.20), we find the modification of Eqs. (7.8) in the large- φ (or, equivalently, large- $\bar{\varphi}$) regime,

$$\partial_\rho \left(\frac{\rho^3 \bar{\varphi}'}{f a_{SI}} \right) = -\frac{1}{M_P} \delta(\rho), \quad f^2 = 1 - \frac{\rho^2 \bar{\varphi}'^2}{6 a_{SI} M_P^2}, \quad (7.12)$$

²Up to a coefficient of the order of one, according to Eq. (8.9).

where a_{SI} is given in Eq. (7.9), and the asymptotic behavior of the scalar field is now (cf. Eq. (6.21))

$$\bar{\varphi} = -M_P \sqrt{6a_{SI}} \log r M_P + C, \quad r \rightarrow 0 \quad (7.13)$$

with C a constant used to match with the asymptotics (7.7) at large r . We observe that the exponentiation of the φ -variable leads to the fixation of the position of the center of the singular shots and makes one of them the legitimate solution of the variational problem $\delta W / \delta \bar{\varphi} = 0$ with the boundary condition (7.7). To simplify the consideration, in the rest of the chapter we will work with the $\bar{\varphi}$ -variable in the entire range of magnitudes, bearing in mind that, by construction, it carries the valid dof only at $\bar{\varphi} \gtrsim M_P \log(1/\sqrt{\xi})$. We would like to use the singular instanton as a saddle point of the functional W , that contributes to the vev $\langle \varphi \rangle$. In the SPA, this amounts to saying that

$$\langle \varphi \rangle \approx M_P e^{-\bar{W}}, \quad (7.14)$$

where \bar{W} is the value of W computed on the instanton.

Formula (7.14) manifests the appearance of a new scale in the model (7.5). We are interested in the case when this scale is much smaller than the original scale M_P (or $M_P/\sqrt{\xi}$). For this to happen, one should require

$$\bar{W} \gg 1. \quad (7.15)$$

As was mentioned in chapter 5, the SPA is not applicable in the situation when \bar{W} is nearly zero or negative. The possible interpretation of this case is that the non-perturbative effects of quantum gravity are strong, and, hence, no new scale appears. If, on the other hand, Eq. (8.49) is fulfilled, these effects are suppressed, and the hierarchy of scales is generated. Our goal for the rest of this section is to find when it is possible to satisfy Eq. (8.49) in the model (7.5) or its modifications.

7.2.2 Attempting to compute the vev in the simple model

In trying to compute \bar{W} in the model (7.5), one immediately encounters multiple issues. We describe them here, and in section 7.2.3 and 7.2.4 the large- $\bar{\varphi}$ modifications of the model are studied with the aim to cure them.

(i) It is immediately seen from Eq. (7.13) that $\bar{\varphi}(0) = \infty$, hence \bar{W} is divergent. In order to extract a meaningful information about the contribution of the

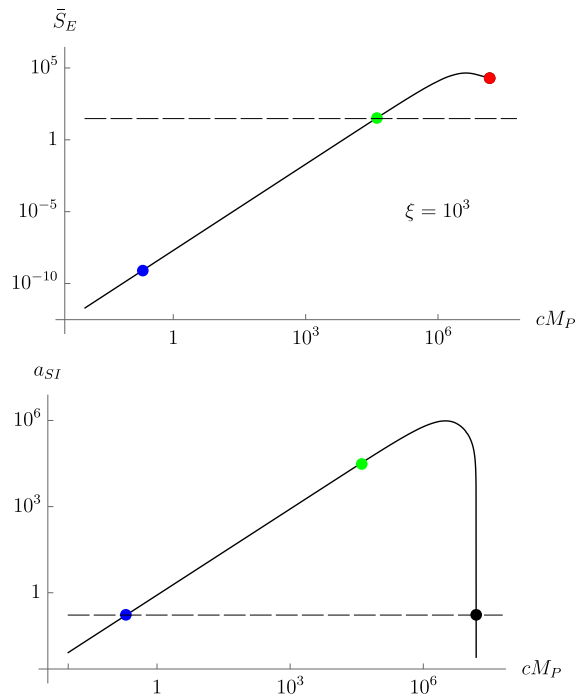


FIGURE 7.3: The family of singular configurations of the model (7.5), parametrized by their fall-off at infinity, $\varphi = cr^{-2}$, $r \rightarrow \infty$. We take the same potential for the scalar field as in Fig. 7.2. The colored circles correspond to the shots shown in Fig. 7.2. The top panel shows the euclidean action of the shot plotted against the parameter c , the dashed line corresponds to $\bar{S}_E = 40$. The bottom panel shows the value of the scalar field source necessary to match with the short-distance asymptotics of the solution, the dashed line corresponds to the value $(6 + 1/\xi)^{-1}$ (see Eq. (7.18)). The black circle indicates another singular instanton with the correct asymptotic behavior; contrary to other configurations, this instanton lies close to the bounce everywhere except the core, and its euclidean action is nearly the same as the one of the bounce. In the SPA, one should exclude this instanton from consideration in favour of the one with the small euclidean action.

singular instanton to the vev $\langle \varphi \rangle$, an accurate treatment of this divergence is required.

(ii) We did not present the semiclassical parameter that would justify the SPA made in arriving at Eq. (7.14). However, such justification can be made *a posteriori* provided that we have an explicit solution.

(iii) Let us compute the euclidean action of the singular instanton \bar{S}_E in the model (7.5). Making use of the Einstein equations, one obtains

$$\bar{S}_E = - \int d^4x \sqrt{\tilde{g}} \tilde{V}(\tilde{\varphi}). \quad (7.16)$$

If one leaves aside for the moment the issue with the singular term in W , then \bar{S}_E is to provide the desired suppression of the Planck scale in Eq. (7.14). This

would imply

$$\bar{S}_E \gg 1. \quad (7.17)$$

For \bar{S}_E to be positive, the field-dependent coupling constant λ must be negative at some values of $\bar{\varphi}$, thus admitting the bounce solution alongside with the instanton solution. Bearing in mind phenomenological applications of our analysis, we require the euclidean action of the bounce to be large enough in order to ensure the sufficiently large lifetime of the false vacuum. With this condition and the condition (8.9) implemented, we investigate numerically the singular shots obeying the asymptotics (7.7) and, in particular, the singular instanton for which

$$\frac{1}{a_{SI}} \frac{r^3 \bar{\varphi}'}{f} \rightarrow -\frac{1}{M_P}, \quad r \rightarrow 0. \quad (7.18)$$

The results of the analysis are presented in Fig. (7.2) and (7.3). We take $\xi = 10^3$, and the $\bar{\varphi}$ -dependence of λ as if it underwent the RG-running in the SM with the central values of the parameters of the latter.³ We observe that the requirement of the correct asymptotic behavior in the large- $\bar{\varphi}$ limit is in a sharp contrast with the requirement to have the large value of \bar{S}_E . In fact, the incompatibility of the two conditions cannot be overcome regardless the shape of the potential for the scalar field. The reason is that the singular instanton turns out to be insensitive to the details of the potential at low magnitudes of $\bar{\varphi}$, since it shoots too fast through this region of magnitudes, and no substantial contribution to the euclidean action can be produced. This forces us to conclude that in the model (7.5) it is impossible to make the singular shot with the conditions (7.17) and (7.18) both satisfied. The euclidean action of the singular instanton turns out to be nearly zero, the SPA is not applicable, and the non-perturbative effects are expected to drive the value of $\langle \varphi \rangle$ close to the Planck scale.

Problems (i) – (iii) pose serious obstacles to our analysis. The possible way out is to modify the model (7.5) in the large- $\bar{\varphi}$ regime. The necessity for such modification comes naturally once we notice that at $\xi \varphi^2 \ll M_P^2$ the Lagrangian (7.5), in fact, describes the low-energy limit of the theory we are ultimately interested in. Hence, considering different higher-dimensional operators supplementing the model (7.5) at large values of $\bar{\varphi}$ and its derivative is in agreement with the strategy of probing different possible UV properties of the theory reducing to the conformally-invariant SM and General Relativity at low energy scales, of which

³Here and below we assume that the RG-running of the non-minimal coupling ξ in the theory can be neglected. This is justified by noticing that ξ evolves rather slowly with the energy scale increasing, provided that it is always far from the conformal limit. Moreover, the results of our analysis will eventually be insensitive to the particular value of ξ .

proper UV completion we are not aware. The applicability limit of the low-energy description is determined by considering unitarity bounds of n -particles scattering amplitudes on top of the background vacuum configuration. The UV cutoff Λ of the model (7.5), determined in this way, is found to be [160–162]

$$\Lambda \sim M_P/\xi . \quad (7.19)$$

This justifies the usage of the Planck-suppressed in the low- $\bar{\varphi}$ limit operators which are composed of the scalar and the metric fields. Below we consider some particular classes of such operators in an attempt to improve the large- $\bar{\varphi}$ properties of the singular instanton and, eventually, to cure problems (i) – (iii).

7.2.3 Shaping the large-field limit with derivative operators

We would like to study how the short-distance behavior of the singular shots of the model of section 7.1 is changed when new operators are added into the model. We start by introducing an operator containing the higher degree of the derivative of the scalar field,

$$\mathcal{O}_n = \sqrt{g} \delta_n \frac{(\partial\varphi)^{2n}}{(M_P\Omega)^{4n-4}} \quad (7.20)$$

with Ω given in Eq. (7.4) and δ_n a dimensionless constant. The operator (7.20) is suppressed by M_P^{4n-4}/δ_n in the low-energy low- φ limit and becomes independent of M_P in the large- φ limit. For simplicity, here we limit the consideration to a single ($n = 2$)-operator. The general case will be commented on in section 7.4. Making the Weyl rescaling of the metric (7.4) and changing the variable according to Eq. (7.11), we obtain the modification of the model in the SI regime by the operator

$$\tilde{\mathcal{O}}_2 = \sqrt{\tilde{g}} \delta \frac{(\tilde{\partial}\bar{\varphi})^4}{M_P^4} , \quad \delta = \delta_2/\xi^2 , \quad (7.21)$$

and we assume $\delta \lesssim 1$. Note that the variation of the operator (7.21) with respect to $\bar{\varphi}$ is a total derivative; this simplifies significantly the analytical treatment of the singular shots in the model (7.5)+(7.21). Applying the ansatz (6.13), we obtain the modified equation of motion for the scalar field in the SI regime,

$$\frac{1}{a_{SI}} \frac{r^3 \bar{\varphi}'}{f} + \frac{4\delta}{M_P^4} \frac{r^3 \bar{\varphi}'^3}{f^3} = -\frac{1}{M_P} . \quad (7.22)$$

Denote by \bar{r} the size of the region in which the second term in the l.h.s. of Eq. (7.22) is dominant. The asymptotic behavior of the singular instanton in this

region is given by

$$\bar{\varphi}' \sim M_P^2 \delta^{-1/6}, \quad f \sim r M_P \delta^{1/6}, \quad r \lesssim \bar{r}. \quad (7.23)$$

First of all, we observe that $\bar{\varphi}$ is not divergent at the origin any more. Hence, the magnitude of the scalar field at the center of the instanton becomes finite. This cures problem (i) of section 7.2.2. Note that, despite being finite, the instanton remains to be singular; in particular, the scalar curvature in the E-frame behaves as

$$\tilde{R} \sim r^{-2}, \quad r \rightarrow 0, \quad \delta \neq 0. \quad (7.24)$$

Hence, the instantaneous source of the field $\bar{\varphi}$ is still necessary in obtaining the solution. Next, we notice that the core region $r \lesssim \bar{r}$ of the instanton provides a finite contribution to the euclidean action. Indeed, the latter becomes

$$\bar{S}_E = \int dr \bar{\mathcal{L}}, \quad \bar{\mathcal{L}} = 2\pi^2 r^3 f \left[\delta \frac{\bar{\varphi}'^4}{f^4 M_P^4} - \tilde{V}(\bar{\varphi}) \right], \quad (7.25)$$

where $\bar{\mathcal{L}}$ is the Lagrangian of the model (7.5)+(7.21), computed at the singular instanton. In the large- $\bar{\varphi}$ regime, it is given by

$$\bar{\mathcal{L}}|_{r \lesssim \bar{r}} = 2^{-4/3} M_P \delta^{-1/6}. \quad (7.26)$$

Finally, the total-derivative form of the scalar field equation of motion, given in Eq. (7.22), implies that the short-distance asymptotics of the solution (7.18), achieved in the SI sub-region well below M_P , remains unchanged once the operator (7.21) becomes important. Hence, according to the discussion in section 7.2.2, the low- $\bar{\varphi}$ part of the instanton cannot provide a suitable contribution to the euclidean action. As for the large- $\bar{\varphi}$ part, one would expect its contribution to be tunable by the parameter δ . However, from Eqs. (7.13), (7.22) and (7.23) it follows that

$$\bar{r} \sim M_P^{-1} \delta^{1/6} a_{SI}^{1/2}. \quad (7.27)$$

From this and Eq. (7.26) one now sees that \bar{S}_E does not experience any power-like dependence on δ . Note that this fact remains true for any operator of the form (7.20) inserted into Lagrangian (7.1), as well as for any analytic function summable from the series of such operators. Hence, for the model (7.5)+(7.21) one expects again $\langle \varphi \rangle$ to lie close to the Planck scale, and the question of how to generate the large value of W persists.

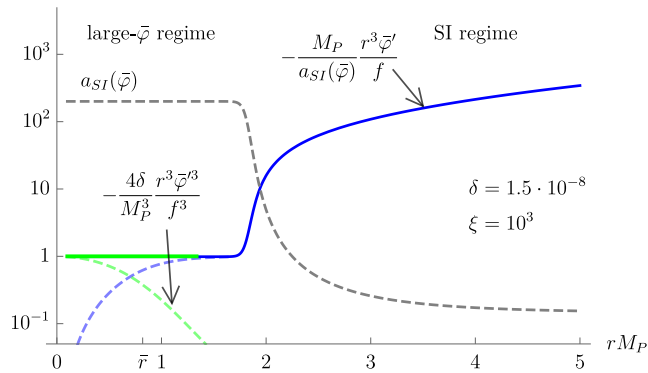


FIGURE 7.4: The l.h.s. of Eq. (7.22) in the units of M_P^{-1} and with a_{SI} given in Eq. (7.33). The solid line represents the sum of the two terms; it approaches M_P^{-1} but does not coincide with it unless a_{SI} freezes. The colored dashed lines show the contributions from each of the terms. The potential for the scalar field and the value of ξ are the same as in Fig. 7.2.

7.2.4 Making the hierarchy of scales with polynomial operators

Knowing the asymptotics of the scalar field in the large- $\bar{\varphi}$ and low- $\bar{\varphi}$ regions of the instanton, one can make a rude estimation of its magnitude at the center of the instanton. In the model (7.5)+(7.21) it is found to be

$$\bar{\varphi}(0)/M_P \sim a_{SI}^{1/2} (\log \delta - 3 \log a_{SI} + \mathcal{O}(1)). \quad (7.28)$$

From this and Eqs. (7.26), (7.27), we deduce the power-like dependence of \bar{W} on a_{SI} ,

$$\bar{W} \sim a_{SI}^{1/2}, \quad (7.29)$$

where we have made use of the fact that the contribution of the singular instanton to W outside the large- $\bar{\varphi}$ region is negligible.⁴ Hence, one can expect that the large values of W can be achieved by tuning the value of a_{SI} . However, from Eq. (7.9) we see that a_{SI} is confined in the region

$$0 < a_{SI} < 1/6, \quad (7.30)$$

which makes it impossible to fulfill relation (8.49). Hence, no hierarchy is generated in the model (7.5)+(7.21). The possible resolution of this issue is to look for further modifications of the model in the large- $\bar{\varphi}$ regime, that would lead to the modification of the allowable range of values of a_{SI} . To this end, consider

⁴In what follows, this will remain true.

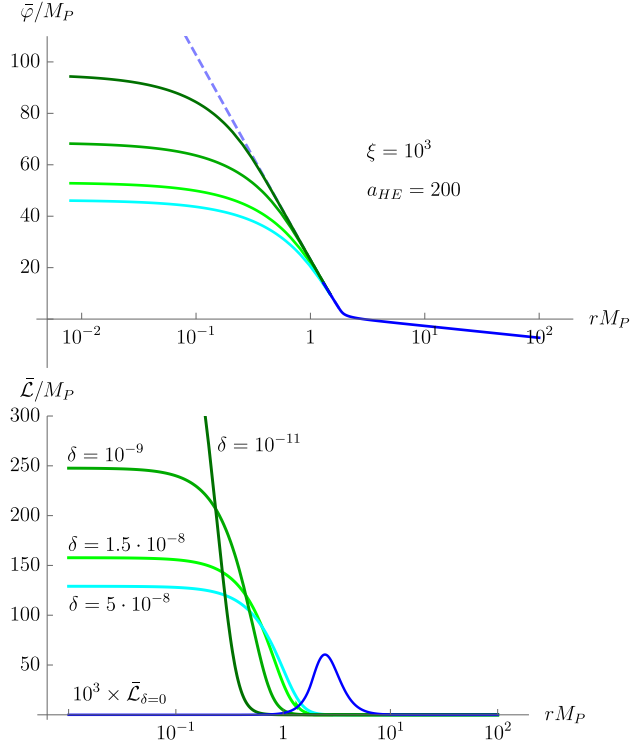


FIGURE 7.5: The family of singular instantons in the model specified by Eqs. (7.31), (7.32), to which the Weyl rescaling (7.4) is applied. The top panel demonstrates the finite short-distance asymptotics of the instantons, the dashed line shows the case $\delta = 0$. The bottom panel shows the corresponding Lagrangians. We observe an agreement with Eqs. (7.26) and (7.27). One also sees that the sizeable contribution to the euclidean action comes from the large- $\bar{\varphi}$ region. The potential for the scalar field and the value of ξ are the same as in Fig. 7.2.

the following Lagrangian,

$$\frac{\mathcal{L}_{\varphi,g}}{\sqrt{g}} = -\frac{M_P^2}{2}F(\varphi/M_P)R + \frac{1}{2}G(\varphi/M_P)(\partial\varphi)^2 + \delta\xi^2 \frac{(\partial\varphi)^4}{(M_P\Omega)^4} + \frac{\lambda}{4}\varphi^4, \quad (7.31)$$

where F and G are rational functions of φ/M_P taken so as to reproduce the Lagrangian (7.1) in the low- φ limit, and Ω is given in Eq. (7.4). The simplest, but not unique, possibility leading to the desired change of the range of a_{SI} , is to choose

$$F = 1 + \xi\varphi^2/M_P^2, \quad G = \frac{1 + \kappa\varphi^2/M_P^2}{1 + \varphi^2/M_P^2} \quad (7.32)$$

with κ some constant. Then, one can show that the coefficient a_{SI} becomes field-dependent,

$$a_{SI} = \frac{1}{\alpha/\xi + 6}, \quad (7.33)$$

where, in terms of the field variable $\bar{\varphi}$,

$$\alpha = \frac{1}{2}(1 - \tanh(\bar{\varphi}/M_P)) + \frac{\kappa}{2}(1 + \tanh(\bar{\varphi}/M_P)). \quad (7.34)$$

Hence, the asymptotic value of a_{SI} in the large- $\bar{\varphi}$ regime modifies to

$$a_{SI} \rightarrow a_{HE} = \frac{1}{\kappa/\xi + 6}, \quad r \rightarrow 0, \quad \bar{h} \gtrsim M_P, \quad (7.35)$$

as compared with Eq. (7.9). By tuning κ , one can make a_{HE} as large as necessary, thus “enhancing” the strength of the scalar field source by a suitable amount. Finally, Eq. (8.51) becomes

$$\bar{W} \sim a_{HE}^{1/2}. \quad (7.36)$$

Let us now study the singular instantons arising in the model specified by Eqs. (7.31), (7.32), to which the Weyl rescaling (7.4) is applied. For simplicity, we assume that the transition between the low- $\bar{\varphi}$ and the large- $\bar{\varphi}$ values of a_{SI} occurs before the asymptotics of the instanton becomes dominated by the quartic derivative term (7.21). This provides us with a separation of regions at which the quartic derivative operator and the polynomial operators start affecting the behavior of the solution. According to Eq. (7.27), the requirement of such separation puts an upper bound on δ ,

$$a_{HE}^{1/2} \delta^{1/6} \ll 1, \quad (7.37)$$

which can easily be satisfied in our analysis. Overall, we look for a classical configuration obeying the asymptotics (7.7) at large distances, and Eq. (7.22) with a_{SI} replaced by a_{HE} according to Eq. (7.35) — at short distances.

Bearing in mind the insensitivity of the singular shot to the details of the model below the large- $\bar{\varphi}$ regime, which was discussed in section 7.2.2, we focus on the variation of the large- $\bar{\varphi}$ parameters a_{HE} and δ . Then, numerics shows that it is possible for a fixed value of δ to choose a_{HE} so that relation (8.49) is satisfied. An example of the solution is presented in Fig. 7.4. As expected from the discussion in section 7.2.3, the variation of δ does not change the picture qualitatively. Fig. 7.5 exemplifies the difference in the large- $\bar{\varphi}$ behavior of the singular instanton and in the shape of the Lagrangian computed on it, as δ varies.

It is important to note that the euclidean action in the functional W is saturated in the large- $\bar{\varphi}$ domain, $\bar{\varphi} \gtrsim M_P$, and the contribution from the region of lower magnitudes of the scalar field is completely negligible. This is clearly seen from

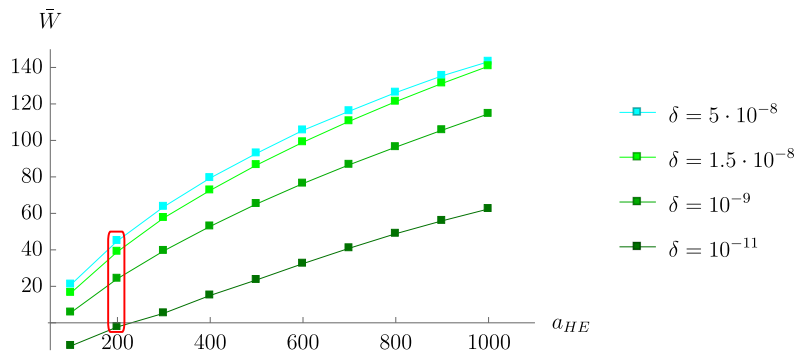


FIGURE 7.6: The instanton value of the functional \bar{W} plotted against the coefficient a_{HE} and with the different choices of the parameter δ . One observes the ambiguity in the choice of a_{HE} , δ leading to a given \bar{W} . The red frame marks the solutions studied in Fig. 7.5. The small deviations from the power-law behavior (7.36) are due to a sub-dominant dependence on a_{SI} and an imperfect separation of the region where a_{SI} varies from the region where the quartic derivative term dominates (see Eq. (7.37)).

the bottom side of Fig. 7.5, which shows the Lagrangian of the model as a function of the distance from the core of the instanton and at different values of δ . We conclude that the power-like estimation for the suppression exponent (7.36) is valid for our solutions; this is checked explicitly in Fig. 7.6, where \bar{W} is plotted against a_{HE} . Furthermore, $a_{HE}^{-1/2}$ can be seen as a small parameter whose appearance as a common multiplier in \bar{W} justifies the SPA made in obtaining Eq. (7.14). This observation resolves issue (ii) of section 7.2.2, thus completing the analysis.

7.3 Implications for the hierarchy problem

The results of the previous section are applied directly to the EW hierarchy problem. We consider the Lagrangian of section 7.2.4 as describing the Higgs-gravity sector of the theory under consideration. The real scalar field φ is identified with the Higgs field degree of freedom in the unitary gauge,

$$\phi = 1/\sqrt{2} (0, \varphi)^T. \quad (7.38)$$

The Higgs-gravity Lagrangian is supplemented with the rest of the low energy content of the theory. One can choose the latter to be that of the SM. All extra fields entering the theory are taken at their vacuum values. The fluctuations of the fields affect the prefactor which in Eq. (7.14) is chosen to be approximately equal to M_P . The validity of the SPA enables us to believe that the higher-order corrections to Eq. (7.14) do not change drastically the leading-order calculation.

Furthermore, Fig. 7.6 assures that any corrections coming from the prefactor can be compensated by readjusting the parameters of the theory. According to Eq. (7.14), the observed ratio of the Fermi scale to the Planck scale is reproduced when

$$\bar{W} = \log(M_P/v) \approx 37. \quad (7.39)$$

The singular instanton with this value of W is studied in Fig. 7.4.

One may wonder how the modifications brought to the Higgs-gravity sector by the derivative and polynomial operators affect the dynamics of the SM fields coupled to the Higgs field. The worrisome observation here is that the coefficient α in Eq. (7.33) appears in the Higgs field kinetic term of the lowest order after the Weyl rescaling of the metric is performed. If a_{HE} is demanded to be large enough for the mechanism to work, α becomes negative. When supplementing the Higgs-gravity Lagrangian with the rest of the SM fields, one replaces in the Higgs kinetic term

$$\partial_\mu \rightarrow \mathcal{D}_\mu. \quad (7.40)$$

This endangers the dynamics of the gauge fields, as the latter become tachyonic as soon as they interact with the Higgs field through the SM coupling terms only. This problem can be overcome by modifying suitably the coupling to the gauge fields at high energies. For example, adding the following operator

$$\frac{(\phi \overleftrightarrow{\mathcal{D}}_\mu \phi^\dagger)(\phi^\dagger \overleftrightarrow{\mathcal{D}}^\mu \phi)}{2\xi\phi^2 + M_P^2} \quad (7.41)$$

does the required job.

7.4 Summary

The model of section 7.2.4 is the one in which we have found the singular instanton with the large value of W . The reason we have provided the detailed exposition of other models is that we wanted to make clear the essential ingredients of the mechanism. It is their step-by-step implementation that guided us from the basic model (7.1) to the one described by Eqs. (7.31), (7.32). We list these ingredients in this short summary, while postponing a more general discussion to chapter 9.

- The non-minimal coupling of the scalar field to gravity, regulated by the parameter ξ . This coupling allowed us to change the variable according to

Eq. (7.11) and, eventually, to introduce the point source of the scalar field. In turn, the source provided us with an additional boundary condition selecting a unique solution from the family of singular configurations.

- The higher-dimensional operators of the form (7.20), which regularize the otherwise divergent solution. Adding such operators allowed us to avoid dealing with the divergence of the instanton at the source point.
- The source enhancement in the large field limit, performed by using the polynomial operators of the form (7.32). They enabled us to make a large value of W .

Regarding the last point, it is interesting to note that in the limit $a_{HE} \rightarrow \infty$, $\delta \rightarrow 0$ the model of section 7.2.4 acquires the Weyl symmetry in the large field region. To see this, we rewrite the Lagrangian of the model in the SI regime as follows,

$$\frac{\mathcal{L}_{\varphi,g,SI}}{\sqrt{g}} = \frac{1}{2} \frac{1}{6 - a_{HE}^{-1}} \varphi^2 R + \frac{1}{2} (\partial\varphi)^2 + \delta \frac{(\partial\varphi)^4}{\varphi^4}. \quad (7.42)$$

As a_{HE} grows and δ decreases, the Lagrangian approaches a Weyl-invariant point. Thus, in generating the hierarchy of scales, one can make use of the (approximate) asymptotic Weyl symmetry of the theory. As Fig. 7.6 demonstrates, the rate of suppression of the original scale M_P can, in fact, be arbitrarily large.

By construction, this mechanism does not require a fine-tuning among the coupling constants of the theory. In the model considered in section 7.2.4, the value of the ratio $\langle\varphi\rangle/M_P$ is mainly controlled by two parameters, a_{HE} and δ . Yet, already in this case, this value is degenerate in the parameter space, as Fig. 7.6 demonstrates. We would like to note that, because δ appears in Eq. (7.27) with the small fractional power, the small values of it are required to satisfy Eq. (7.37). This fact is not related to the original hierarchy problem, and the smallness of δ does not bring about new interactions scales much below M_P .

Let us stress again that the non-minimal coupling of the scalar field to gravity is one of the crucial parts of the mechanism. With this coupling preserved, one can expect instantons of a similar kind to exist in other scalar-tensor theories of gravity. In particular, being inspired by the idea of scale symmetry as a fundamental symmetry of Nature, it is tempting to study SI scalar-tensor theories that are reduced to the SM and General Relativity in the process of spontaneous breaking of the scale invariance. A notable example is the Higgs-Dilaton theory which we outlined in chapter 3. It is interesting to see if it also allows for non-perturbative generation of the parameter determining the Higgs field vev,

provided that the latter is classically zero. We proceed to this question in the next chapter.

Chapter 8

“Higgs+dilaton+gravity” models

In this chapter, we study the class of models containing two scalar fields coupled to gravity in a non-minimal way. For convenience, the scalar fields are arranged into a two-component vector $\vec{\varphi} = (\varphi^1, \varphi^2)^T$. We are interested in the case when the vev of one of the fields is classically non-zero and can be associated with the Planck scale. By studying singular instantons similar to those of the Dilaton model or the models of chapter 7, we will show how they can contribute to the vev of the second scalar field. These results will then be applied to the hierarchy problem within the setting of the Higgs-Dilaton theory.

Bearing in mind phenomenological applications of our analysis, we require for the models considered here to be convertible into a viable theory upon identifying one of its scalar field with the Higgs field dof and supplementing them with the rest of the SM content. We also require a model to enjoy global scale symmetry. As was mentioned in section 1.3, this can ensure the stability of the scalar fields vev against perturbative quantum corrections. Finally, the results of the previous studies give us the hints about the desirable structure of the model in the regime probed by the core of the singular instanton.

The chapter is organized as follows. The next section is dedicated to the analysis of singular solutions in a particular class of SI models of gravity. In section 8.2 we apply these solutions to compute the (classically zero) vev of one of the scalar fields. Section 8.3 contains an implication for the hierarchy problem. This chapter follows directly from chapter 6 and is essentially independent from chapter 7.

8.1 Instantons in scale-invariant gravity with two scalar fields

8.1.1 Model setup

Consider the following Lagrangian,

$$\begin{aligned} \frac{\mathcal{L}}{\sqrt{g}} = & -\frac{1}{2}\mathcal{G}(\vec{\varphi})R + \frac{1}{2}\gamma_{ij}^{(2)}(\vec{\varphi})g^{\mu\nu}\partial_\mu\varphi^i\partial_\nu\varphi^j \\ & + \sum_{n=2}^{\infty}\gamma_{i_1,\dots,i_{2n}}^{(2n)}(\vec{\varphi})g^{\mu\nu}\partial_\mu\varphi^{i_1}\partial_\nu\varphi^{i_2}\dots g^{\rho\sigma}\partial_\rho\varphi^{i_{2n-1}}\partial_\sigma\varphi^{i_{2n}} + V(\vec{\varphi}). \end{aligned} \quad (8.1)$$

It must be supplemented with the boundary term

$$I = - \int d^3x \sqrt{\gamma} K \mathcal{G}(\vec{\varphi}), \quad (8.2)$$

which is, however, unimportant for our purposes, according to the discussion in section 6.2, and we will omit it from now on. The model is required to be invariant under the global scale transformations

$$g_{\mu\nu}(x) \mapsto g_{\mu\nu}(qx), \quad \vec{\varphi}(x) \mapsto q\vec{\varphi}(qx), \quad (8.3)$$

and for the sake of simplicity we choose scaling dimensions of the scalar fields to be equal 1. Next, we require the model to admit the classical ground state with the constant value of the Ricci scalar and

$$\vec{\varphi}_{vac.} = \begin{pmatrix} \varphi_0 \\ 0 \end{pmatrix}. \quad (8.4)$$

Finally, the derivative part of the Lagrangian must be organized so that to avoid the appearance of ghosts. We will specify the latter condition quantitatively when we rewrite the model in the form which is more suitable for analytical analysis.

The functions introduced in the Lagrangian are taken as follows,¹

$$\begin{aligned}
 \mathcal{G} &= \xi_1 \varphi_1^2 + \xi_2 \varphi_2^2, \\
 \gamma_{ij}^{(2)} &= \delta_{ij} + \varkappa \mathcal{G} \mathcal{F} \mathcal{J}^{-4} (1 + 6\xi_i)(1 + 6\xi_j) \varphi_i \varphi_j, \\
 \gamma_{ijkl}^{(4)} &= \delta \mathcal{J}^{-8} (1 + 6\xi_i)(1 + 6\xi_j)(1 + 6\xi_k)(1 + 6\xi_l) \varphi_i \varphi_j \varphi_k \varphi_l, \\
 \gamma_{i_1 \dots i_{2n}}^{(2n)} &= 0, \quad n > 2.
 \end{aligned} \tag{8.5}$$

Here

$$\mathcal{J}^2 = (1 + 6\xi_1) \varphi_1^2 + (1 + 6\xi_2) \varphi_2^2, \tag{8.6}$$

$$\mathcal{F} = \frac{(1 + 6\xi_1) \varphi_2^2}{(1 + 6\xi_2) \varphi_1^2 + (1 + 6\xi_1) \varphi_2^2}, \tag{8.7}$$

and ξ_1 , ξ_2 , \varkappa and δ are constants. The potential for the scalar fields is chosen as

$$V = \frac{\lambda}{4} \varphi_2^4. \tag{8.8}$$

The comments are in order on this choice of the ingredients of the model. The first of Eqs. (8.5) represents the simplest compatible with the symmetries non-minimal coupling of the scalar fields to gravity. It is of the same form as in the Dilaton model, in which it was shown to lead naturally to the appearance of the scalar field source when evaluating its vev.

The second of Eqs. (8.5) specifies the quadratic in derivatives part of the scalar sector of the model. The parameter \varkappa controls its deviation from the canonical form. For the sake of simplicity, in sections 8.1.2–8.1.4 we consider the case $\varkappa = 0$, while the general case is postponed until section 8.1.5. There, we will see that \varkappa serves to regulate certain properties of the singular instanton and instanton action near the source, much in the same way as its counterpart in Eqs. (7.32).

The third of Eqs. (8.5) determines the quartic in derivatives kinetic term of the model. It is absent in the Dilaton model, and, similarly to the theories with one scalar field studied above, it plays a crucial role in controlling the short-distance behavior of the instanton. The derivative terms of higher degrees are set to zero, because the effect they produce is analogous to the one of the quartic term. We address this question in some detail in appendix B.

Finally, the scalar field potential (8.8) is chosen so as to be in accordance with a real-world theory in which φ_2 is to be identified with the Higgs field dof. For the

¹The indices of the components of the vector $\vec{\varphi}$ are raised and lowered with the euclidean metric δ_{ij} in the field space.

same reason, the coupling constant λ may be chosen to be field-dependent in a way that does not spoil the scale symmetry of the model. This dependence would mimic the RG evolution of the Higgs self-coupling in a realistic setting.² Note that we do not introduce the interaction terms $\propto \varphi_1^2 \varphi_2^2$ and $\propto \varphi_1^4$ into the classical potential, although their presence is allowed by scale symmetry. In other words, we require the scalar sector of the model to respect the “shift symmetry” of the dilaton field φ_1 . As will be discussed in section 8.3.1 on a concrete example, the shift symmetry protects the mass of φ_2 from radiative corrections.

Evidently, with the choice of the operators given above, the model is invariant under the scale transformations (8.3). Requiring the quadratic part of the kinetic terms for $\vec{\varphi}$ to be positive-definite puts a constraint on \varkappa , which will be specified below. The positive-definiteness of the derivative sector at high energies is ensured by setting $\delta > 0$. We also require

$$\xi_2 > \xi_1 > 0. \quad (8.9)$$

Last but not least, it is straightforward to see that Eq. (8.4) defines the classical ground state of the model, in which

$$\mathcal{G}(\vec{\varphi}_{vac.}) = \xi_1 \varphi_0^2 \equiv M_P^2. \quad (8.10)$$

8.1.2 Polar field variables

Let us rewrite the Lagrangian of the model in the form convenient for the analysis of classical configurations. As usual, we perform the Weyl rescaling of the metric,

$$\tilde{g}_{\mu\nu} = \Omega^2 g_{\mu\nu}, \quad \Omega^2 = \frac{\mathcal{G}(\vec{\varphi})}{\mathcal{G}(\vec{\varphi}_{vac.})}. \quad (8.11)$$

and obtain the E-frame Lagrangian in the form

$$\begin{aligned} \frac{\tilde{\mathcal{L}}}{\sqrt{\tilde{g}}} = & -\frac{1}{2} M_P^2 \tilde{R} + \frac{1}{2} \tilde{\gamma}_{ij}^{(2)}(\vec{\varphi}) \tilde{g}^{\mu\nu} \partial_\mu \varphi^i \partial_\nu \varphi^j \\ & + \gamma_{ijkl}^{(4)}(\vec{\varphi}) \tilde{g}^{\mu\nu} \tilde{g}^{\rho\sigma} \partial_\mu \varphi^i \partial_\nu \varphi^j \partial_\rho \varphi^k \partial_\sigma \varphi^l + \tilde{V}(\vec{\varphi}), \end{aligned} \quad (8.12)$$

²Recall that the field-dependence of a normalization point in RG equations is essential in maintaining the scale invariance of the theory at the perturbative quantum level, see section 3.2.2. Also, in what follows we neglect the running of other constants, since it does not change the results qualitatively.

where

$$\tilde{\gamma}_{ij}^{(2)} = \Omega^{-2} \left(\delta_{ij} + \frac{3}{2} M_P^2 \partial_i \log \Omega^2 \partial_j \log \Omega^2 \right), \quad \tilde{V}(\vec{\varphi}) = V(\vec{\varphi}) \Omega^{-4}, \quad (8.13)$$

and we made use of Eqs. (8.5) with $\varkappa = 0$.

Following the exposition of section 3.1, we now look for a suitable redefinition of the scalar field variables. To trace the actual scalar dof in the Lagrangian (8.12), we would like to bring the quadratic in derivatives part of the kinetic term to a diagonal form. In the new variables $\vec{\chi} = \vec{\chi}(\vec{\varphi})$, let the latter take the form

$$\frac{1}{2} \tilde{\gamma}_{nm}^{(2)}(\vec{\chi}(\vec{\varphi})) \tilde{g}^{\mu\nu} \partial_\mu \chi^n \partial_\nu \chi^m. \quad (8.14)$$

Then, one demands that

$$\tilde{\gamma}_{12}^{(2)}(\vec{\chi}(\vec{\varphi})) = 0, \quad (8.15)$$

which provides us with a first-order differential equation on the two components of the vector $\vec{\chi}$, thus leaving some freedom in the choice of new variables. It proves to be useful to choose χ^1, χ^2 in such a way that the scale transformations (8.3) leave one of the fields intact, while shifting another by a constant,

$$\chi^1 \mapsto \chi^1 + q, \quad \chi^2 \mapsto \chi^2. \quad (8.16)$$

From Eqs. (8.16) one sees that χ^1, χ^2 are reminiscent of polar coordinates on a plane on which the scale transformations act by an isotropic dilation by a factor q . To find an equation $\vec{\chi}(\vec{\varphi})$ must satisfy in this case, we make use of the Noether current associated with the scale invariance of the model. In view of Eq. (8.3), the latter is given by

$$\sqrt{\tilde{g}} J^\mu = \frac{\partial \tilde{\mathcal{L}}}{\partial \partial_\mu \varphi^i} \varphi^i. \quad (8.17)$$

For simplicity, let us put $\delta = 0$ for the moment. Then, on the one hand,

$$\begin{aligned} \sqrt{\tilde{g}} J^\mu &= \tilde{g}^{\mu\nu} \varphi^i \tilde{\gamma}_{ij}^{(2)}(\vec{\varphi}) \partial_\nu \varphi^j \\ &= M_P^2 \tilde{g}^{\mu\nu} \frac{\partial_\nu \mathcal{J}^2}{\mathcal{G}} \end{aligned} \quad (8.18)$$

with \mathcal{J}^2 given in Eq. (8.6). On the other hand, when expressed in terms of the variables $\vec{\chi}$ satisfying Eq. (8.16), the current becomes

$$\sqrt{\tilde{g}} J^\mu = M_P \tilde{g}^{\mu\nu} \tilde{\gamma}_{11}^{(2)}(\vec{\chi}(\vec{\varphi})) \partial_\nu \chi^1. \quad (8.19)$$

Equating (8.18) and (8.19), we obtain two more equations on $\vec{\chi}$. One can show

that they are compatible and, combined with Eq. (8.15), can be simultaneously solved. Denote this solution by $\chi^1 = \rho$, $\chi^2 = \theta$. Then, its explicit form is (cf. Eq. (3.22), (3.23))

$$\rho = \frac{M_P}{2} \log \frac{\mathcal{J}^2}{M_P^2}, \quad \theta = \arctan \left(\sqrt{\frac{1 + 6\xi_1 \varphi_2}{1 + 6\xi_2 \varphi_1}} \right). \quad (8.20)$$

It is now straightforward to derive the form of the Lagrangian in the new variables. It is given by

$$\begin{aligned} \frac{\tilde{\mathcal{L}}}{\sqrt{\tilde{g}}} = & -\frac{1}{2} M_P^2 \tilde{R} + \frac{1}{2a(\theta)} (\tilde{\partial}\rho)^2 + \frac{b(\theta)}{2} (\tilde{\partial}\theta)^2 \\ & + \delta \frac{(\tilde{\partial}\rho)^4}{M_P^4} + \tilde{V}(\theta) \end{aligned} \quad (8.21)$$

with

$$a(\theta) = a_0 (\sin^2 \theta + \zeta \cos^2 \theta), \quad b(\theta) = \frac{M_P^2 \zeta}{\xi_1} \frac{\tan^2 \theta + \xi_1/\xi_2}{\cos^2 \theta (\tan^2 \theta + \zeta)^2}, \quad (8.22)$$

$$\tilde{V}(\theta) = \frac{\lambda M_P^4}{4\xi_2^2} \frac{1}{(1 + \zeta \cot^2 \theta)^2}, \quad (8.23)$$

and

$$\zeta = \frac{(1 + 6\xi_2)\xi_1}{(1 + 6\xi_1)\xi_2}, \quad a_0 = \frac{1}{6 + 1/\xi_2}. \quad (8.24)$$

First, we note that, due to the invariance of the model under the scale transformations (8.16), the field ρ enters the Lagrangian only through derivatives. As we will see, this makes its role analogous to that of the field $\bar{\varphi}$ in the Dilaton model. Second, the form of the quartic derivative term becomes strikingly simple in the new variables. Its suppression by M_P is due to the classical vev which is now given by

$$\rho_{vac.} = \frac{M_P}{2} \log \frac{1 + 6\xi_1}{\xi_1}, \quad \theta_{vac.} = 0. \quad (8.25)$$

Hence, the higher-dimensional derivative term determines the structure of the theory at high energies. Regarding the classical analysis, this term starts to be important in the limit of large derivatives of the ρ -component of the instanton and, hence, is expected to change the behavior of the latter in this limit.

As was already mentioned, the fields ρ and θ can be thought of as polar coordinates on the plane spanned by $\sqrt{1 + 6\xi_1}\varphi_1$ and $\sqrt{1 + 6\xi_2}\varphi_2$. In particular, θ is analogous to the angle on that plane, and ρ — to the logarithm of the radius.

Because of this, in what follows we will refer to ρ as the radial and to θ as the angular field variables.

Let us finally quote the inverse formulas,

$$\varphi_1 = \frac{M_P \cos \theta}{\sqrt{1 + 6\xi_1}} e^{\rho/M_P}, \quad \varphi_2 = \frac{M_P \sin \theta}{\sqrt{1 + 6\xi_2}} e^{\rho/M_P}. \quad (8.26)$$

One observes that the original scalar fields are expressed through the exponent of the field ρ . Hence, according to the discussion in chapter 5, the source of the radial field naturally appears in the course of evaluation of the vev of φ_2 .³ This points again at the similarity between ρ and the field $\bar{\varphi}$ of the Dilaton model.

Note also that from Eq. (8.1) and the first of Eqs. (8.5) it follows that in the limit when φ_1 and φ_2 vanish simultaneously the model is not well-defined. The classical configurations we study below avoid this point; in fact, for them

$$\rho \geq \rho_{vac.}. \quad (8.27)$$

8.1.3 Instanton in a model without higher-dimensional terms

We begin to study classical configurations arising in the model specified by Eqs. (8.21)—(8.24). As in the previous chapters, we restrict ourselves to the analysis of $O(4)$ -symmetric configurations and choose the metric ansatz as in Eq. (6.13). The configuration must approach the classical ground state (8.25) at infinity. Since the quartic derivative term affects only the short-distance part of the instanton, it is convenient to study first the case when $\delta = 0$.

From Eq. (8.21) we obtain the equation of motion for the radial field ρ ,

$$\partial_r \left(\frac{\rho' r^3}{a(\theta) f} \right) = 0, \quad (8.28)$$

which is fully analogous to Eq. (6.14). Thanks to the form of the metric ansatz and the fact that ρ enters the Lagrangian derivatively, both ρ' and f can be expressed explicitly through the angular field θ and its derivatives. Therefore, finding a solution reduces to solving a single second-order differential equation on θ . Switching on the source of ρ selects a unique solution from the family of singular shots obeying Eq. (8.28). In view of Eqs. (8.26), we specify the source

³Although the change of variables (8.26) is applicable for all $\vec{\varphi} \neq \vec{0}$, one can think of ρ, θ as replacing the original scalar dof in the regime where the latter are not canonical, $|\varphi_1 - \varphi_0| \gtrsim \varphi_0$, $|\varphi_2| \gtrsim \varphi_0$.

as follows,

$$W = S - \int d^4x \delta^{(4)}(x) \rho(x) / M_P . \quad (8.29)$$

Equation of motion becomes

$$\frac{\rho' r^3}{f} = -\frac{a(\theta)}{M_P} . \quad (8.30)$$

Let us focus on the classical configurations satisfying Eq. (8.30) and approaching the ground state (8.25) at infinity. The large-distance asymptotics of these solutions are inferred directly from equations of motion, they coincide with the ones of the massless fields,⁴

$$\rho - \rho_0 \sim r^{-2} , \quad \theta \sim r^{-2} , \quad r \rightarrow \infty . \quad (8.31)$$

We now turn to the short-distance behavior of the solutions. We require the fields constituting the instanton to behave monotonically with the distance. Then, the angular field must have a definite limit $\theta \rightarrow \theta_0$ at $r \rightarrow 0$. Inspecting Eq. (8.30) and 00-component of the Einstein equations reveals that

$$\rho \sim -\gamma M_P \log M_P r , \quad \tilde{R} \sim r^{-6} , \quad r \rightarrow 0 , \quad (8.32)$$

where \tilde{R} is the Ricci scalar in the E-frame and

$$\gamma = \sqrt{6a_0} . \quad (8.33)$$

We conclude that ρ carries the same properties as the scalar field $\bar{\varphi}$ in the Dilaton model.

In looking for allowable values of θ_0 , we made use of the analysis of the bounce performed in chapter 3. There, it was shown that the finite values of θ_0 , different from $\pi k/2$, $k = 0, 1, 2, \dots$, are possible only if one requires

$$\rho' = 0 . \quad (8.34)$$

The singular instanton we are interested in here violates this condition, hence it differs qualitatively from the possible bounce. One can show that the only admissible values of θ_0 for this solution are

$$\theta_0 = \frac{\pi}{2} + \pi k , \quad k = 1, 2, \dots \quad (8.35)$$

⁴Note that self-consistency dictates the fields to approach the values corresponding to the actual vev of φ_1, φ_2 . The difference can be neglected on practice provided that the characteristic size of the configuration contributing to the vev is much smaller than $\langle \varphi_2 \rangle^{-1}$.

We focus on the case $k = 0$, since, as will be seen shortly, this is the only case when the configuration approaching the ground state at infinity exists. Then, one has

$$a(\theta_0) = a_0 . \quad (8.36)$$

Recall that $a(\theta_0)$ regulates the strength of the source felt by the radial field. The short-distance asymptotics of θ is found to be

$$\frac{\pi}{2} - \theta \sim r^\eta , \quad r \rightarrow 0 \quad (8.37)$$

with

$$\eta = \sqrt{6a_0(1 - \xi_1/\xi_2)} , \quad (8.38)$$

provided that inequality (8.9) holds. The exponents (8.33) and (8.38) demonstrate essential non-analyticity of the configuration in the core region, caused by the presence of the source. The solution satisfying Eqs. (8.31), (8.32) and (8.37) is the singular instanton of the theory specified by Eqs. (8.21)—(8.24) with $\delta = \varkappa = 0$.

To understand better the properties of the singular instanton near the source, we write its asymptotics in terms of the original field variables,

$$\varphi_1 \sim r^{-\gamma+\eta} , \quad \varphi_2 \sim r^{-\gamma} . \quad (8.39)$$

Since $\eta < \gamma$, we conclude that both fields diverge at the center of the instanton. It is important to note that the divergence of φ_1 , φ_2 originates fully from the divergence of the radial field. Hence, Eqs. (8.26) provide a splitting of the scalar fields on the singular exponential part and the finite angular prefactor. The core region of the instanton is determined by the relation $|\varphi_2| \gg |\varphi_1|$ or, equivalently, $|\partial\varphi_2| \gg |\partial\varphi_1|$.

As an example, Fig. 8.1 shows the singular instanton for a particular choice of parameters of the model. The solution is found by solving numerically equation for θ , by the means of shooting. For illustrative purposes, the configurations with no limit of θ at $r \rightarrow 0$ are also shown. One can see that only for $\theta_0 = \pi/2$ does the solution have the appropriate large-distance behavior.

The singular instanton of the type found above exists regardless the shape of the potential for the field θ , encoded in the function $\lambda = \lambda(\theta)$. It is so because the potential does not affect neither long-distance nor short-distance asymptotics of the solution. Note also that Fig. 8.1 demonstrates the difference of the singular instanton from the possible bounce, which is noticeable even in the limit $r \rightarrow \infty$.

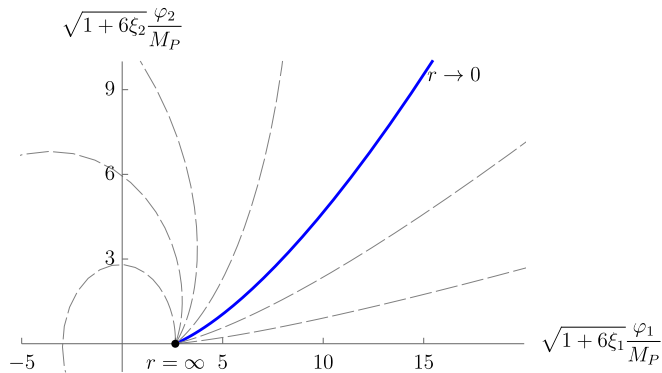


FIGURE 8.1: The classical configurations of the model (8.21)–(8.24), satisfying the vacuum boundary conditions, Eq. (8.31), at infinity. The solid blue line represents the singular instanton obeying Eqs. (8.32), (8.37). It is the only configuration with the finite asymptotics of θ . The dashed lines are examples of other singular shots. All solutions are distinguished by their fall-off at infinity, $\theta \sim cr^{-2}$, $r \rightarrow \infty$. The parameter c is used as a shooting parameter in numerical calculations. The parameters of the model are $\xi_1 = 1$, $\xi_2 = 1.1$ and $\delta = \lambda = 0$.

Indeed, from Eqs. (8.26) and (8.34) we see that for the bounce in this limit $d\varphi_2/d\varphi_1 \rightarrow \infty$, while for the instanton the ratio remains finite.

8.1.4 Regularization of the instanton by a higher-dimensional term

Let us now switch on the Planck-suppressed quartic derivative operator in the Lagrangian (8.21). As compared to the Dilaton model, it gives us a new ingredient, analogous to the operator (7.21) of the one-scalar field theory. Importantly, the variation of this operator with respect to ρ is a total derivative, hence, equation of motion for ρ following from varying the functional (8.29) takes the form

$$\frac{4\delta}{M_P^4} \frac{\rho'^3 r^3}{f^3} + \frac{\rho' r^3}{a(\theta)f} = -\frac{1}{M_P}. \quad (8.40)$$

This is again an exact equation. Denote by \bar{r} the size of the region where the first term in Eq. (8.40) is dominant. In what follows, we will choose δ to be such that the length \bar{r} is well within the region where $a(\theta)$ does not differ noticeably from its asymptotic value a_0 . This will allow us to neglect the dynamics of the angular field when discussing the effects of the higher-dimensional operator on the behavior of the instanton. Note also that the interpretation of a_0 as the parameter regulating the strength of the source is preserved, since the short-distance asymptotics defined by Eq. (8.30) develops before the first term in Eq. (8.40) comes into play.

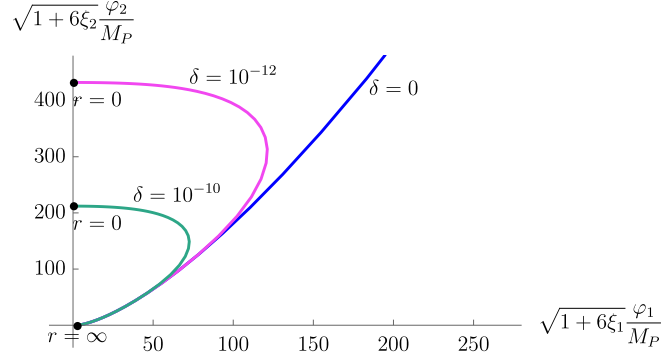


FIGURE 8.2: The family of singular instantons of the model (8.21)–(8.24), corresponding to different values of the parameter δ in the higher-dimensional derivative term. One observes that this derivative term regularizes the logarithmic divergence of the radial field and makes the latter finite at the center of the instanton. The parameters of the model are $\xi_1 = 1$, $\xi_2 = 1.1$ and $\lambda = 0$.

At $r \lesssim \bar{r}$, the behavior of the singular instanton is

$$\rho' \sim -M_P^2 \delta^{-1/6}, \quad f \sim M_P r \delta^{1/6}. \quad (8.41)$$

From this and Eqs. (8.40) and (8.32) one can infer the value of \bar{r} ,

$$\bar{r} \sim M_P^{-1} \delta^{1/6} a_0^{1/2}. \quad (8.42)$$

The crucial observation is that, thanks to the first of Eqs. (8.41), the radial field is not divergent any more, and its magnitude at the center of the instanton is finite. It can be estimated from Eqs. (8.32), (8.41) and (8.42) that (cf. Eq. (7.28))

$$\rho(0)/M_P \sim a_0^{1/2} (\log \delta - 3 \log a_0 + \mathcal{O}(1)). \quad (8.43)$$

Despite the finiteness, the instanton remains to be singular. In particular, the scalar curvature in the E-frame behaves as

$$\tilde{R} \sim r^{-2}, \quad r \rightarrow 0, \quad \delta \neq 0. \quad (8.44)$$

Therefore, introducing the source of the radial field is still a necessary step in obtaining the solution.

An example of how the higher-dimensional term regularizes the divergence of the instanton is presented in Fig. 8.2. Because of Eqs. (8.41), the small values of δ are required to ensure the separation of the region where $a(\theta)$ varies from the region where the regularization acts. Note, however, that the smallness of δ does not bring in the model any new interaction scales below the Planck scale.

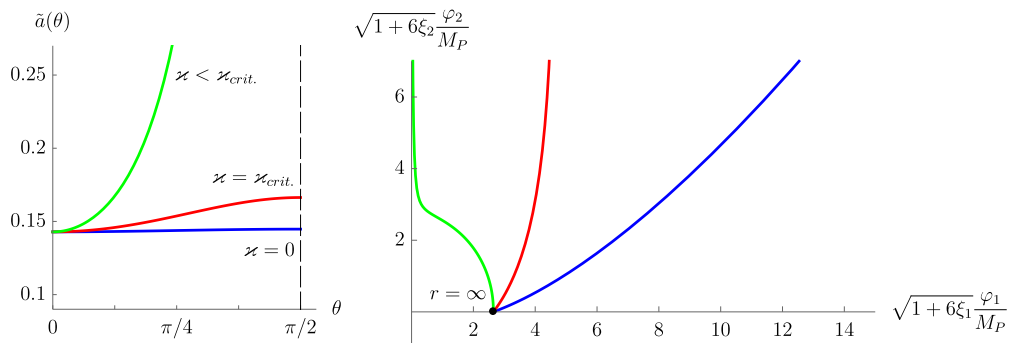


FIGURE 8.3: The singular instantons of the model (8.21)—(8.24) with $a(\theta)$ replaced by $\tilde{a}(\theta)$ according to Eq. (8.46), and with \varkappa varied. The left panel shows the function $\tilde{a}(\theta)$. In the limit $\varkappa = 0$, the original model is reproduced. The critical value, $\varkappa = \varkappa_{crit.}$, corresponds to the case when $\eta = \gamma$ in Eqs. (8.39), see appendix C for details. The value below the critical, $\varkappa < \varkappa_{crit.}$, is chosen so that $\tilde{a}(\theta_0) \equiv \tilde{a}_0 = 100$. This value lies close to the positivity bound in Eq. (8.47). The right panel shows the corresponding instanton solutions. At $\varkappa = 0$, the instanton studied in Fig. 8.1 and 8.2 is reproduced. The parameters of the model are $\xi_1 = 1$, $\xi_2 = 1.1$ and $\lambda = 0$.

8.1.5 Source enhancement

From Eq. (8.43) one sees that the parameter $a_0 = a(\theta_0)$, alongside with δ , controls the large- ρ properties of the singular instanton. In the model (8.21)—(8.24), the value of a_0 is determined by the non-minimal coupling ξ_2 and, according to Eq. (8.24), is confined in the region

$$0 < a_0 < 1/6. \quad (8.45)$$

Since a_0 is associated with the strength of the source of the radial field, it is important to investigate the possibility that it can take values other than those prescribed by inequality (8.45). In particular, we are interested in making the upper bound in this inequality arbitrarily large. This can be achieved by switching on the parameter \varkappa in Eqs. (8.5), which was set to zero in the previous analysis. Starting from the Lagrangian in the form (8.1), we follow the steps performed in section 8.1.2 to obtain the description of the modified model in terms of the polar field variables. It is straightforward to see that the modified Lagrangian is still given by Eq. (8.21), but with the function $a(\theta)$ replaced by a new function $\tilde{a}(\theta)$ so that

$$\frac{1}{\tilde{a}(\theta)} = \frac{1}{a(\theta)} + \varkappa \sin^2 \theta. \quad (8.46)$$

As θ approaches the vacuum value, $\tilde{a}(\theta)$ becomes indistinguishable from $a(\theta)$, hence the properties of the model near the ground state remain unchanged. In

particular, the large-distance properties of the singular instanton are independent of \varkappa .

Let us focus on the short-distance behavior of the instanton solution. One can make sure that the asymptotic value of θ obeys Eq. (8.35) with $k = 0$ regardless the presence of \varkappa . Requiring the quadratic in derivatives part of the Lagrangian to be positive-definite yields

$$\varkappa > -\frac{1}{a_0}. \quad (8.47)$$

Varying \varkappa within this region, one can achieve any positive strength of the radial field source $\tilde{a}_0 \equiv \tilde{a}(\theta_0)$.

In Fig. 8.3 some particular values of \varkappa are considered. One observes that the properties of the singular instanton at short distances depend significantly on the choice of \varkappa . The dependence is encoded in the exponents γ and η whose form for $\varkappa \neq 0$ is not given by Eqs. (8.32), (8.37) any more. Leaving the quantitative analysis to appendix C, here we just note that η exceeds γ for \varkappa lying close to the bound specified by Eq. (8.47). From Eq. (8.39) we see that in this case the field φ_1 tends to zero as the source is approached even without the regularization provided by the quartic derivative term. The latter, however, is still necessary to remove the divergence of the field φ_2 .

We would like to stress that the explicit form of the function $\tilde{a}(\theta)$ resulting in a particular source strength \tilde{a}_0 is, in fact, a matter of convenience, provided that the properties of the model near the ground state are respected. We choose this function according to Eq. (8.46) because of the simple form it takes in the polar field variables and because it will fit well into the phenomenological analysis of section 8.3. Finally, the effect produced by the quartic derivative term remains unchanged as long as $\tilde{a}(\theta)$ approaches the asymptotic value before this term takes over.

To summarize, in sections 8.1.3–8.1.5 we have constructed and studied the singular instantons arising in the class of SI models specified by Eqs. (8.1) and (8.5)–(8.8). The principal difference of these models from the one-field Dilaton theory of chapter 6 is the presence of two parameters, \varkappa and δ , associated with the structure of the theory at high energies, which determine its properties in the regime when $|\varphi_2| \gg |\varphi_1|$ and $|\partial\varphi_2| \gg |\partial\varphi_1|$. Their roles are quite analogous to those in the theories of chapter 7. Namely, the parameter δ serves to regularize the logarithmic divergence of the radial field and to make $\rho(0)/M_P$ finite. We will now see how the parameter \varkappa affects the properties of the instanton at short distances in the models under investigation.

8.2 New scale via the instanton

As was already discussed, the ground state (8.4) provides us with a single mass parameter $\varphi_0 \approx M_P$ at the classical level, at least when the non-minimal couplings ξ_1, ξ_2 are of the order of one. We would like to see if the singular instantons obtained before can generate a new scale, by contributing non-perturbatively to the vev of φ_2 . We are interested in the case when the contribution is such that the hierarchy

$$\langle \varphi_2 \rangle / \langle \varphi_1 \rangle \ll 1 \quad (8.48)$$

emerges.

Following the reasoning of chapter 5, we attempt to evaluate the vev of φ_2 with the new functional W . The latter is defined in Eq. (8.29). The appropriate saddle points of W are the singular instantons studied above. We will investigate if it is possible to adjust the parameters of the model to yield

$$\bar{W} \gg 1, \quad (8.49)$$

where \bar{W} is the instanton value of W . Applying the SPA, one arrives at

$$\langle \varphi_2 \rangle \sim M_P e^{-\bar{W}}. \quad (8.50)$$

If for a particular choice of the parameters the condition (8.49) is violated, one concludes that the SPA is not applicable and Eq. (8.50) is not valid. In this case one can conclude that non-perturbative quantum gravity effects are strong and drive the value of $\langle \varphi_2 \rangle$ close to M_P so that no new scale appears. If, on the other hand, Eq. (8.49) is satisfied, these effects are suppressed, and the hierarchy of scales (8.48) is generated. Note that the Planck mass appears as a prefactor in Eq. (8.50), as it is the only classical scale of the model.

Let us proceed to computation of \bar{W} . Since the potential \tilde{V} , given in Eq. (8.23), tends to zero when θ approaches its vacuum value, the geometry of the solution is asymptotically flat and the ground state action is zero. Contributions to \bar{W} come from the source term and the instanton action \bar{S} . Making use of the Einstein equations and applying the ansatz (6.13), we have

$$\bar{W} = -\frac{\rho(0)}{M_P} + \int_0^\infty dr (\bar{\mathcal{L}}_\delta - \bar{\mathcal{L}}_V), \quad (8.51)$$

where

$$\bar{\mathcal{L}}_\delta = 2\pi^2 r^3 f \left(\frac{\rho'}{M_P f} \right)^4, \quad \bar{\mathcal{L}}_V = 2\pi^2 r^3 f \tilde{V}(\theta). \quad (8.52)$$

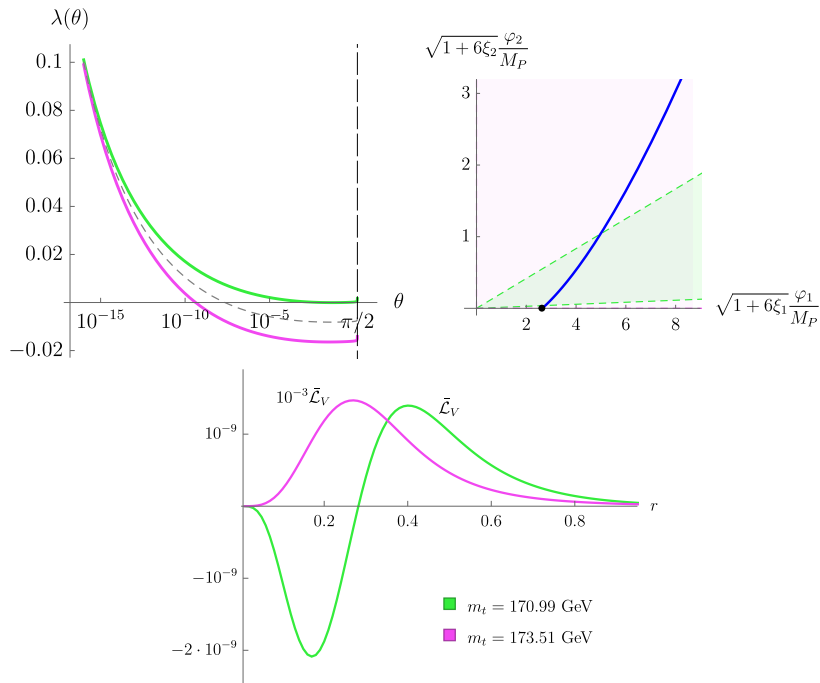


FIGURE 8.4: Top left: the SM Higgs self-coupling $\lambda(\hat{\mu})$ at NNLO with the θ -dependent momentum scale $\hat{\mu}$ given in Eq. (8.53). The RG equations are solved using the code based on [29, 72]. The solid lines represent the 2σ -uncertainty region of the top quark mass, the dashed line corresponds to the central value $m_t = 172.25$ GeV [36]. The Higgs mass is taken to be $m_H = 125.09$ GeV [35]. Top right: the singular instanton in the potential (8.23) with λ plotted on the left side. The dashed lines encompass the regions of negative λ . One observes no difference between the solutions corresponding to the different choices of λ . Bottom: the potential part of the instanton Lagrangian, see Eq. (8.52). One sees the contribution from $\bar{\mathcal{L}}_V$ to the instanton action \bar{S} to be negligible compared to the overall contribution which is supposed to give $\bar{S} \gg 1$. The parameters of the model are $\xi_1 = 1$, $\xi_2 = 1.1$.

We will study separately the contributions from the long-distance and short-distance parts of the instanton. The dominant term in the long-distance region is the one provided by the potential, $\bar{\mathcal{L}}_V$. According to Eq. (8.23), it is mainly determined by the quartic coupling λ . Bearing in mind phenomenological applications of our analysis, we consider λ as a function of θ in order to mimic the RG evolution of the Higgs self-coupling in the SM setting.⁵ Specifically, we take the running of λ corresponding to the 2σ -uncertainty region around the central value of the top quark mass $m_t = 172.25$ GeV [36], and to the central value of the Higgs mass $m_H = 125.09$ GeV [35]. The field-dependent momentum scale $\hat{\mu} = \hat{\mu}(\theta)$ is chosen according to the prescription (see section 3.2.2)

$$\hat{\mu}^2 = \frac{y_t^2 M_P^2}{2\xi_2} \frac{1}{1 + \zeta \cot^2 \theta}, \quad (8.53)$$

⁵The dependence of the self-coupling on the radial field would be inconsistent with the (quantum perturbative) scale invariance of the theory.

where y_t is the top quark Yukawa coupling and ζ is given in Eq. (8.24). With the potential specified in this way, we find the singular instanton numerically and compute its contribution to the potential part of the Lagrangian $\bar{\mathcal{L}}_V$. The results of the computation are shown in Fig. 8.4. The main observation is that the potential term contributes negligibly to the instanton action. The reason lies in the fact that the instanton shoots too fast through the region where the action can be saturated by $\bar{\mathcal{L}}_V$. Hence, provided that we are interested in the total contribution to satisfy inequality (8.49), one can safely ignore the potential term in Eq. (8.51). Note that this result points again at the qualitative difference between the singular instanton and the bounce for which the overall contribution comes exclusively from the potential.

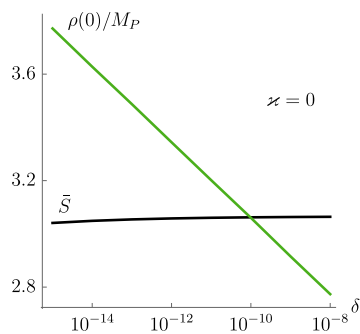


FIGURE 8.5: The singular term $\rho(0)/M_P$ and the instanton action $\bar{S} = \int dr \bar{\mathcal{L}}$, contributing to \bar{W} according to Eq. (8.51). Here we take $\varkappa = 0$ and $\xi_1 = 1$, $\xi_2 = 1.1$. The left panel shows the two contributions depending on the choice of δ . One sees that, although \bar{W} is positive for $\delta \gtrsim 10^{-10}$, it is impossible to achieve the regime when $\bar{W} \gg 1$.

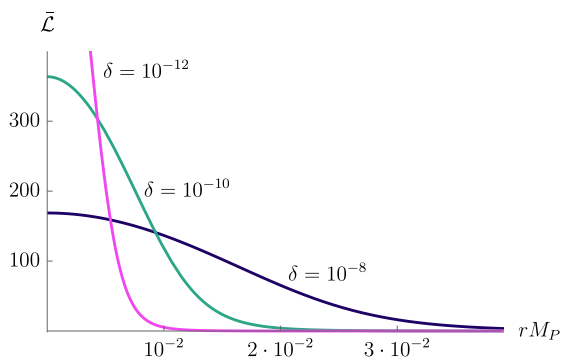


FIGURE 8.6: Instanton Lagrangian $\bar{\mathcal{L}}$ as a function of the radial coordinate and for different values of δ . The parameters are the same as in Fig. 8.5. An agreement with Eqs. (8.42) and (8.54) is observed.

The net contribution of the short-distance part of the instanton is determined by a balance between the source term coming with the negative sign in Eq. (8.51) and the positive quartic derivative term. As Fig. 8.5 demonstrates, the difference between the two terms can be of either sign. Having confined ourselves in the region of parameters for which this difference is positive, one can try to amplify

\bar{W} by the means of some small constant justifying the SPA. An obvious candidate for such a constant is the parameter δ appearing in the quartic derivative term. However, from Eqs. (8.41) and (8.52) it follows that (see Fig. 8.6)

$$\bar{\mathcal{L}}_\delta|_{r \lesssim \bar{r}} \sim M_P \delta^{-1/6}. \quad (8.54)$$

From this and Eqs. (8.42) and (8.43) one now sees that \bar{W} , in fact, does not contain any power-like dependence on δ . This can also be inferred from Fig. 8.5, where the dependencies of the instanton action \bar{S} and of the maximum value of the radial field $\rho(0)/M_P$ on δ are shown.

It turns out that the suitable semiclassical parameter can be provided by the asymptotics \tilde{a}_0 of $\tilde{a}(\theta)$. Indeed, from Eqs. (8.42), (8.43) and (8.52) one obtains that

$$\bar{W} \sim \sqrt{\tilde{a}_0}, \quad (8.55)$$

where we have made use of the fact that the contribution of the singular instanton to W outside the large- ρ region is negligible. As was discussed in section 8.1.5, in the models under consideration the large \tilde{a}_0 can be achieved by choosing the parameter \varkappa to lie close to the bound in Eq. (8.47). In this case, \tilde{a}_0^{-1} is the desired small parameter arising when computing the instanton value of W . In Fig. 8.7 and 8.8 we study the behavior of \bar{W} as δ and \tilde{a}_0 vary. While the dependence on δ is seen to be logarithmic, in accordance with Eq. (8.43), the dependence on \tilde{a}_0 is power-like and matches the analytical estimation (8.55). Note also that Eq. (8.55) is valid assuming that the length scale $r \sim \bar{r}$ at which the quartic derivative operator becomes dominant is smaller than the characteristic length at which the function $\tilde{a}(\theta)$ changes, and it is this fact that enabled us to replace the latter by the asymptotic value \tilde{a}_0 in Eq. (8.42).

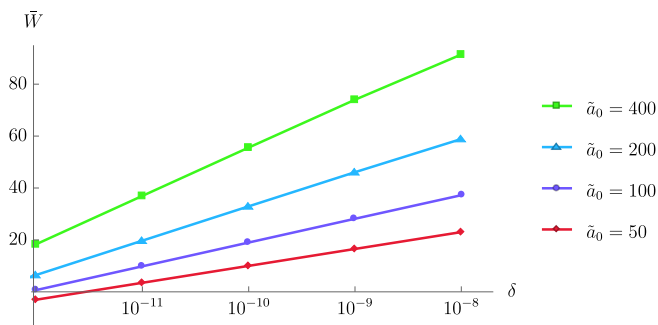


FIGURE 8.7: The suppression rate \bar{W} as a function of δ and for several choices of \tilde{a}_0 . One observes the logarithmic dependence, which excludes the possibility to treat δ as a semiclassical parameter.

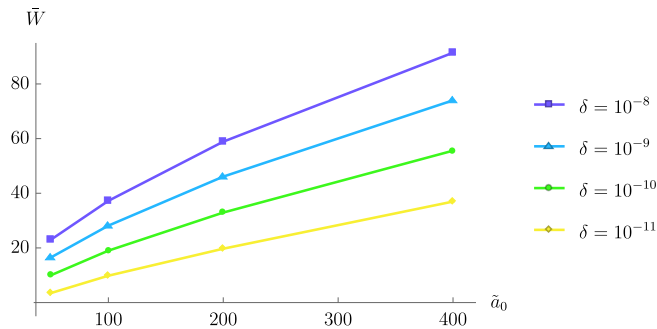


FIGURE 8.8: The suppression rate \bar{W} as a function of \tilde{a}_0 and for several choices of δ . One observes the power-like behavior, in agreement with Eq. (8.55). The small deviations from the power law are due to a sub-dominant dependence on \tilde{a}_0 and an imperfect separation of the region where $\tilde{a}(\theta)$ varies from the region where the quartic derivative term dominates.

8.3 Implications for the hierarchy problem

In this section, we apply the results of our analysis to the Higgs-Dilaton theory described in section 3.1. The part of the theory, comprising the metric, the dilaton and the Higgs fields matches the models of section 8.1 after the higher-dimensional operators containing the parameters \varkappa and δ are introduced. As we will see, these operators do not spoil any phenomenological consequences of the theory. Within the Higgs-Dilaton model modified in this way, we demonstrate how the hierarchy between the Fermi and the Planck scales can emerge from the non-perturbative gravitational effects.

8.3.1 On quantum corrections in the Higgs-Dilaton theory

In section 3.2.2 we outlined the application of SI regularization procedure to the Higgs-Dilaton theory. Let us now discuss quantum corrections to the Higgs mass produced within this procedure. It can be shown that potentially dangerous corrections from the dilaton field of the form $\lambda^n \chi_0^2$ cannot be generated in any order of perturbation theory [100]. In particular, at one-loop level the dilaton contribution is of the form $\delta m_H^2 \sim \alpha^2 \chi_0^2$ and can be neglected in view of the constraint (3.6) and Eq. (3.7). We conclude that scale symmetry makes the Higgs mass stable against radiative corrections produced by the dilaton field. Note also that in the limit $\alpha = 0$ the dilaton decouples from the SM sector and provides no contribution to m_H .

The corrections to the Higgs potential from the various SM fields are well-known and were discussed in section 3.2.2. As it was done there, we choose the momentum scale $\hat{\mu}$ to minimize those corrections. This leads to the normalization prescriptions (3.39), depending on the choice of the renormalization scheme (3.34).

Finally, graviton loops do not destabilize the Higgs mass as well. Indeed, the graviton mass m_g^2 in the uniform χ_0 and h_0 background (leading to the vacuum energy $\propto \lambda h_0^4$) is $m_g^2 \sim \lambda h_0^4 / (\xi_\chi \chi_0^2 + \xi_h h_0^2)$, and the graviton contribution to the effective potential is $\propto m_g^4$.

Let us now comment on the requirement of the absence of dof with the mass scales exceeding the EW scale. Being non-renormalizable, the Higgs-Dilaton model experiences an infinite series of counter-terms to be added to the Lagrangian (3.2) in a process of renormalization. If one works at energies well below the scale at which the perturbation theory breaks down, these terms do not bring about new dof, since the particle spectrum is read from the original expression (3.2).⁶ Then, the assumption about the absence of heavy particles amounts to the hypothesis that, as one approaches the tree-level unitarity breaking scale, the theory reorganizes itself in such a way that no undesired singularities appear in its propagators.

8.3.2 Higgs vev generation in the Higgs-Dilaton setting

Let us put $\alpha = 0$ in the potential (3.3). Then, $m_H = 0$ at the classical level, according to Eq. (3.6), and, in view of the discussion in section 8.3.1, one can be sure that the radiative corrections to the Higgs mass do not shift it towards the observed value.⁷ In particular, thanks to the shift symmetry, the interaction term $\propto h^2 \chi^2$ is not generated in any order of perturbation theory. Another way to see this is to notice that the RG flow of the couplings α and β in the potential (3.3) is governed by

$$\mu \frac{d}{d\mu} \alpha = \mathcal{F}_\alpha(\alpha, \beta, \dots), \quad \mu \frac{d}{d\mu} \beta = \mathcal{F}_\beta(\alpha, \beta, \dots), \quad (8.56)$$

where $\mathcal{F}_\alpha, \mathcal{F}_\beta$ are functions of α, β and other couplings present in the theory, such that $\mathcal{F}_{\alpha, \beta} \rightarrow 0$ if both $\alpha, \beta \rightarrow 0$.⁸ Thus, the Higgs-Dilaton theory provides a suitable framework to tackle the hierarchy problem with non-perturbative tools.

⁶See, e.g., chapter 16 in [163].

⁷We neglect the corrections to m_H coming from non-zero β at the classical level.

⁸For an equivalent discussion in terms of second-order phase transitions see [164].

The results of sections 8.1 and 8.2 are applied straightforwardly to the Higgs-Dilaton theory. In order for the mechanism to work, one must modify the theory in the limit of large magnitudes and momenta of the Higgs field. This is done by introducing the higher-dimensional operators of the form given in Eqs. (8.5). Because of their suppression by M_P , the vev of the Higgs field is stable against perturbative corrections coming from these operators [69].

Following the steps performed in section 8.1.2, we apply the Weyl rescaling to the theory (3.2) to disentangle the dilaton and the Higgs fields from the Ricci scalar. We then introduce the polar field variables ρ and θ , and rewrite the Higgs-dilaton sector of the theory as in Eq. (8.21), with $a(\theta)$ replaced by $\tilde{a}(\theta)$ given in Eq. (8.46). Our goal is to find numerically the singular instanton and compute its contribution to the suppression rate \bar{W} .

From the results of section 8.2 it follows that the form of the potential for the Higgs field is irrelevant for the analysis of the singular instanton. In numerical calculations we choose the potential to coincide with the RG-improved SM Higgs potential corresponding to the central values of the top quark and Higgs masses, $m_t = 172.25$ GeV [36], $m_H = 125.09$ GeV [35]. We choose the first normalization prescription for the Higgs self-coupling λ in Eqs. (3.39). We also expect the suppression rate \bar{W} to be insensitive to the precise shape of the function $\tilde{a}(\theta)$ outside the vicinity of the point $\theta = \pi/2$, and, hence, to the values of the non-minimal couplings ξ_χ, ξ_h .

Calculations confirm that, varying the parameters δ and \varkappa , one can adjust \bar{W} to be equal

$$\bar{W} = \log M_P/v \approx 37, \quad (8.57)$$

in which case the hierarchy between the Fermi and the Planck scales is reproduced in the leading-order SPA. This is demonstrated in Fig. 8.9. One observes an ambiguity in the choice of the parameters leading to a given value of \bar{W} .

it is interesting to note that the conditions imposed on the coefficients δ and \tilde{a}_0 of the higher-dimensional operators point at a near Weyl-invariance of the theory in the limit $\theta \rightarrow \pi/2$. Indeed, when recast in terms of the original variables, the Lagrangian (8.21) in this limit can be written as

$$\frac{\mathcal{L}_{\theta \rightarrow \pi/2}}{\sqrt{g}} \sim -\frac{1}{2} \frac{1}{\tilde{a}_0^{-1} - 6} \varphi_2^2 R + \frac{1}{2} (\partial \varphi_2)^2 + \frac{\delta}{1 + 6\xi_2} \frac{(\partial \varphi_2)^4}{\varphi_2^4}. \quad (8.58)$$

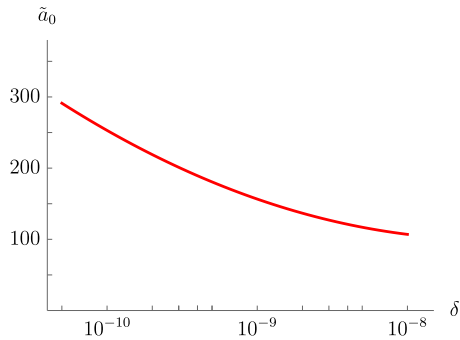


FIGURE 8.9: The set of parameters (\tilde{a}_0, δ) , for which Eq. (8.57) is satisfied. Here we choose $\xi_\chi = 5 \cdot 10^{-3}$, $\xi_h = 5 \cdot 10^3$ and λ coinciding with the SM running Higgs self-coupling at NNLO with the central values of the top quark and Higgs masses (see Fig. 8.4).

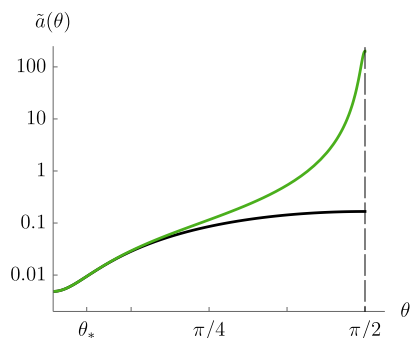


FIGURE 8.10: The function $\tilde{a}(\theta)$ in the original Higgs-Dilaton theory (the lower curve) and in the modified theory with \varkappa chosen so that $\tilde{a}_0 = 200$ (the upper curve). The angle θ_* corresponds to the scale of inflation $\sim M_P/\xi_h$. ξ_χ , ξ_h and λ are the same as in Fig. 8.9.

Hence, for large \tilde{a}_0 and small δ , the theory acquires an approximate Weyl symmetry. Note again that the small coupling δ , required for the mechanism to work, does not bring about new interaction scales much below M_P .

The modification of the Higgs-Dilaton theory by the higher-dimensional operators does not affect the properties which are important for phenomenology. Indeed, as Fig. 8.10 demonstrates, the function $\tilde{a}(\theta)$ is indistinguishable from its counterpart in the original theory at least up to the inflationary scales.

Let us finally comment on the dynamics of the SM dof coupled to the Higgs field. The same observation as in section 7.3 holds here. Namely, the coefficient \varkappa appears in the quadratic part of the Higgs field kinetic term, according to the second of Eqs. (8.5). The successful implementation of the non-perturbative mechanism requires large values of \tilde{a}_0 , which yields \varkappa to be negative. This endangers the dynamics of the gauge fields, as the latter become tachyonic as soon

as they interact with the Higgs field through the SM coupling terms. This drawback can be fixed by modifying suitably the coupling of the gauge fields at high energies. For example, introducing the operator (7.41) with an appropriate coupling constant compensates the negative mass terms coming from the quadratic in derivatives operator in Eq. (8.1).

Chapter 9

Discussion and outlook

Let us summarize the results obtained in chapters 7 and 8. We attempted to look at the vev of the Higgs field as arising due to some non-perturbative effect that relates low-energy phenomena with physics at the Planck scale. We proposed that the small ratio between the Fermi and the Planck scales could be generated via the instanton configuration of a special type. It was argued that in this case the Fermi scale appears as a result of the exponentially strong suppression of the Planck scale by the instanton. This effect relies strongly on a structure of the theory in the strong-gravity regime, of which explicit form we are not aware. To make the quantitative analysis possible, several conjectures about the properties of the theory in this regime were adopted. Namely, the global scale invariance was assumed to be a fundamental symmetry in the high-energy domain, while being broken explicitly or spontaneously in the gravitational sector at low energies. We also assumed the absence of heavy dof associated with new physics above the EW scale. Within these conjectures, we studied several toy models comprising the gravitational and scalar fields. We constructed singular instanton configurations and investigated their contribution to the vev of the scalar field. The results of the studies were then applied to the actual hierarchy problem. It was shown that the hierarchy between the Fermi and the Planck scales can indeed be generated with a particular structure of higher-dimensional operators added to the theory.

The power-like dependence of the instanton action on the parameter a_{HE} (in chapter 7) or \tilde{a}_0 (in chapter 8) and its degeneracy in the parameter space imply that the value of \bar{W} reproducing the hierarchy (4.1) in the leading-order SPA is not featured among other possible values. Thus, although the suggested mechanism allows to generate an exponentially small ratio of scales without a

fine-tuning among the parameters of the theory, it does not explain a particular value of this ratio.

Speaking more generally, the mechanism is not specific to the scalar-tensor models studied in the previous chapters. For example, replacing the quartic derivative operator in Eqs. (8.5)—(8.8) by an operator with the derivatives of the scalar fields of higher degrees or by a linear combination thereof results in the same picture. The reason is that the impact of any such operator on the short-distance behavior of the instanton is qualitatively the same. Further, due to the fact that the instanton action is saturated in the core region of the instanton, the precise shape of the function regulating the strength of the radial field source is inessential, as soon as it interpolates between the fixed low-field and large-field values. Finally, including higher-dimensional operators of the types different from those considered here does not spoil the mechanism provided that they do not affect the properties of the solution near the source. As it is not so in general, we would like to stress again that, instead of performing a barely possible analysis of euclidean classical configurations arising in a general SI scalar-tensor theory of gravity, we preferred to focus on particular examples at which we demonstrate the mere possibility of the existence of the desired non-perturbative effect.

The singular instantons found above turn out to be insensitive to the properties of the theory at low energies and low magnitudes of the Higgs field. In fact, these properties are irrelevant for the mechanism of generating the hierarchy of scales, since the latter operates essentially in the Planck region. It follows that from the perspective of a low-energy theory, the vev of the Higgs field appears as a classical quantity. For example, the leading-order instanton contribution to the n -point correlation function of the Higgs field is given by

$$\langle \phi(x_1) \dots \phi(x_n) \rangle \sim v^n, \quad (9.1)$$

provided that the points x_1, \dots, x_n are farther from each other than the characteristic size of the instanton, $|x_i - x_j| \gtrsim M_P^{-1}$, so that the dilute-gas approximation is applicable. Eq. (9.1) points at the classical interpretation of the Higgs field vev, as long as the physics at the energies much below M_P^{-1} is concerned. Still, there are no a priori reasons for the instanton action to be saturated exclusively in the core region of the instanton. Nevertheless, we find it intriguing that the observed hierarchy between the Fermi and the Planck scales could actually result purely from the features of quantum gravity *above* the Planck scale. We leave the further investigation of this question for future.

It is natural to ask if singular instantons of a similar kind can be of use in resolving another great puzzle of theoretical physics — the cosmological constant problem. Leaving the discussion of this question aside, here we just note that a straightforward attempt to implement the mechanism of chapter 5 to compute the non-perturbative correction to the curvature vev $\langle R \rangle$ fails. Moreover, the scale symmetry used to make the Higgs field vev stable against radiative corrections is, in general, not suitable to protect the cosmological constant, as one can make sure using the Higgs-Dilaton theory as an example.

A systematic treatment of fluctuations correcting the leading-order estimation (8.50) is not easy. Some progress in a related problem of finding cosmological perturbations above a configuration with the singularity of the type (7.13) was made in [151]. We find this task important, since knowing the determinant in Eq. (8.50) may clarify whether the exponential change of the field variable is indeed the preferred way to describe the dynamics at high energies. We leave to future work the investigation of different modes arising on top of the singular instanton, and their possible physical implications.

In the language of the Higgs-Dilaton theory, our motivation in searching for a non-perturbative mechanism of generating the Higgs vev was an unnatural smallness of the coefficient α in the potential (3.3). One more parameter of the theory which is required to be small in order to match phenomenological data is the non-minimal dilaton coupling ξ_χ . In the limit $\xi_\chi = 0$, the Lagrangian (3.2) without the potential term acquires an additional invariance under the constant shifts of the dilaton field. It would be interesting to see whether the interaction $\propto \chi^2 R$ can be induced by some non-perturbative effect similar to the one studied, e.g., in [165–167], provided that the shift symmetry is exact at the classical level.

One more interesting question regarding the singular instantons is whether they can be responsible for generating the masses of right-handed neutrinos, say, in the ν MSM setting [168, 169].¹

¹ One idea of how gravity can be responsible for neutrino mass generation was elaborated in [170].

Chapter 10

Conclusion

Let us conclude. In this thesis, two groups of questions were studied. The first of them concerns with the stability of the electroweak vacuum in different settings. As was stated in introduction, this topic attracts significant attention in the recent literature, partly because the lifetime of the low-energy vacuum is, in general, sensitive to the the structure of the theory at high energy scales. Having observed the sufficiently long-lived universe, we can, therefore, put constraints on new physics in the domain that we cannot probe directly in experiment. Given below is the summary of our results in this direction of research.

In chapter 2 we studied Coleman-De Luccia tunneling of the Standard Model Higgs field during inflation in the case when the electroweak vacuum is metastable. We verified that the tunneling rate is exponentially suppressed. The main contribution to the suppression is the same as in flat space-time. We analytically estimated the corrections due to the expansion of the universe and an effective mass term in the Higgs potential that can be present at inflation.

In chapter 3 we investigated stability of the electroweak vacuum in the Higgs-Dilaton theory — a scale-invariant extension of the Standard Model and General Relativity. The safety of the low-energy vacuum against possible transition towards another minimum of the Higgs potential is a necessary condition for the model to be phenomenologically acceptable. We found that, within a wide range of parameters of the theory, the decay rate is significantly suppressed compared to that of the Standard Model. We also discussed properties of the tunneling solutions that are specific to the Higgs-Dilaton theory.

The second group of questions addressed in the thesis is dedicated to one puzzling fact arising when one treats gravity on equal footing with other fundamental

interactions. Suppose we are given two theories equally well explaining experimental and observational data. Let one theory possess the input parameter of order $10^{-17} \sim v/M_P$, while another theory contains a dynamical mechanism of generating such parameter. If, based on this difference, one would take the second theory as the “better” one, then the ratio of the electroweak to gravitational forces is a challenge one must deal with. We attempted to look for the resolution of this challenge in the high-energy domain of the theory and suggested that the weak scale is a manifestation of the non-perturbative gravitational effect whose existence relies on the structure of the theory in the strong-gravity regime.

The summary of the results of the second part of the thesis is as follows. In chapter 4 we provided arguments in favor of the non-perturbative perspective on the problem of hierarchy between the Fermi and the Planck scales. In chapter 5 the main idea behind all subsequent calculations was given and the challenges standing on the way of its justification were described. In chapter 6 we considered the simple scale-invariant model of one scalar field coupled to gravity in a non-minimal way. We studied analytically singular euclidean solutions of equations of motion supplemented by an instantaneous source of the scalar field. The results of these studies were then used in chapters 7 and 8, where we analyzed similar configurations in several toy models and in phenomenologically viable theories encompassing the Standard Model and gravity. We chose the Planck scale to start with, as it is the only scale appearing inevitably in any theory comprising the Standard Model and General Relativity. We then showed that, under specific assumptions about the high-energy behavior of a theory, it is possible to generate the electroweak scale via the instanton effect that suppresses the Planck scale by a necessary amount.

Needless to say, the suggested mechanism of generating the hierarchy of scales calls for further investigation. It opens many interesting questions, some of which were mentioned in chapter 9. Speaking more globally, on this example we tried to learn how certain conjectures about UV behaviour can help in resolving apparently low-energy issues. As is seen from this perspective, presented in the thesis are just few steps on this way to approach the yet unknown final theory.

Appendix A

Singular instanton in curved space

Let us switch on the quartic coupling λ in the Lagrangian (6.1) of the Dilaton model. Then, the second of Eqs. (6.14) becomes

$$\frac{1}{f^2} = 1 + \frac{a}{6M_P^4 r^4} \pm b^2 r^2, \quad b^2 = \frac{|\lambda| M_P^2}{12\xi^2}, \quad (\text{A.1})$$

where the plus (minus) sign in the second expression holds for negative (positive) λ . The classical ground state (6.5) of the Dilaton model is given by

$$\bar{\varphi} = 0, \quad f^2 = \frac{1}{1 \pm b^2 r^2}, \quad (\text{A.2})$$

Repeating the steps leading to Eq. (6.21), we obtain the expression for the singular instanton in the space of constant curvature,

$$\bar{\varphi}(r) = - \int_{r_b}^r \frac{f(r')}{r'^3 M_P} dr', \quad \frac{1}{f(r)^2} = 1 + \frac{a}{6M_P^4 r^4} \pm b^2 r^2, \quad (\text{A.3})$$

where r_b is sent to infinity for $\lambda < 0$ or is equal to a positive root of the inverse of the metric function f^{-2} for $\lambda > 0$. Eq. (A.3) contains two scales. The first of them is defined by the combination $a^{1/4} M_P^{-1}$ and determines the size of the instanton, as explained in section 6.2. The second is the cosmological scale b determined by the classical ground state. We require the vacuum energy of the ground state to be well below M_P^4 ,

$$b M_P^{-1} \ll 1. \quad (\text{A.4})$$

From this and the fact that a is confined in the region

$$0 < a < 1/6 \tag{A.5}$$

the separation of the instanton and cosmological sizes follows. Eq. (A.4) imposes an upper bound on the absolute value of λ , which can always be satisfied provided that $\xi \neq 0$.

It is worth to note that when the vacuum geometry is the de Sitter one, $\lambda > 0$, the instanton is not regular at the boundary point $r = r_b$. However, computation of the metric invariants yields, in notations of [171],¹

$$\begin{aligned} \tilde{R} &= 12b^2(1 + \mathcal{O}(ab^4 M_P^{-4})), & \tilde{E} &= b^4 \cdot \mathcal{O}(a^2 b^8 M_P^{-8}), \\ \tilde{F} &= b^8 \cdot \mathcal{O}(a^4 b^{16} M_P^{-16}), & \tilde{G} &= b^{12} \cdot \mathcal{O}(a^6 b^{24} M_P^{-24}). \end{aligned} \tag{A.6}$$

To the leading order in $a^{1/4} b M_P^{-1}$, they coincide with those of the euclidean de Sitter space. Hence, one can expect that the singularity of the metric at $r = r_b$ does not contribute to the instanton action.

As the last step, we evaluate the euclidean action and the boundary term of the instanton in curved background. With the ansatz (6.13) applied, the exterior curvature of a surface defined by the equation $r = r_s$ is seen to be

$$\tilde{K} = \frac{3}{f(r_s)r_s}. \tag{A.7}$$

For λ positive, the boundary term is absent both for the vacuum solution and the singular instanton. In the case $\lambda < 0$, the boundary is determined by sending r_s to infinity and we have (cf. Eq. (6.22))

$$\bar{I}_{GH} - I_{GH,0} \sim a^{-1} b^{-1} M_P^{-2} r_s^{-3} \rightarrow 0, \quad r_s \rightarrow \infty, \quad \lambda < 0. \tag{A.8}$$

To find the euclidean action, we make use of the Einstein equations. The difference in the actions between the instanton and the vacuum for $\lambda \neq 0$ is evaluated as

$$\bar{S} - S_0 \sim ab^2 M_P^{-2} \ll 1 \tag{A.9}$$

given Eqs. (A.4) and (A.5).

We conclude that the nontrivial background geometry does not lead to a significant contribution to the net instanton action, neither to the net boundary term.

¹Among the fourteen metric invariants, ten are expressed using the Weyl tensor which is zero in our case [171].

Hence, in proceeding with the classical analysis in more complicated theories, one can focus solely on the core region of the instanton. Moreover, as was mentioned in section 6.2, in order to make the instanton action large, the structure of the theory in this region must be different from that of the Dilaton model.

Appendix B

Derivative operators of higher degrees

Here we discuss the generalization of the models of section 8.1, which amounts to replacing the quartic derivative term for the radial field by a more general operator of the form

$$\tilde{\mathcal{O}} = \delta M_P^4 p(z), \quad p(z) = \sum_{n=1}^N \alpha_n z^n, \quad z = \frac{(\tilde{\partial}\rho)^4}{M_P^8}. \quad (\text{B.1})$$

The original operator is reproduced when $p(z) = z$, $\alpha_1 = 1$. The coefficients α_n are chosen to be less or of the order of one, the overall coupling δ is adjusted to provide the separation of the region where the angular field varies from the region where the operator $\tilde{\mathcal{O}}$ dominates the dynamics of the instanton. Each of the terms in $p(z)$ can be easily traced back to the original field variables, invoking non-zero coefficients $\tilde{\gamma}_{i_1, \dots, i_{2k}}$ up to $k = N/2$ in the Lagrangian (8.1).

Making use of the Einstein equations, one finds the instanton action

$$\bar{S} = \int d^4x \sqrt{\tilde{g}} \delta M_P^4 (2z p'(z) - p(z)), \quad (\text{B.2})$$

where the potential term is neglected. We would like to study how this action depends on the coupling δ for different choices of the function $p(z)$. Applying the ansatz (6.13), we arrive at equations of motion in the high-energy regime,

$$4r^3 \delta M_P^2 z^{\frac{3}{4}} p'(z) = -\frac{1}{M_P}, \quad (\text{B.3})$$

$$\frac{M_P^2}{2} \frac{3 - 3f^2}{r^2 f^2} = \delta M_P^4 (2z p'(z) - p(z)/2). \quad (\text{B.4})$$

Let us take

$$p(z) = z^k, \quad k \geq 1. \quad (\text{B.5})$$

From Eqs. (B.3) the high-energy asymptotics of the radial and metric fields are deduced,

$$\begin{aligned} \rho' &\sim -M_P^2 \delta^{\frac{1}{2-8k}} (M_P r)^{\frac{2k-2}{4k-1}}, \\ f &\sim \delta^{\frac{1}{8k-2}} (M_P r)^{\frac{2k+1}{4k-1}}, \end{aligned} \quad (\text{B.6})$$

where we keep track of the dependence on δ and \tilde{a}_0 . These asymptotics prevail at the distances $r \lesssim \bar{r}$, where

$$\bar{r} \sim \delta^{\frac{1}{6(2k-1)}} M_P^{-1} \tilde{a}_0^{\frac{4k-1}{6(2k-1)}}. \quad (\text{B.7})$$

Setting $k = 1$, one reproduces Eqs. (8.41), (8.42). The instanton action becomes,

$$\bar{S} \sim \int_0^\infty dr r^3 f \delta M_P^4 \left(\frac{\rho'^4}{f^4 M_P^8} \right)^k. \quad (\text{B.8})$$

We now use Eqs. (B.6) and (B.7) to compute the high-energy part of the action. Remarkably, it shows no power-like dependence on δ :

$$\bar{S} \sim \tilde{a}_0^{\frac{1}{2}}. \quad (\text{B.9})$$

The same is true for the value of the radial field at the center of the instanton,

$$\rho(0)/M_P \sim \tilde{a}_0^{\frac{1}{2}} (\log \delta + \mathcal{O}(1)). \quad (\text{B.10})$$

It is clear that using the more general form of the function $f(z)$, given in Eq. (B.1), reveals the same behavior of \bar{S} and $\rho(0)/M_P$. We conclude that the reasoning of section 8.1.5 applies universally regardless the particular derivative operator chosen to regularize the instanton.

From Eqs. (B.6) it also follows that the high energy asymptotics of the fields are confined as

$$|\rho'| \gtrsim r^{\frac{1}{2}}, \quad r^{\frac{1}{2}} \gtrsim f \gtrsim r. \quad (\text{B.11})$$

Hence, the non-analyticity invoked by the source of the radial field cannot be completely removed by the operators of the form (B.1).

Appendix C

More on short-distance behavior of the instanton

Following the discussion in section 8.1.5, here we study the exponents γ , η in the asymptotics of the scalar fields at $r \rightarrow 0$ and for different values of \varkappa . Recall that

$$\tilde{a}_0 \equiv \tilde{a}(\pi/2), \quad (\text{C.1})$$

where $\tilde{a}(\theta)$ is a function defined in Eq. (8.46). From equations of motion for the radial and angular fields it follows that

$$\rho \sim -M_P \gamma \log(M_P r), \quad \frac{\pi}{2} - \theta \sim r^\eta \quad (\text{C.2})$$

with

$$\gamma = \sqrt{6\tilde{a}_0}, \quad \eta = \sqrt{\frac{\tilde{a}_0(1+6\xi_2)(2\xi_2(1+3\xi_1) - \xi_1) - \xi_2^2(1+6\xi_1)}{\xi_1(\xi_1 + 1/6)}}. \quad (\text{C.3})$$

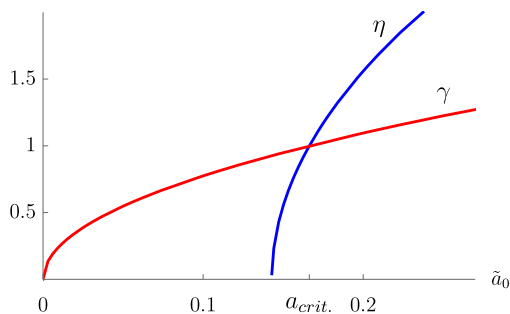


FIGURE C.1: The exponents of the short-distance asymptotics of the fields ρ and θ with no higher-dimensional derivative terms included. Here we take $\xi_1 = 1$, $\xi_2 = 1.1$. The critical value of the source of the radial field, $a_{crit.}$, is indicated according to Eq. (C.5).

This reduces to Eqs. (8.33) and (8.38) for $\tilde{a}_0 = a_0 \equiv (6 + 1/\xi_2)^{-1}$.

Fig. C.1 demonstrates the relative values of γ and η for different possible values of the coefficient $\tilde{a}_0 = (\varkappa + a_0^{-1})^{-1}$. We observe two featured values of \tilde{a}_0 . The first one represents the minimal possible strength of the source for which the singular instanton of the type studied here exists. It is given by

$$a_{min.} = a_0 \frac{\xi_2(1 + 6\xi_1)}{\xi_2(2 + 6\xi_1) - \xi_1}. \quad (C.4)$$

If $\varkappa = 0$, the requirement $\tilde{a}_0 > a_{min.}$ gives $\xi_2 > \xi_1$, in agreement with Eq. (8.38). The second featured value of \tilde{a}_0 is the one at which $\eta = \gamma$. It is given by

$$a_{crit.} = a_0 \frac{\xi_2(1 + 6\xi_1)}{\xi_2(1 + 6\xi_1) - \xi_1} \quad (C.5)$$

and is always larger than a_0 . For $\tilde{a}_0 > a_{crit.}$ we have, according to Eq. (8.39),

$$\varphi_1 \rightarrow 0, \quad r \rightarrow 0. \quad (C.6)$$

Thus, the large sources make the dilaton field associated with φ_1 convergent at the center of the instanton. Note, however, that the behavior of the dilaton is still non-analytic in r , which is justified by the presence of the source. Furthermore, the Higgs field associated with φ_2 diverges the stronger, the larger the value of \tilde{a}_0 , hence the regularization provided, for example, by the higher-dimensional derivative operator is still needed.

Bibliography

- [1] R. Rajaraman, Solitons and instantons: an introduction to solitons and instantons in quantum field theory (Amsterdam, Netherlands: North-holland (1982) 409p).
- [2] N.N. Bogolyubov and D.V. Shirkov, Intersci. Monogr. Phys. Astron. 3 (1959) 1.
- [3] S.R. Coleman, Subnucl. Ser. 15 (1979) 805, [,382(1978)].
- [4] T.D. Lee and Y. Pang, Phys. Rept. 221 (1992) 251, [,169(1991)].
- [5] N.J. Zabusky and M.D. Kruskal, Phys. Rev. Lett. 15 (1965) 240.
- [6] S.R. Coleman, Subnucl. Ser. 13 (1977) 297.
- [7] N.S. Manton and P. Sutcliffe, Topological solitons (Cambridge University Press, 2004).
- [8] Y.M. Shnir, Topological and Non-Topological Solitons in Scalar Field Theories (Cambridge University Press, 2018).
- [9] A. Hasegawa and M. Matsumoto Optical Solitons in Fibers Vol. 9 (Springer, Berlin, Heidelberg, 2003).
- [10] S.T. A.R. Bishop, J.A. Krumhansl, Physica D: Nonlinear Phenomena 1 (1980) 1 .
- [11] V.A. Rubakov, Classical theory of gauge fields (Princeton, USA: Univ. Pr. (2002) 444 p, 2002).
- [12] V.A. Rubakov and D.S. Gorbunov, Introduction to the Theory of the Early Universe (World Scientific, Singapore, 2017).
- [13] E.J. Weinberg, Classical solutions in quantum field theory (Cambridge University Press, 2012).

-
- [14] V. Belinski and E. Verdaguer, Gravitational solitons (Cambridge University Press, 2005).
- [15] G. 't Hooft, Phys. Rev. D14 (1976) 3432, [,70(1976)].
- [16] S.R. Coleman, Phys. Rev. D15 (1977) 2929, [Erratum: Phys. Rev.D16,1248(1977)].
- [17] M. Shifman, Advanced topics in quantum field theory. (Cambridge Univ. Press, Cambridge, UK, 2012).
- [18] G.W. Gibbons and S.W. Hawking, Commun. Math. Phys. 66 (1979) 291.
- [19] A. Shkerin and S. Sibiryakov, Phys. Lett. B746 (2015) 257, 1503.02586.
- [20] A. Shkerin, JHEP 05 (2017) 155, 1701.02224.
- [21] M. Shaposhnikov and A. Shkerin, Phys. Lett. B783 (2018) 253, 1803.08907.
- [22] M. Shaposhnikov and A. Shkerin, (2018), 1804.06376.
- [23] S.R. Coleman and F. De Luccia, Phys. Rev. D21 (1980) 3305.
- [24] S.R. Coleman and E.J. Weinberg, Phys. Rev. D7 (1973) 1888.
- [25] S. Weinberg, Phys. Rev. D7 (1973) 2887.
- [26] A.D. Linde, JETP Lett. 23 (1976) 64, [,73(1975)].
- [27] M. Sher, Phys. Rept. 179 (1989) 273.
- [28] G. Altarelli and G. Isidori, Phys. Lett. B337 (1994) 141.
- [29] F. Bezrukov et al., JHEP 10 (2012) 140, 1205.2893, [,275(2012)].
- [30] G. Degrassi et al., JHEP 08 (2012) 098, 1205.6497.
- [31] D. Buttazzo et al., JHEP 12 (2013) 089, 1307.3536.
- [32] F. Bezrukov and M. Shaposhnikov, J. Exp. Theor. Phys. 120 (2015) 335, 1411.1923, [Zh. Eksp. Teor. Fiz.147,389(2015)].
- [33] S. Spannagel, PoS DIS2016 (2016) 150, 1607.04972.
- [34] ATLAS, K. Yau Wong, Proceedings, 9th International Workshop on Top Quark Physics (TOP 2016): Olomouc, Czech Republic, September 19-23, 2016, 2016, 1610.06707.
- [35] ATLAS, CMS, G. Aad et al., Phys. Rev. Lett. 114 (2015) 191803, 1503.07589.

-
- [36] CMS, A. Castro, 10th International Workshop on Top Quark Physics (TOP2017) Braga, Portugal, September 17-22, 2017, 2017, 1712.01027.
- [37] A. Andreassen, W. Frost and M.D. Schwartz, *Phys. Rev. D* **97** (2018) 056006, 1707.08124.
- [38] G. Isidori et al., *Phys. Rev. D* **77** (2008) 025034, 0712.0242.
- [39] V. Branchina, E. Messina and D. Zappala, *EPL* **116** (2016) 21001, 1601.06963.
- [40] A. Rajantie and S. Stopyra, *Phys. Rev. D* **95** (2017) 025008, 1606.00849.
- [41] A. Salvio et al., *JHEP* **09** (2016) 054, 1608.02555.
- [42] J.R. Espinosa, G.F. Giudice and A. Riotto, *JCAP* **0805** (2008) 002, 0710.2484.
- [43] O. Lebedev and A. Westphal, *Phys. Lett. B* **719** (2013) 415, 1210.6987.
- [44] M. Herranen et al., *Phys. Rev. Lett.* **115** (2015) 241301, 1506.04065.
- [45] Y. Ema, K. Mukaida and K. Nakayama, *JCAP* **1610** (2016) 043, 1602.00483.
- [46] P. Burda, R. Gregory and I. Moss, *Phys. Rev. Lett.* **115** (2015) 071303, 1501.04937.
- [47] P. Burda, R. Gregory and I. Moss, *JHEP* **08** (2015) 114, 1503.07331.
- [48] P. Burda, R. Gregory and I. Moss, *JHEP* **06** (2016) 025, 1601.02152.
- [49] D. Gorbunov, D. Levkov and A. Panin, *JCAP* **1710** (2017) 016, 1704.05399.
- [50] J. Garcia-Bellido et al., *Phys. Rev. D* **84** (2011) 123504, 1107.2163.
- [51] F. Bezrukov et al., *Phys. Rev. D* **87** (2013) 096001, 1212.4148.
- [52] G.F. Giudice, (2008) 155, 0801.2562.
- [53] G.F. Giudice, *PoS EPS-HEP2013* (2013) 163, 1307.7879.
- [54] W.A. Bardeen, *Ontake Summer Institute on Particle Physics Ontake Mountain, Japan, August 27-September 2, 1995, 1995.*
- [55] S.R. Coleman and R. Jackiw, *Annals Phys.* **67** (1971) 552.
- [56] S. Weinberg, *Phys. Lett.* **82B** (1979) 387.
- [57] S. Weinberg, *Phys. Rev. Lett.* **36** (1976) 294.

-
- [58] A.D. Linde, Phys. Lett. 70B (1977) 306.
- [59] E. Witten, Nucl. Phys. B177 (1981) 477.
- [60] C.D. Froggatt and H.B. Nielsen, Phys. Lett. B368 (1996) 96, hep-ph/9511371.
- [61] E. Gildener and S. Weinberg, Phys. Rev. D13 (1976) 3333.
- [62] K.A. Meissner and H. Nicolai, Phys. Lett. B648 (2007) 312, hep-th/0612165.
- [63] S. Iso, N. Okada and Y. Orikasa, Phys. Lett. B676 (2009) 81, 0902.4050.
- [64] L. Boyle et al., (2011), 1111.0273.
- [65] A.J. Helmboldt et al., JHEP 07 (2017) 113, 1603.03603.
- [66] A. Karam and K. Tamvakis, Phys. Rev. D92 (2015) 075010, 1508.03031.
- [67] A. Karam and K. Tamvakis, Phys. Rev. D94 (2016) 055004, 1607.01001.
- [68] G. 't Hooft and M.J.G. Veltman, Nucl. Phys. B44 (1972) 189.
- [69] G. 't Hooft and M.J.G. Veltman, Ann. Inst. H. Poincare Phys. Theor. A20 (1974) 69.
- [70] G. Dvali, Subnucl. Ser. 53 (2017) 189, 1607.07422.
- [71] A.M. Polyakov, Contemp. Concepts Phys. 3 (1987) 1.
- [72] K.G. Chetyrkin and M.F. Zoller, JHEP 06 (2012) 033, 1205.2892.
- [73] A. Kobakhidze and A. Spencer-Smith, Phys. Lett. B722 (2013) 130, 1301.2846.
- [74] M. Fairbairn and R. Hogan, Phys. Rev. Lett. 112 (2014) 201801, 1403.6786.
- [75] K. Enqvist, T. Meriniemi and S. Nurmi, JCAP 1407 (2014) 025, 1404.3699.
- [76] A. Hook et al., JHEP 01 (2015) 061, 1404.5953.
- [77] M. Herranen et al., Phys. Rev. Lett. 113 (2014) 211102, 1407.3141.
- [78] F.L. Bezrukov and M. Shaposhnikov, Phys. Lett. B659 (2008) 703, 0710.3755.
- [79] S.W. Hawking and I.G. Moss, Phys. Lett. 110B (1982) 35.

-
- [80] V.A. Rubakov and S.M. Sibiryakov, *Theor. Math. Phys.* 120 (1999) 1194, gr-qc/9905093, [*Teor. Mat. Fiz.*120,451(1999)].
- [81] G.W. Gibbons and S.W. Hawking, *Phys. Rev. D*15 (1977) 2738.
- [82] K. Kamada, *Phys. Lett. B*742 (2015) 126, 1409.5078.
- [83] I. Affleck, *Nucl. Phys. B*191 (1981) 429, [,247(1980)].
- [84] G. Isidori, G. Ridolfi and A. Strumia, *Nucl. Phys. B*609 (2001) 387, hep-ph/0104016.
- [85] BICEP2, Planck, P.A.R. Ade et al., *Phys. Rev. Lett.* 114 (2015) 101301, 1502.00612.
- [86] V. Branchina and E. Messina, *Phys. Rev. Lett.* 111 (2013) 241801, 1307.5193.
- [87] M. Shaposhnikov and D. Zenhausern, *Phys. Lett. B*671 (2009) 187, 0809.3395.
- [88] J. Rubio, *J. Phys. Conf. Ser.* 631 (2015) 012032, 1502.07952.
- [89] S. Chigusa, T. Moroi and Y. Shoji, *Phys. Rev. D*97 (2018) 116012, 1803.03902.
- [90] F. Bezrukov, D. Gorbunov and M. Shaposhnikov, *JCAP* 0906 (2009) 029, 0812.3622.
- [91] J. Garcia-Bellido, D.G. Figueroa and J. Rubio, *Phys. Rev. D*79 (2009) 063531, 0812.4624.
- [92] F. Bezrukov, J. Rubio and M. Shaposhnikov, *Phys. Rev. D*92 (2015) 083512, 1412.3811.
- [93] G.W. Gibbons and S.W. Hawking, *Phys. Rev. D*15 (1977) 2752.
- [94] A. Masoumi, S. Paban and E.J. Weinberg, *Phys. Rev. D*94 (2016) 025023, 1603.07679.
- [95] A.Yu. Kamenshchik and C.F. Steinwachs, *Phys. Rev. D*91 (2015) 084033, 1408.5769.
- [96] Y. Fujii and K. Maeda, *The scalar-tensor theory of gravitation* (Cambridge University Press, 2007).
- [97] S.R. Coleman, V. Glaser and A. Martin, *Commun. Math. Phys.* 58 (1978) 211.

-
- [98] K. Blum et al., JHEP 05 (2017) 109, 1611.04570, [Erratum: JHEP06,060(2017)].
- [99] M.E. Shaposhnikov and F.V. Tkachov, (2009), 0905.4857.
- [100] M. Shaposhnikov and D. Zenhausern, Phys. Lett. B71 (2009) 162, 0809.3406.
- [101] F. Englert, C. Truffin and R. Gastmans, Nucl. Phys. B117 (1976) 407.
- [102] C. Tamarit, JHEP 12 (2013) 098, 1309.0913.
- [103] D.M. Ghilencea, Z. Lalak and P. Olszewski, Eur. Phys. J. C76 (2016) 656, 1608.05336.
- [104] D.M. Ghilencea, Z. Lalak and P. Olszewski, Phys. Rev. D96 (2017) 055034, 1612.09120.
- [105] G. 't Hooft, Nucl. Phys. B61 (1973) 455.
- [106] V. Branchina, E. Messina and M. Sher, Phys. Rev. D91 (2015) 013003, 1408.5302.
- [107] V. Branchina and E. Messina, EPL 117 (2017) 61002, 1507.08812.
- [108] K.G. Wilson, Phys. Rev. D3 (1971) 1818.
- [109] E. Gildener, Phys. Rev. D14 (1976) 1667.
- [110] L. Susskind, Phys. Rev. D20 (1979) 2619.
- [111] F. Vissani, Phys. Rev. D57 (1998) 7027, hep-ph/9709409.
- [112] M. Shaposhnikov, Astroparticle Physics: Current Issues, 2007 (APCI07) Budapest, Hungary, June 21-23, 2007, 2007, 0708.3550.
- [113] G.K. Karananas and M. Shaposhnikov, Phys. Lett. B771 (2017) 332, 1703.02964.
- [114] G.F. Giudice and M. McCullough, JHEP 02 (2017) 036, 1610.07962.
- [115] J.L. Feng, Ann. Rev. Nucl. Part. Sci. 63 (2013) 351, 1302.6587.
- [116] B. Bellazzini, C. Cski and J. Serra, Eur. Phys. J. C74 (2014) 2766, 1401.2457.
- [117] N. Arkani-Hamed, S. Dimopoulos and G.R. Dvali, Phys. Lett. B429 (1998) 263, hep-ph/9803315.

-
- [118] L. Randall and R. Sundrum, Phys. Rev. Lett. 83 (1999) 3370, hep-ph/9905221.
- [119] J.D. Wells, Stud. Hist. Phil. Sci. B49 (2015) 102, 1305.3434.
- [120] J. Barnard and M. White, JHEP 10 (2015) 072, 1507.02332.
- [121] M. Farina, D. Pappadopulo and A. Strumia, JHEP 08 (2013) 022, 1303.7244.
- [122] A. Arvanitaki et al., JHEP 05 (2017) 071, 1609.06320.
- [123] G.M. Pelaggi et al., Front.in Phys. 5 (2017) 49, 1701.01453.
- [124] A. Salvio and A. Strumia, Eur. Phys. J. C78 (2018) 124, 1705.03896.
- [125] P.W. Graham, D.E. Kaplan and S. Rajendran, Phys. Rev. Lett. 115 (2015) 221801, 1504.07551.
- [126] G. Dvali and A. Vilenkin, Phys. Rev. D70 (2004) 063501, hep-th/0304043.
- [127] G. Dvali, Phys. Rev. D74 (2006) 025018, hep-th/0410286.
- [128] D.L. Bennett and H.B. Nielsen, Int. J. Mod. Phys. A9 (1994) 5155, hep-ph/9311321.
- [129] M. Shaposhnikov and C. Wetterich, Phys. Lett. B683 (2010) 196, 0912.0208.
- [130] S. Weinberg, Phys. Rev. D81 (2010) 083535, 0911.3165.
- [131] Y. Fujii, Phys. Rev. D9 (1974) 874.
- [132] Y. Fujii, General Relativity and Gravitation 6 (1975) 29.
- [133] D.J. Amit and E. Rabinovici, Nucl. Phys. B257 (1985) 371.
- [134] E. Rabinovici, B. Saering and W.A. Bardeen, Phys. Rev. D36 (1987) 562.
- [135] C. Wetterich, Nucl. Phys. B302 (1988) 668, 1711.03844.
- [136] A. Zee, Phys. Rev. Lett. 42 (1979) 417.
- [137] L. Smolin, Nucl. Phys. B160 (1979) 253.
- [138] W. Buchmuller and N. Dragon, Nucl. Phys. B321 (1989) 207.
- [139] J. Rubio and M. Shaposhnikov, Phys. Rev. D90 (2014) 027307, 1406.5182.

-
- [140] P.G. Ferreira, C.T. Hill and G.G. Ross, *Phys. Lett.* B763 (2016) 174, 1603.05983.
- [141] G.K. Karananas and J. Rubio, *Phys. Lett.* B761 (2016) 223, 1606.08848.
- [142] P.G. Ferreira, C.T. Hill and G.G. Ross, *Phys. Rev.* D95 (2017) 043507, 1610.09243.
- [143] P.G. Ferreira, C.T. Hill and G.G. Ross, *Phys. Rev.* D95 (2017) 064038, 1612.03157.
- [144] G. 't Hooft, *NATO Sci. Ser. B* 59 (1980) 135.
- [145] C. Wetterich, *Phys. Lett.* B718 (2012) 573, 1112.2910.
- [146] G.W. Horndeski, *Int. J. Theor. Phys.* 10 (1974) 363.
- [147] A. Nicolis, R. Rattazzi and E. Trincherini, *Phys. Rev.* D79 (2009) 064036, 0811.2197.
- [148] D. Langlois and K. Noui, *JCAP* 1602 (2016) 034, 1510.06930.
- [149] A.M. Polyakov, *Phys. Lett.* 72B (1978) 477.
- [150] G.W. Gibbons, *Phys. Lett.* A61 (1977) 3.
- [151] S. Gratton and N. Turok, *Phys. Rev.* D60 (1999) 123507, *astro-ph/9902265*.
- [152] D. Blas, M. Shaposhnikov and D. Zenhausern, *Phys. Rev.* D84 (2011) 044001, 1104.1392.
- [153] G.K. Karananas and M. Shaposhnikov, *Phys. Rev.* D93 (2016) 084052, 1603.01274.
- [154] A. Padilla and V. Sivanesan, *JHEP* 08 (2012) 122, 1206.1258.
- [155] S.W. Hawking and N. Turok, *Phys. Lett.* B425 (1998) 25, *hep-th/9802030*.
- [156] J. Garriga, *Phys. Rev.* D61 (2000) 047301, *hep-th/9803210*.
- [157] A. Vilenkin, *Phys. Rev.* D57 (1998) 7069, *hep-th/9803084*.
- [158] N. Turok, *Phys. Lett.* B458 (1999) 202, *gr-qc/9901079*.
- [159] A. Andreassen et al., *Phys. Rev.* D95 (2017) 085011, 1604.06090.
- [160] C.P. Burgess, H.M. Lee and M. Trott, *JHEP* 09 (2009) 103, 0902.4465.

-
- [161] J.L.F. Barbon and J.R. Espinosa, Phys. Rev. D79 (2009) 081302, 0903.0355.
- [162] F. Bezrukov et al., JHEP 01 (2011) 016, 1008.5157.
- [163] S.W. Hawking and W. Israel, General Relativity (Univ. Pr., Cambridge, UK, 1979).
- [164] C. Wetterich, Phys. Lett. 140B (1984) 215.
- [165] S.L. Adler, AIP Conf. Proc. 68 (1980) 915.
- [166] B. Hasslacher and E. Mottola, Phys. Lett. 95B (1980) 237.
- [167] S.L. Adler, Rev. Mod. Phys. 54 (1982) 729, [,539(1982)].
- [168] T. Asaka, S. Blanchet and M. Shaposhnikov, Phys. Lett. B631 (2005) 151, hep-ph/0503065.
- [169] T. Asaka and M. Shaposhnikov, Phys. Lett. B620 (2005) 17, hep-ph/0505013.
- [170] G. Dvali and L. Funcke, Phys. Rev. D93 (2016) 113002, 1602.03191.
- [171] P.J. Greenberg, Studies in Applied Mathematics 51 277, <https://onlinelibrary.wiley.com/doi/pdf/10.1002/sapm1972513277>.